Molecular Crystals and Liquid Crystals Incorporating Nonlinear Optics

Publication details, including instructions for authors and subscription information:
http://www.tandfonline.com/loi/gmcl17

1. Introduction

Version of record first published: 28 Mar 2007.

To cite this article: (1988): 1. Introduction, Molecular Crystals and Liquid Crystals Incorporating Nonlinear Optics, 162:1, 1-96

To link to this article: http://dx.doi.org/10.1080/00268948808083041

1. INTRODUCTION

An exceptional variety of phase transitions is characteristic of a liquid crystalline state.[1] Quite often one encounters several different liquid crystalline phases appearing in an interval of only a few degrees (Figure 1). These transitions are usually the second order or weakly first order. Therefore they are accompanied by critical phenomena. Here "critical phenomena" is meant to denote those phenomena which are peculiar to the vicinity of second order transitions or critical points, i.e., they exhibit a huge increase of susceptibility, an anomaly in the specific heat, large fluctuations of order parameter, etc. Critical phenomena in liquid crystals have specific features due to the variety of the symmetries of the different phases and coupling of the different order parameters. These features complicate theoretical considerations and restrict methods which are well proved in other cases (e.g. renormalization group method). Lack of a strict theory often leads the experimentalists to interpret the results of their investigations in terms of mean-field approximation only. From the experimental point of view, the liquid crystal near a phase transition is a more "capri-

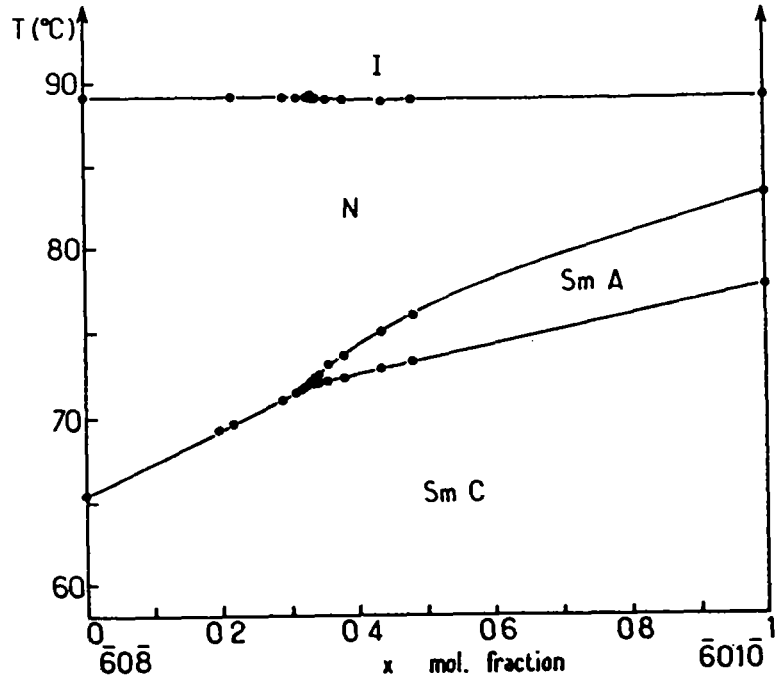

FIGURE 1 Phase diagram of $\bar{6}O\bar{8}$–$\bar{6}O1\bar{0}$ mixture. Phases: isotropic (I), nematic (N), smectic A (SmA) and smectic C (SmC).

cious" object than fluids in the vicinity of their critical points. All defects of solids are peculiar to liquid crystals: dislocations, quenched ("frozen") impurities, and the practical inability to intermix the viscous phases.

A correct fit and interpretation of the experimental data is also a difficult problem for liquid crystals. The temperature interval for fitting almost always appears to be nonasymptotic for various reasons. As a rule there is a crossover from one type of critical behaviour to another. The difficulties mentioned above sometimes lead to the result that even the order of the phase transition becomes subject to prolonged discussion. Nevertheless in recent years the experimental situation has been substantially clarified. High-resolution adiabatic calorimetry and accurate acoustic, light and X-rays scattering studies have succeeded in a coordination of the various physical properties near the following phase transitions: isotropic–nematic (NI), nematic–smectic A (NA), nematic–smectic C (NC) and smectic A–smectic C (AC). The exposition is devoted only to these transitions which are well studied experimentally.

2. LANDAU-DE GENNES THEORY

Identification of the order parameter is the key point in the description of any phase transition. The traditional approach to liquid crystals[1] consists in the introduction of the order parameters for the N, A and C phases independently.

Nematic phase

Nematics differ from isotropic liquids only by ordering (an average) of the long axes of anisotropic molecules (Figure 2). This is the least ordered of all liquid crystalline phases. If one considers molecules to be simple rods, the orientational order can be characterized by the scalar parameter

$$Q = \frac{1}{2}\langle(3\cos^2\theta - 1)\rangle \tag{1}$$

where θ is the angle between the molecular axes and the chosen direction. In the isotropic phase molecular orientations are chaotic, then $\langle\cos^2\theta\rangle = 1/3$ and $Q = 0$. In the nematic phase $\langle\cos^2\theta\rangle > 1/3$ and $Q > 0$. In reality the molecules of liquid crystals are not rods

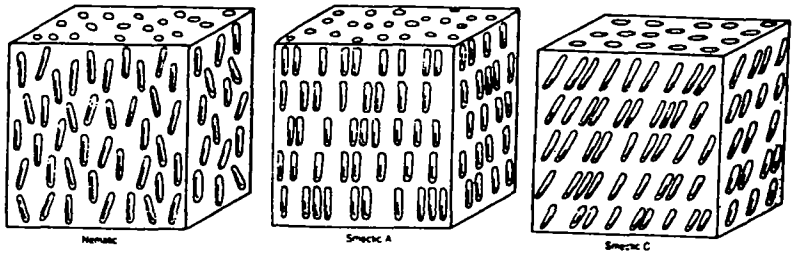

FIGURE 2 Some types of liquid crystalline ordering.[12]

but complex three-dimensional formations with more or less flexible fragments. They are not like pencils in a box, but rather packed like sardines. Therefore a more adequate a determination of the order parameter would not depend on the assumptions concerning the details of the molecule form and flexibility. The macroscopic description of nematic ordering with the help of a tensor order parameter is generally accepted now. The anisotropic part of the magnetic or dielectric susceptibility tensor can be taken as an order parameter. In this case certain difficulties arise when trying to link the macroscopic tensor properties of a liquid with the characteristics of a separate molecule.[1] To simplify this connection one can consider the anisotropic molecules to be rigid in the first approximation. The unit vector **n** indicating the direction of the preferred orientation of the long molecular axes is called a director. The tensor order parameter can be expressed through the director components:

$$Q_{ij} = Q\left(n_i n_j - \frac{\delta_{ij}}{3}\right) \tag{2}$$

where $\delta_{ij} = 1$ at $i = j$ and $\delta_{ij} = 0$ at $i \neq j$, Q is the scalar determined by the expression (1), it characterizes the fraction of the orientated molecules. Q_{ij} is the symmetric second-rank traceless tensor. Its matrix has the form

$$Q_{ij} = \begin{bmatrix} -\frac{1}{2}Q & 0 & 0 \\ 0 & -\frac{1}{2}Q & 0 \\ 0 & 0 & Q \end{bmatrix} \tag{3}$$

The simplest and well-known description of the thermodynamic

behaviour in the vicinity of the NI transition is given by the Landau-de Gennes theory.[1,2] This phenomenological theory corresponds to the mean-field approximation. Detailed discussions of the Landau-de Gennes theory of the NI transition can be found in many places (see e.g. Refs. 1 and 3). In this part the main predictions concerning the interpretation of some static properties will be recalled. The expansion of the density of the free energy in powers of the tensor order parameter

$$F - F_0 = \frac{3}{4}AQ_{ij}Q_{ji} - \frac{3}{2}BQ_{ij}Q_{jk}Q_{ki} + \frac{9}{16}CQ_{ij}Q_{jk}Q_{km}Q_{mi} + \ldots \qquad (4)$$

contains a cubic invariant as the states with Q_{ij} and $-Q_{ij}$ are non-equivalent energetically. The free energy F is measured in $\rho_{NI}RT_{NI}$ units (ρ_{NI} and T_{NI} are the density and temperature at the NI transition point, R is a gas constant), then A, B, and C are dimensionless coefficients. The values of the numerical coefficients in Eq. (4) are chosen for the convenience in further calculations. By putting the expression (2) into the expansion (4) one can obtain the expansion of the free energy in the modulus of the order parameter:

$$F - F_0 = \frac{1}{2}AQ^2 - \frac{1}{3}BQ^3 + \frac{1}{4}CQ^4 + \ldots \qquad (5)$$

The presence in Eq. (4) and (5) of the cubic term, which does not disappear at the NI transition point, leads to the fact that the NI transition appears to be a first order one. The smaller value of B the weaker first-order character of the transition. For a uniaxial phase with the positive anisotropy ($Q > 0$) $B > 0$. The minimization of (5) yields the following solutions:

$$\begin{aligned} &Q = 0 && \text{(isotropic phase)} \\ &Q = \frac{B}{2C}\left\{1 + \left(1 - \frac{4AC}{B^2}\right)^{1/2}\right\} && \text{(uniaxial nematic phase).} \end{aligned} \qquad (6)$$

In the expansion (5)

$$A = at\left(t = \frac{T - T^*}{T_{NI}}\right) \qquad (7)$$

If B were absent, T^* would be the mean-field second-order transition temperature. Since $B > 0$, T^* is the (mean-field) absolute stability limit of the isotropic phase. It is of course different from the actual transition temperature, which is given by

$$T_{NI} = \frac{T^*}{(1 - 2B^2/9aC)} \tag{8}$$

Similarly the order parameter at the transition point is

$$Q_{NI} = \frac{2B}{3C} \tag{9}$$

At the absolute limit of stability of the isotropic phase ($T = T^*$), the order parameter is

$$Q^* = \frac{B}{C} \tag{10}$$

If the expansion up to fourth order is valid, there is a universal ratio between the order parameter at T_{NI} and T^*:

$$\frac{Q_{NI}}{Q^*} = \frac{2}{3} \tag{11}$$

Note however that, if the first-order character is such that higher order terms in the expansion have to be kept, this ratio will no longer be universal.

The temperature of the absolute stability limit of the nematic phase is determined by the disappearance of the $Q \neq 0$ solution:

$$T^{**} = T^* + T_{NI}\frac{B^2}{4aC} = T_{NI}\left(1 + \frac{B^2}{36aC}\right) \tag{12}$$

Then

$$Q^{**} = \frac{B}{2C} \tag{13}$$

Contrarily to Q^*, Q^{**} is not directly accessible in experiments.

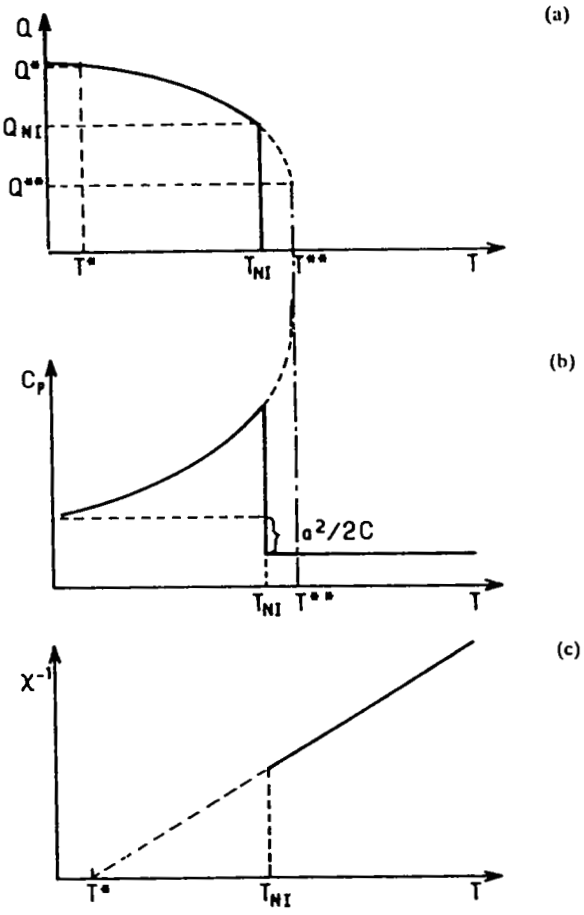

FIGURE 3 Predictions of the Landau-de Gennes theory for the NI transition: a) Order Parameter, b) Specific heat, c) Susceptibility.

The temperature dependence of Q in the nematic phase is contained in (6) more explicitly (see Figure 3a):

$$Q = \frac{B}{2C}\left[1 + \left(1 - \frac{4aC}{B^2}t\right)^{1/2}\right] = \frac{B}{2C}\left[1 + \frac{2(aC)^{1/2}}{B}\left(\frac{T^{**} - T}{T_{NI}}\right)^{1/2}\right] \tag{14}$$

The specific heat excess in the nematic phase is

$$C_P = aRQ\left(\frac{\partial Q}{\partial T}\right)_P = R\frac{a^2}{2C}\left[1 + \frac{B}{2(aC)^{1/2}}\left(\frac{T^{**} - T}{T_{NI}}\right)^{-1/2}\right] \quad (15)$$

Note the square root singularity, which is absent in the mean-field second order case (Figure 3b). The jump of the specific heat at T_{NI} is

$$\Delta C_p = R\frac{2a^2}{C} \quad (16)$$

i.e.: it is four times larger than at a second order transition. Note that it does not depend on B.

Similarly, the entropy, molar volume and enthalpy discontinuities (with obvious notations) are

$$S_I - S_N = \frac{1}{2}aQ_{NI}^2 R = \frac{2aB^2}{9C^2}R$$

$$V_I - V_N = (S_I - S_N)\left(\frac{dP}{dT}\right)_{NI} = \frac{2aB^2}{C^2}R\left(\frac{dP}{dT}\right)_{NI} \quad (17)$$

$$H_I - H_N = T_{NI}(S_I - S_N) = \frac{2aB^2}{9C^2}RT_{NI}$$

In the isotropic phase the Curie-Weiss law for the susceptibility should be valid (Figure 3c):

$$\chi^{-1} = \frac{\partial^2 F}{\partial Q^2} = a\frac{T - T^*}{T_{NI}} \quad (18)$$

In the nematic phase three different susceptibilities exist: the longitudinal susceptibility (if the field is parallel to the optical axes)

$$\chi_l^{-1} = A - 2BQ + 3Q^2$$

$$= \frac{aB}{C}\left(\frac{T^{**} - T}{T_{NI}}\right)^{1/2} + 2a\frac{T^{**} - T}{T_{NI}} \quad (19a)$$

the biaxial order susceptibility

$$\chi_b^{-1} = A + 2BQ + 3Q^2$$

$$= \frac{3B^2}{C} + 2a\frac{T^{**} - T}{T_{NI}} + 5B\left(\frac{a}{C}\right)^{1/2}\left(\frac{T^{**} - T}{T_{NI}}\right)^{1/2} \quad (19b)$$

and the susceptibility which characterizes the director fluctuations

$$\chi_{xz}^1 = L_1 k_x^2, \qquad \chi_{yz}^{-1} = L_2 k_y^2 \quad (19c)$$

(here z is the director axes, x and y are the directions of the field, L_1 and L_2 are the elastic constants, k_x and k_y are the components of the wave vector. One should note that the Curie-Weiss law is not valid for the longitudinal susceptibility, the biaxial susceptibility is a constant at $T = T^{**}$, whereas both χ_{xz} and χ_{yz} diverge at $k \to 0$, i.e. they are always "critical".

All the known thermotropic nematics are uniaxial. Pokrovskii and Katz have shown that the uniaxiality of nematics is connected with the existence of the cubic invariant in the Landau-de Gennes expansion. Generally the phase diagram of the nematic liquid crystal with an isolated critical point is possible. In a such point $B = 0$.

Vigman, Larkin and Filev[5] have shown that there should be the biaxial phase region near this point. The width of this region is determined by the sixth order term of the expansion (4). Moreover the transitions between the uniaxial and biaxial phases may be second order (Figure 4). The isolated critical point divides the uniaxial phases with the positive and negative anistropy (they are characterized by the opposite signs of the coefficients B). The similar phase diagram has been found in the liotropic nematics where the orientational ordering of the disk-like and the rod-like micelles may occur simultaneously.[6] In the thermotropic nematics the coefficient B slightly changes when pressure increases.[7] Therefore it is unlikely to discover the isolated critical point on this way. Mixing discotic liquid crystals and ordinary nematics might be the only such possibility (predicted in Ref. 8). If they are soluble there is a hope to obtain a phase diagram similar to that represented in Figure 4.

Nevertheless the biaxiality of molecules forming a uniaxial nematic can lead to the renormalization of the Landau-de Gennes expansion coefficients, effectively diminishing the value of B.[9] Let us assume, for example, that the molecules are rectangular plates. The ordering in the direction normal to the plate is described by a uniaxial tensor

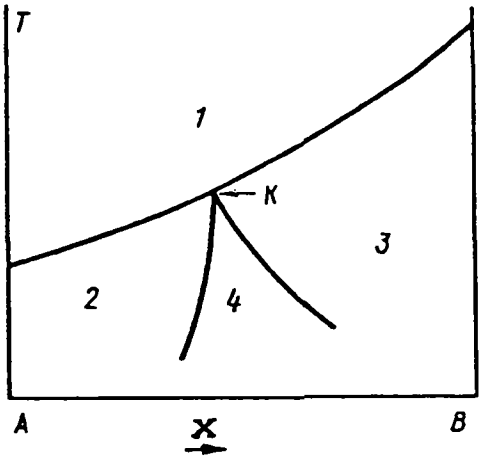

FIGURE 4 Possible phase diagram of a liquid crystalline mixture: isotropic liquid (1), uniaxial nematic with a positive anisotropy (2) uniaxial nematic with a negative anisotropy (3), biaxial nematic (4), K is an isolated critical point, x is a concentration of the component B.

R_{ij}. Then the expansion in powers of R_{ij} and the term accounting the coupling between Q_{ij} and R_{ij} should be added to the expansion given by Eq. (4). The simplest form of the coupling term is

$$F_{\text{int}} = \lambda\, Q_{ij}R_{ij} \tag{20}$$

A minimization of the free energy in order the parameter with account of Eq. (20) results in the following renormalization of the expansion (4) coefficients[9]

$$\begin{aligned} \tilde{A} &= A - \frac{\lambda^2}{A^*} \\ \tilde{B} &= B - \frac{\lambda^3 B^*}{A^{*3}} \\ C^* &= C - \frac{12B^{*2}\lambda^4}{A^{*5}} + \frac{C^*\lambda^4}{A^{*4}} \end{aligned} \tag{21}$$

where A^*, B^* and C^* are the coefficients of the free energy expansion in powers of R_{ij}. It is seen from Eq. (21) that account of the interaction between Q_{ij} and R_{ij} leads to the decrease of B and the increase of T^* since $A^* > 0$ (biaxial ordering is not achieved).

The influence of molecular flexibility may be another factor leading to the renormalization of the Landau-de Gennes expansion coefficients.[9] Let l_0 be the equilibrium value of a molecule of the length l in the absence of any orientational order. Then the expansion given by Eq. (4) should be supplemented by the terms depending on l:

$$F - F_0 = \ldots + \frac{1}{2} A^* \left(\frac{l - l_0}{l_0} \right)^2 + \frac{3}{4} \frac{\partial A}{\partial l} (l - l_0) Q_{ij} Q_{ji} \quad (22)$$

Transformation of Eq. (22) to the one-parameter potential depended on Q (see e.g. Ref. 10) leads to the renormalization of the coefficient at the fourth-order term:

$$\tilde{C} = C - \frac{1}{2} \left(\frac{\partial A}{\partial l} \right)^2 A^* \quad (23)$$

This one can expect anomalously small coefficients at the fourth power of Q_{ij} for the molecules with very "soft" fragments. The effect of dependence of the orientational ordering on the transformations of the flexible chains of the anisotropic mesogenic molecules was observed by Averianov.[11]

Smectic A phase

Anisotropic molecules of mesogenic liquids are usually arranged in such a way that the rigid central nucleus is connected with one or two flexibile tails. Moreover the tail–tail and nucleus–nucleus interactions may appear to be essentially different than those of the tail–nucleus. Thus at the decrease of temperature the formation of such an ordering may appear to be more profitable energetically when the similar molecular fragments are more likely to be in the neighbourhood. The described situation corresponds to the partial (in one dimension) violation of the translational symmetry (see Figure 2).

The formed smectic A phase differs from nematics by existence of a one-dimensional density wave along the director†):

$$\rho(\mathbf{r}) = \rho_0 \{1 - \psi(\mathbf{r}) \exp(i k_0 Z\} \quad (24)$$

where ρ_0 is the average density, $k_0 = 2\pi/l$, l is the average distance

†One can say that the smectics A are one-dimensional solids but two dimensional fluids (see Ref. 12).

between smectic layers, and

$$\psi(\mathbf{r}) = |\psi|e^{ik_0u(x,y,z)}$$

(here $u(x,y,z)$ is the displacement of the layers away from their equilibrium position). It is natural to consider the complex function $\psi(r)$ as the order parameter for a smectic A phase. The complex order parameter $\psi(z)$ is equivalent to a two-component vector. The analogous situation realizes in the superfluid helium-4 where the order parameter is a wave function. This fact leads to the so-called "helium analogy" between NA transition and λ-point in He4. Expansion of the free energy in powers of the smectic A order parameter modulus has the form

$$F - F_0 = \frac{1}{2}A|\psi|^2 + \frac{1}{4}C|\psi|^4 + \frac{1}{6}E|\psi|^6 + \ldots \tag{25}$$

where $A = a\dfrac{T - T^*_{NA}}{T_{NA}}$. When $C > 0$, $T^*_{NA} = T_{NA}$.

Since symmetry considerations requite that the odd invariants in Eq. (25) are absent, the NA transition may be either second or first order. Specifically, the NA transition can become the first order due to the coupling between the smectic and nematic ordering.[1,13]

The orientational order parameter can be written as

$$Q = Q_N + \delta Q \tag{26}$$

where Q_N is the order parameter in the nematic phase and δQ is the value which corresponds to the additional orientational ordering due to formation of the smectic layers. Then the free energy expansion is

$$F - F_0 = \frac{1}{2}a_0\frac{T - T^0_{NA}}{T^0_{NA}}|\psi|^2 + \frac{1}{4}C|\psi|^4 + \frac{1}{6}E|\psi|^6 + \frac{1}{2}A_NQ^2 + \lambda|\psi|^2Q \tag{27}$$

where T^0_{NA} is the NA transition temperature in the absence of the coupling between ψ and Q, λ is the coupling constant. Transforming

$F(T,\psi,Q)$ to the one-parameter potential $F(T,\psi)$, we obtain the expansion (25) with the renormalized coefficients:

$$A = a_0(T^0_{NA})^{-1}\left[T - \left(T^0_{NA} + \frac{2Q_N\lambda}{a_0}\right)\right] \tag{28}$$

$$C = C_0 - \frac{2\lambda^2}{A_N} \tag{29}$$

here

$$\begin{aligned} T^0_{NA} + 2Q_N a_0^{-1}\lambda &= T^*_{NA} \\ \lambda &= -\frac{a_0}{2T_{NA}}\frac{dT_{NA}}{dQ} \end{aligned} \tag{30}$$

Thus the coupling between ψ and Q leads to the shift of the NA transition temperature and to the renormalization of the fourth-order term coefficient. If the NA and NI transitions are close enough to each other, the nematic susceptibility is large since $\chi \sim A_N^{-1} = (an(T - T^*/T_{NI})^{-1}$. Hence the sign of the coefficient C can invert. When $C = 0$ a tricritical point appears and when $C < 0$ the NA transition becomes a first-order one. For a tricritical point there are peculiar dependences of the order parameter and specific heat on temperature. The minimization of Eq. (25) yields in the ordered phase at $C = 0$

$$|\psi| = \left(-\frac{A}{E}\right)^{1/4} = \left[-\frac{a(T - T_{tcp})}{ET_{tcp}}\right]^{1/4} \tag{31}$$

where T_{tcp} is the tricritical temperature.

Putting Eq. (31) into Eq. (25) and differentiating twice we obtain the specific heat:

$$C_p = \frac{1}{4} R\, a^{3/2}\, E^{-1/2}(-t)^{1/2} \tag{32}$$

where $t = (T - T_{tcp})/T_{tcp}$, i.e. C_p of the ordered phase has a square root

singularity at the tricritical point. If C is small and positive

$$C_p = \frac{1}{4} R\, a^2 \left(\frac{1}{4}C^2 - aEt\right)^{-1/2} \tag{33}$$

The temperature of the specific heat singularity T_0 one can obtain from the condition

$$\frac{1}{4} C^2 - aEt = 0$$

Then

$$t_0 = \frac{T_0 - T_{NA}}{T_{NA}} = \frac{C^2}{4aE} \tag{34}$$

Obviously T_0 is only the parameter of extrapolation. Equilibrium conditions

$$F - F_0 = 0 \text{ and } \partial F/\partial\psi = 0$$

lead to the following value of the order parameter at $T = T_{NA}$ when C is small and negative:

$$|\psi| = \left(-\frac{3C}{4E}\right)^{1/2} \tag{35}$$

The first order NA transition line equation can be obtained by putting Eq. (35) to Eq. (25) with account of the condition $F - F_0 = 0$:

$$\frac{16}{3} AE - C^2 = 0 \tag{36}$$

Hence the shift between the NA first order transition temperature and the temperature of a nematic phase absolute stability limit is

$$t^* = \frac{T_{NA} - T^*_{NA}}{T_{NA}} = \frac{3C^2}{16aE} \tag{37}$$

and the shift between T_{NA} and T^{**} is

$$t^{**} = \frac{T^{**} - T_{NA}}{T_{NA}} = \frac{C^2}{16aE} \tag{38}$$

Putting Eq. (36) to Eq. (33) we obtain the jump of the smectic A phase specific heat at $T = T_{NA}$

$$C_p = \frac{a^2}{C} \tag{39}$$

which is twice more than the specific heat jump at the second-order transition line. At last the latent heat of the transition is given by the following expression:

$$\frac{\Delta H_{NA}}{RT_{NA}} = \frac{1}{2} a|\psi|^2 = \frac{3aC}{8E} \tag{40}$$

Smectic C Phase

A further decrease in temperature can lead to the next less symmetric smectic C phase. In this case the uniaxial symmetry is broken, which physically corresponds to the appearance of a tilt in the molecular axes with respect to the density wave direction (Figure 2). De Gennes[1] proposed to describe smectics C by the complex order parameter

$$\bar{S} = \theta e^{i\Phi} \tag{41}$$

where θ is the angle of the molecular slope with respect to the director, ϕ is the azimuth. This order parameter is equivalent to a two-component vector, i.e. the helium analogy might be also expected for the AC transition. As in the case of the NA transition, it can be either second or first order.

Mean-field models for coupled order parameters

The more consistent consideration of the AC transition should take into account the coupling between different order parameters. There are several mean-field models which describe uniformly the N, A and C phases. Chu and McMillan[14] took into account coupling between smectic A and C order parameters in the form $|\psi|^2\theta^2$ in the expansion of the thermodynamic potential in powers of ψ and θ. In the phase diagram a triple NAC point may appear at which the lines of the

NA, AC and NC transitions converge, all of them being of the second order. Pikin and Idenbom[15] proposed an order parameter with modulus equal to $S = \theta|\psi|$, which takes into account the fact that the angle θ is inevitably equal to zero in the absence of smectic ordering. Then the expansion of the free energy has the form

$$F - F_0 = \frac{1}{2} A_1 |\psi|^2 + \frac{1}{4} C_1|\psi|^4 + \frac{1}{6}E|\psi|^6 + \frac{1}{2}A_2\theta^2|\psi|^2 + \frac{1}{4}C_2\theta^4|\psi|^4 - \frac{1}{2}\lambda\theta^2|\psi|^4 \quad (42)$$

where the last item describes the coupling between $|\psi|$ and $S = \theta|\psi|$. A positive sign for the coupling constant λ means that the density wave amplitude increases in the C phase. If the critical temperatures T_1 and T_2 of the NA and AC transitions depend on any external parameter (e.g. pressure), a NAC point appears when $T_1 = T_2$. Both of the AC and NC transitions may either be of the first or of the second order near the NAC point. Under certain correlations of the expansion (42) constants a coincidence of the NAC point with the tricritical one is also possible.

Gorodetskii and Podnek[16] constructed a model which can give a unified description of the main types of liquid crystalline phases and the transitions between them. Their starting point was the fact that in liquid crystals generally there are two independent directions: one of them determines the orientational order of the nematic type and another gives the orientation of the smectic layers. The existence of these two directions means that a liquid crystal should be described by two order tensors, one of which is responsible for the formation of the nematic phase, the other for the smectic phases. The two tensor order parameters can be introduced either phenomenologically, or by separating the long-wave (nematic) and short-wave (smectic) components of a single tensor. One should note that in the Gorodetskii and Podnek model the appearance and the behaviour of the angle θ in the smectic C phase are completely determined by the value of the nematic order parameter. In the smectic phase, starting from the line $Q = Q_c$, there is a nonzero mean angle θ, determined in the C phase by the equation

$$\sin^2\theta = \frac{2}{3}\frac{Q - Q_c}{Q} \quad (43)$$

The maximum value of θ is limited by $\arcsin\sqrt{\frac{2}{3}} \approx 55°$. Line $Q = Q_c$ is a curve of AC second-order transitions. But according to this model the AC transition free energy has no independent term proportional to θ^2, i.e. θ is not a separate order parameter. Thus the angle θ could appear from a finite value at the NC transition line even the transition would be a second-order. The model[16] describes naturally so-called re-entrant behaviour[17] (see Figures 5 and 6) which is determined by competition between orientation and smectic ordering. The calculations in Ref. 16 show that the disposition ("slope") of the "re-entrant parabola" strongly depends on the slope of the NI transition line.

Chen and Lubensky[20] as early as in 1976 proposed a model which is essential for understanding the nature of smectic phases. In this case, a single order parameter describing the modulation of the density was used. However, for the C phase there was additional modulation in a direction perpendicular to the director. This additional modulation is mathematically related to the change in the sign of the

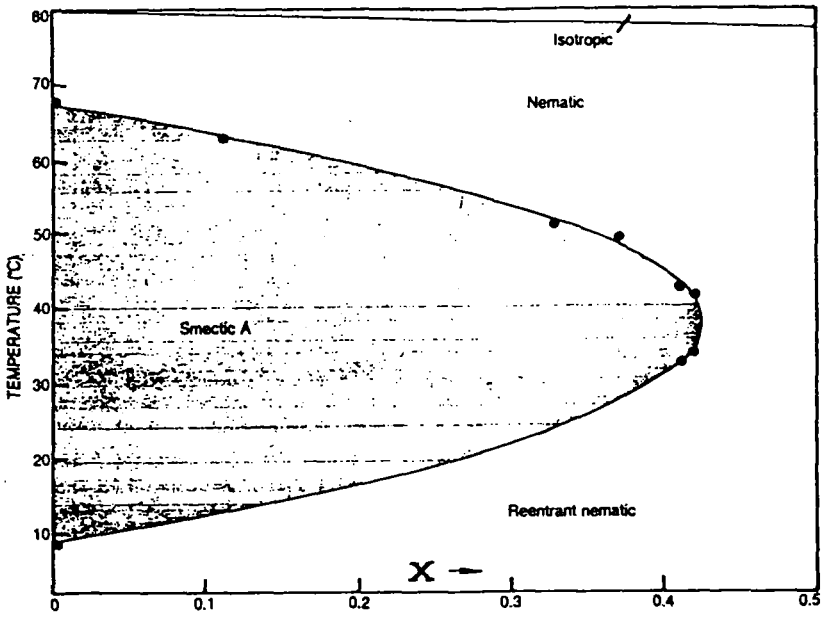

FIGURE 5 Phase diagram of 6OCB–8OCB mixture.[12,18] X is the weight ratio (6OCB/8OCB).

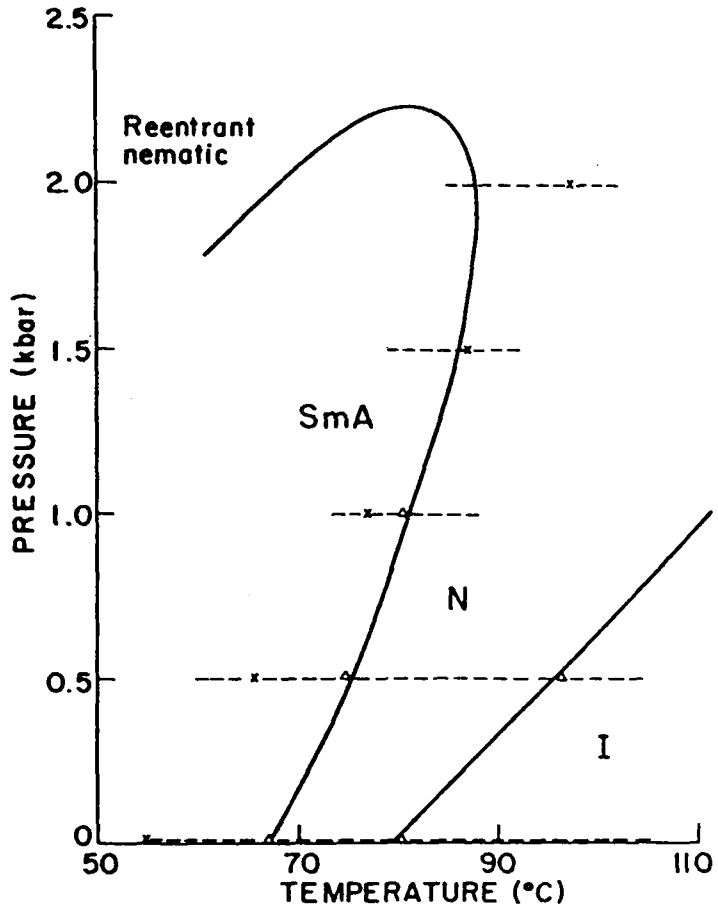

FIGURE 6 Phase diagram of 80CB.[19] The dashed lines indicate the C_p-studied isobars, crosses indicate the equilibrium melting point of the solid state, i.e. the re-entrant point is located in a metastable region.

coefficient in front of $\nabla_\perp^2$ in the smectic free energy expansion, which has the form

$$F - F_0 = \frac{1}{2}A|\psi|^2 + \frac{1}{4}C|\psi|^4 + \frac{1}{2}L_{\|}|\nabla_{\|}^2\psi| + \frac{1}{2}L_\perp|\nabla_\perp - ik_0\delta\mathbf{n})\psi|^2 \qquad (44)$$

where symbols $\|$ and $\perp$ are related with the direction along the director and perpendicular to it. The term $ik_0\delta\mathbf{n}$ takes into account

so-called gauge invariance, i.e. the invariance of the system under a simultaneous rotation of the director and the direction of modulation of the density. Two correlation lengths can be determined with the help of Eq. (44):

$$\xi_{\parallel} = \sqrt{\frac{L_{\parallel}}{A}} \text{ and } \xi_{\perp} = \sqrt{\frac{L_{\perp}}{A}}$$

The point where the coefficient in front of $\nabla_{\perp}^2$ becomes equal to zero is known as a Lifshitz critical point.[21] Hence the multicritical NAC should be a Lifshitz point.

Accounting the gradient-dependent items in the free energy expansion means accounting the fluctuations of the order parameter in the first approximation. It means that many peculiarities of the liquid crystal behaviour can not be explained without consideration of fluctuations.

3. BASIC RESULTS OF THE FLUCTUATION THEORY

Nematic Fluctuations

The characteristic feature of practically all known thermotropic nematics is the weakness of the first-order character of the NI transition. This weakness can be characterized numerically by the parameter

$$\Delta = \frac{T_{NI} - T^*}{T_{NI}} \sim B^2$$

In most liquid crystals that have been studied, the parameter $\Delta \approx 10^{-2} - 10^{-3}$, i.e. $\Delta << 1$. But in any mean-field theory with a single interaction constant, the order of magnitude of Δ should be ≈ 1. Therefore the weakness of the NI transition can not be accidental. In Section 2 it was shown that an account of molecular biaxiality even within the framework of the Landau-de Gennes theory may result in the effective diminition of the coefficient B and, consequently, to the weakness of the NI transition. However an account of fluctuations may force one to revise the situation in general. For example, the fluctuations of the nematic order parameter may be quite probable and universal reason of the smallness of the constant B. In the nematic phase the director fluctuations are "critical". Nelson and Pelcovits[22]

pointed out that strongly developed director fluctuations could alter the character of the NI transition and make it a very weak first order (see also Ref. 23). On the other hand the weakness of the NI transition results in the large fluctuations of the order parameter modulus. Unfortunately methods of the fluctuation theory (such as renormalization-group method) can be applied consistently only to the pure second-order transitions.

Vigman, Larkin and Filev[5] applied the renormalization-group method to the description of the fluctuation behaviour near the isolated critical point on the NI transition line. In this point (see Figure 4) the cubic invariant in the effective Hamiltonian is equal to zero. The values of the critical exponents were calculated by the ϵ-expansion ($\epsilon = 4 - d$, d is a dimension of space) for the five-component order parameter.† In the linear approximation

$$\nu = \frac{1}{2} + \frac{7}{52}\epsilon,\ \gamma = 1 + \frac{7}{26}\epsilon,\ \alpha = \frac{1}{26}\epsilon,\ \beta = \frac{1}{2} - \frac{6}{52}\epsilon \quad (45)$$

where ν is the critical exponent of the correlation length $\xi \sim (T - T_c)^{-\nu}$, γ is the critical exponent of the susceptibility $\chi \sim (T - T_c)^{-\gamma}$, α is the critical exponent of the specific heat $C_p \sim (T - T_c)^{-\alpha}$ and β is the critical exponent of the order parameter $Q \sim (T - T_c)^{\beta}$. In three dimensions $\epsilon = 1$ and $\nu \approx 0.64$, $\gamma \approx 1.27$, $\alpha \approx 0.04$, $\beta \approx 0.38$. Though the real NI transitions are close to second-order ones, the behaviour of the thermodynamic values here is too far from the predictions of the fluctuation theory. Gorodetskii and Zaprudskii[26] as well as Korzhenevskii and Shalaev,[27] investigating the systems with the effective Hamiltonian contained a cubic invariant, have found an additional fixed point of the renormalization-group equations besides the isolated critical one. This point corresponds to the second-order transition despite the fact that a cubic invariant exists in the initial Hamiltonian. Unfortunately such a point as well as the isolated one is not found in the thermotropic nematics. The character of the anomalies theoretically predicted in Refs. 26 and 27 (e.g. $\gamma \approx 1.6$), is also far from the experimental results for the NI transition (see the next Sections).

The absence of the susceptibility divergence at the NI transition point allows us to expect the possibility of using the Gaussian approximation, i.e. the approximation of weakly interacted fluctuations.

†See the general view and details in Refs. 24 and 25.

In this case the account of the orientational fluctuations in the isotropic phase is reduced to the addition of gradient-dependent terms to the expansion (4):

$$F - F_0 = \ldots + \frac{1}{2} L_1 \left(\frac{\partial}{\partial x_i} Q_{jk}\right)^2 + \frac{1}{2} L_2 \left(\frac{\partial}{\partial x_j} Q_{jk}\right)^2 \qquad (46)$$

where L_1 and L_2 are the elastic constants of the isotropic phase. In a single correlation length approximation

$$\xi = \xi_0 t^{-1/2} \qquad (47)$$

where $\xi_0 = (L/a)^{1/2}$ is a bare correlation length, $L = L_1$, $L_2 = 0$. The corresponding fluctuation addition to the specific heat has the form

$$\delta C_p = \frac{nRv_0}{16\pi\xi_0^3} t^{-1/2} \qquad (48)$$

where n is the number of independently fluctuating modes, v_0 is the molecular volume. In the single correlation length approximation $n = 5$ (in the isotropic phase) and $n = 1$ (in the nematic phase). Comparing the fluctuation part of the specific heat with its second-order transition jump $a^2/2C$ one can find the Ginzburg criterion for the mean-field region:

$$t >> \mathrm{Gi} = \frac{n^2 C^2}{64\pi^2 a^4} \left(\frac{v_0}{\xi_0^3}\right)^2 \qquad (49)$$

For the NI transition $n = 5$ and usually $\frac{v_0}{\xi_0^3} \approx 2$. If one were to assume that $a \approx C \approx 1$, one would expect a violation of the Ginzburg criterion even far from the transition point, since $\mathrm{Gi} \approx 0.2$ and $\Delta << \mathrm{Gi}$. However as experiment shows (see the next sections), the coefficient C usually appears to be anomalously small $C \approx 0.1$, i.e. it is in fact as small as B!. Hence the true value of the Ginzburg number is $2 \cdot 10^{-3}$ and the critical regime is not accessible.

The estimations made above may be invalid since the existence of the cubic term in expansion (4) was not taken into account. If one

compares the fluctuations in the correlation volume $v_c \approx \xi^3$ at $T = T_{NI}$

$$\langle \delta Q^2 \rangle = \frac{v_0}{v_c} \chi = \frac{v_0 \Delta^{1/2}}{\xi_0^3 a} \tag{50}$$

where $\Delta = 2B^2/9aC$ (Eq. 8), and the value of the order parameter at $T = T_{NI}$ (Eq. 9), one can obtain the following condition for the mean-field region:

$$\left(\frac{C^{3/2}}{|B|a^{3/2}}\right)\left(\frac{v_0}{\xi_0^3}\right) << 1 \tag{51}$$

Using the experimental values of the constants for MBBA (see Section 4): $C \approx 0.1$, $B \approx 0.06$, $a \approx 1.4$, $v_0/\xi_0^3 \approx 2$, one can make sure that the inequality (51) is not satisfied at $T = T_{NI}$. Hence in the immediate vicinity of the NI transition point the mean-field approach may fail due to the weak first-order character of the NI transition.

Fan and Stephen[28] showed that the account of the fluctuations of the nematic order parameter modulus in Gaussian approximation renormalized the susceptibility of the isotropic phase:

$$\chi^{-1} = a\,t\left[1 + \frac{7}{2\pi^2}\left(\frac{C}{a^2}\right)\left(\frac{v_0}{\xi_0^3}\right) t^{-1/2} - \frac{7}{4\pi^2}\left(\frac{B^2}{a^3}\right)\left(\frac{v_0}{\xi_0^3}\right) t^{-3/2}\right] \tag{52}$$

Comparing the first and the second terms in Eq. (52) one can obtain the Ginzburg criterion (49) within the accuracy of a numerical coefficient. Evaluation of the contribution of the third item gives another Ginzburg criterion which connected with the cubic term in the Landau-de Gennes expansion. In the last case the mean-field region is

$$t >> \mathrm{Gi} = \left(\frac{7B^2}{4\pi^2 a^3}\right)\left(\frac{v_0}{\xi_0^3}\right)^{2/3} \tag{53}$$

If one replaces t in this criterion by $\Delta = 2B^2/9aC$, the inequality (51) can be easily obtained within the accuracy of a numerical coefficient which does not differ much from 1. Thus the existence of the cubic invariant may appear to be the dominant reason for the possible failure of the mean-field description is the vicinity of the NI transition.

One should note that the coefficient B is also renormalized by the nematic fluctuations, the corresponding correction being always negative.[9] Priest[29] showed that the coupling between uniaxial and biaxial fluctuations in the isotropic phase leads to the diminution of B as well. One can note that in the nematic phase biaxial fluctuations play a minor role since χ_b does not diverge at $T = T^{**}$. Nevertheless biaxial fluctuations can make a noticeable contribution to the physical values at the length

$$l = \frac{2\pi}{k} \approx \frac{(CL)^{1/2}}{|B|}$$

This estimation shows that the characteristic length becomes macroscopic only at $B = 0$. At the real values of $B \approx C \approx 0.1$ and $L \approx a\xi_0^2 \approx 5.10^{-19}\text{m}^2$, $l \approx 10^{-9}\text{m}$ which corresponds to hyperacoustic wavelengths.

The consistent investigation of the nematic fluctuations in the isotropic phase by the perturbation theory method in the Gaussian approximation was carried out in Ref. 30. Contribution of the one and two-loop diagrams was taken into account. Two-loop diagrams were calculated with logarithmic accuracy.

The following expressions for the susceptibility and specific heat in the isotropic phase were obtained:

$$\chi^{-1} = a\,t\left[1 + y_C t^{-1/2} - y_B t^{-3/2} + y_E - \left(\frac{1}{7}y_C^2 - y_{BD}\right) t^{-1}\ln t^{-1} - \frac{25}{63}\,y_B^2 t^{-3} + \frac{5}{14}y_C y_B\, t^{-2}\right] \quad (54)$$

$$\delta C_p = \frac{5Rv_0}{16\pi\xi_0^3}\,t^{-1/2}\left[1 + \frac{2}{3}\,y_B t^{-3/2} + \frac{4}{5}\,y_B^2\,t^{-3} + \frac{1}{2}y_E + \frac{3}{50}\,y_B y_C t^{-2} + \left(\frac{1}{14}\,y_C^2 - \frac{1}{2}\,y_{BD}\right) t^{-1}\ln t^{-1}\right] \quad (55)$$

where y_C, y_B, y_E, y_{BD} are the combinations of the expansions (4) and (46) coefficients with account of the fifth and sixth order terms. One can see that the temperature dependence of the susceptibility has some deviations from the Curie-Weiss law and the specific heat from the square root divergence (compare with formulas (48) and (52). As shown below, the approach proposed in Ref. 30 allows one to adjust

the pretransitional behaviour in the isotropic phase, where only the contribution of fluctuations takes place. In the nematic phase the temperature dependence of the order parameter plays the substantial role.

Smectic fluctuations

The modern fluctuation theory of the NA transition starts from the "helium analogy"[1] between Hamiltonians describing this transition and the superfluid – normal fluid (or superconductor – normal metal) one. The effective Hamiltonian of a smectic A with account of the contribution from the energy of deformation of the director, the so-called Frank elastic energy, has the form[23]

$$\begin{aligned} H = H_S + H_N = \int \Bigg[& \frac{1}{2} a^* t|\psi|^2 + \frac{1}{4} C^*|\psi|^4 \\ & + |(\nabla - ik_0\, \delta\mathbf{n})|^2 \Bigg] d\mathbf{r} \\ & + \int \Bigg[\frac{1}{2} K_1 (\nabla \mathrm{n})^2 + K_2 \sum_{ij} (\nabla_i n_j - \nabla_j n_i)^2 \\ & + \frac{1}{2} K_3 \sum_j (\nabla_{\|} n_j)^2 \Bigg] d\mathbf{r} \end{aligned} \tag{56}$$

where

$$a^* = \frac{a}{L_0},\ C^* = \frac{C}{L_0},\ L_0^3 = L_{\|} L_{\perp}^2,$$

$$K_1 = K_2 = \overline{K}_{1,2} (L_{\|}/L_{\perp})^{2/3},$$

$$K_3 = \overline{K}_3 (L_{\|}/L_{\perp})^{-1/3},$$

$t = (T - T_{NA}^0)/T_{NA}$, T_{NA}^0 is the NA transition temperature in mean-field approximation, $\overline{K}_1$, $\overline{K}_2$ and $\overline{K}_3$ are the bare values of Frank moduli (i.e., if neglecting fluctuations of the smectic order parameter). In Eq. (56) the start-up anisotropy of the correlation lengths was eliminated with the help of scale transformation.

The Hamiltonian for the superconductor—normal metal transition

would coincide exactly with the NA transition Hamiltonian (56) if $K_1 = 0$ and $K_2 = K_3$. This is not true in general for liquid crystals. There is also another very important difference between smectic one-dimension crystallization and superconductivity. According to Landau and Peierls theorem,[2] true long-range order cannot in general exist in smectics. This is related with the fact that in any three-dimensional system with a one-dimensional modulation of density, fluctuations of the displacements ("phase" of the complex order parameter) diverge. Dunn and Lubensky[31] proposed an artificial technique involving the introduction of a special so-called superconducting gauge which allows one to related the smectic problem to superconductivity. Thermodynamic characteristics such as the specific heat do not depend on the gauge, i.e., they can be calculated in any convenient gauge. On the other hand, some important quantities (e.g. the correlation function) depend explicitly on the gauge. Therefore there is no assurance that the theoretical values of the critical exponents are really true.† Moreover universality class depends on the bare values of elastic moduli.[31] One can only expect definitely that the scaling relations between critical exponents must be satisfied:

$$2 - \alpha = \nu_{\|} + (d - 1)\nu_{\perp} \tag{57}$$

$$\gamma = \nu_{\|}(2 - \eta_{\|}) = \nu_{\perp}(2 - \eta_{\perp}) \tag{58}$$

where $\nu_{\|}$ and $\nu_{\perp}$ are the longitudinal (along the director) and transverse correlation length exponents ($\xi_{\|} = \xi_{0\|}|t|^{-\nu_{\|}}$ and $\xi_{\perp} = \xi_{0\perp}|t|^{-\nu_{\perp}}$), $\eta_{\|}$ and $\eta_{\perp}$ are the longitudinal and transverse correlation function exponents ($G_{\|}(r) \sim r^{\perp-\eta_{\|}}$ and $G_{\perp}(r) \sim r^{1-\eta_{\perp}}$). The relations (57) and (58) may be called anisotropic scaling. Incidentally it is quite possible that in the very NA transition point the situation becomes isotropic ($\nu_{\|} = \nu_{\perp}$). Nelson and Toner[32] proposed a model in which the smectic A phase changes to nematic through a proliferation of defects in the layer structure (topological melting). In this case $\nu_{\|} = (5 - d)\nu_{\perp}$ (at $d = 3$, $\nu_{\|} = 2\nu_{\perp}$).[33] The renormalization group equation for K_1 has the following fixed points: $K_1^* = 0$, $K_1^* = \infty$ and $0 < K_1^* < \infty$. In the first case there is a superconducting analogy, in the second there is anisotropic scaling with the nonuniversal relation $\nu_{\|} > \nu_{\perp}$, and in the third we always have $\nu_{\|} = (5\ d)\nu_{\perp}$.

†Critical exponents should be calculated in this case for the two-component order parameter (see Refs. 24 and 25).

The situation near the NA transition is complicated even more by the possible "breakdown" of the continuous NA transition to the first-order one due to the nematic direction fluctuations (Halperin-Lubensky-Ma effect).[34] However the coefficient in front of the cubic term which appears due to the HLM effect, is probably, very small. So from the experimental view point the NA transition may seem to be second order.

Smectic fluctuations near special points of a phase diagram

We have seen that the theoretical situation around the NA transition is very complicated. Indeed, Lubensky[35] had a reason for calling the NA transition problem one of the most intriguing. Therefore the adequate interpretation of the experiment becomes so important. From the very beginning it is necessary to extract the effects related to the special points on a phase diagram which appear due to the order parameter coupling. These effects appear to be more rough in comparison with thin differences of versions of the fluctuation theory. Hence their consideration should precede any detailed analysis of experiments. The smectic fluctuations in Ornstein-Zernike (Gaussian) approximation near the triple NAI, multicritical NAC, tricritical and reentrant NA points were considered in Refs. 36 and 37 on the basis of the model proposed in Ref. 16.

The main result for the isotropic phase[36] is the renormalization of the nematic suseptibility and the nematic bare correlation length by smectic fluctuations. The perturbation theory gives[36]

$$\chi^{-1} = at - \frac{B_{Q\psi}^2}{(t + \Delta_0)^{3/2}} + \frac{C_{Q\psi}}{(t + \Delta_0)^{1/2}} \tag{59}$$

$$\tilde{\xi}_0 = \xi_0 \left[1 + \frac{B_{Q\psi}^2}{32\pi^2(t + \Delta_0)^{5/2}}\right]^{1/2} \tag{60}$$

$$\delta C_p = \frac{nRv_0}{16\pi\tilde{\xi}_0^3}\left[\frac{\partial(\chi a)^{-1}}{\partial t}\right]^2 (\chi a)^{1/2} \tag{61}$$

where

$$t = \frac{T - T_{NI}^*}{T_{NI}^*},$$

$$\Delta_0 = \frac{T_{NI}^* - T_{AI}^*}{T_{AI}^*},$$

T^*_{NI} and T^*_{AI} are the bare (in absence of the coupling between positional and orientational ordering) absolute stability limits of the isotropic phase for NI and AI transitions correspondingly, $B_{Q\psi}$ and $C_{Q\psi}$ are proportional to the coupling constants λ and γ in the free energy expansion

$$F - F_0 = F_N + F_S + \lambda Q|\psi|^2 + \gamma Q^2|\psi|^2 \tag{62}$$

(F_N and F_S are the bare nematic and smectic free energies). The result given by Eq. (59) was also obtained independently by Prost and his coworkers.[38]

One can note that qualitatively the character of deviations from the Curie-Weiss law caused by smectic fluctuations is similar to those connected with taking into account nematic fluctuations (see Eqs. 52 and 54). So the separation of these effects can not be a simple question while fitting the experimental data. However, one should note that the powers $-1/2$ and $-3/2$ are fundamentally different from those in Eq. 52, which in fact under the same circumstances $+1/2$ and $-1/2$ respectively. As a result smectic fluctuation are more "dangerous" for the Curie-Weiss law. Furthermore, the smectic fluctuation corrections depend on the width of the nematic range: the closer NAI point (i.e., the smaller Δ_0) the large deviations. Near the NAI point Δ_0 changes its sign. It means that without the coupling the positional ordering would precede the nematic ordering. But in any case $(t + \Delta_0)$ remains positive at the transition point because the smaller Δ_0 the large "first-order power" of the transition.

Besides the effect mentioned above, the smectic fluctuations make an additional contribution to the specific heat of the isotropic phase:[39]

$$\delta C_p \sim (t + \Delta_0)^{-3/2} \tag{63}$$

This result is closely related to the general consideration made by Brazovskii.[40] He has shown that if a density wave is established with an infinite number of possible characteristic wavevectors, there is a divergent contribution to the entropy. Hence such transitions should be always first order. This effect should exist in the isotropic phase of cholesterics due to the fluctuations of cholesteric ordering and in the nematic phase of smectics C due to azimuthal symmetry of the smectic C-phase. Therefore the NC transition is always first order[41] even though the mean-field approximation, which neglects fluctuations, predicts second-order behaviour.

The NA second-order transition line is determined by the equation

$\Delta_A = 0$, where Δ_A is the inverse susceptibility of the smectic A. At the re-entrant point

$$\left(\frac{\partial \Delta_A}{\partial t}\right)_{NA} = 0 \tag{64}$$

and $\Delta_A \sim |t|^{2\gamma}$, $\xi_{||} = \xi_{0||}|t|^{-2\nu}$, i.e., doubling of the critical exponent should be observed. At the same time the specific heat anomaly vanishes at the re-entrant point. In the mean-field approximation the C_p jump $\left(\frac{a^2}{2C}\right)$ vanishes because $a = 0$ at the re-entrant point, in the fluctuation theory the C_p critical amplitude vanishes because the effective value of the bare longitudinal correlation length tends to infinity. Indeed, if the correlation length is represented in the form

$$\xi_{||} = \tilde{\xi}_{0||}|t|^{-1/2} \tag{65}$$

then the effective value of the bare correlation length

$$\tilde{\xi}_{0||} = \xi_{0||}(\partial \Delta_A/\partial t)^{-1/2} \tag{66}$$

will depend on the proximity of the re-entrant point. As a result, in the vicinity of the re-entrant point all measured critical exponents should be "effective" (dependent on the width of the nematic range).

According to Ref. 37 at the line $Q = Q_c$ (see previous section) the character of the smectic fluctuations in the nematic phase changes. At $Q \geq Q_c$ the mean angle θ appears in the smectic fluctuation clusters. The equilibrium angle θ is determined by Eq. (43). The A-type fluctuation regime is replaced by that of the C-type. The line $Q - Q_c$ (A-C crossover line) should be parallel to the NI transition line, being the line of the constant value of the nematic order parameter. The value of the transverse bare correlation length also depends on the nematic ordering:

$$\xi_{0\perp} \approx k_0^{-1}|Q_c - Q|^{1/2} \tag{67}$$

At the line $Q = Q_c$ $\xi_{0\perp} = 0$. The point of the intersection of this line and the NC transition line should be the Lifshitz point. Hence in the vicinity of the NAC point the relation $\xi_{||}|\xi_\perp$ should strongly depend on temperature.

Analysis of the "rough" effect should precede the discussion about more delicate phenomenon, such as possible anisotropy of the cor-

relation length exponents $\nu_{\|}$ and $\nu_{\perp}$. In the region of the A-C crossover the specific heat is not described by a simple power law, and only in the immediate vicinity of the NC transition point it comes out to the following asymptotics:

$$\delta C_p = \frac{R\nu_0}{16\pi\xi_{0\|}\xi_{0\perp}^2}\left(\frac{\partial\Delta_A}{\partial t}\right)^2 \Delta_A^{-1/2} \tag{68}$$

Comparing the fluctuation part of the specific heat with the mean-field jump

$$\Delta C_p = \frac{a^2}{2C} = \frac{(\partial\Delta_A/\partial t)^2}{2C}$$

one can obtain the Ginzburg criterion for the smectic fluctuations in the nematic phase:

$$\mathrm{Gi} = \frac{C^2}{64\pi^2}\left(\frac{\nu_0}{\xi_{0\|}\xi_{0\perp}^2}\right)^2\left(\frac{\partial\Delta_A}{\partial t}\right)^{-1} \tag{69}$$

It is seen from Eq. (69) that the mean-field range ($t >> \mathrm{Gi}$) increases while approaching the tricritical point ($C = 0$) and decreases while approaching the NAC point ($\xi_{0\perp} = 0$) if the later is not a tricritical at the same time.

4. STATICS NEAR NI TRANSITIONS

Order parameter

The temperature dependence of the order parameter in the nematic phase could provide a first test for the validity of the Landau-de Gennes theory. In this case, the measured quantity is some macroscopic property of a material which characterizes anisotropy of the nematic phase. If one identifies the order parameter with the anisotropic part of the magnetic susceptibility tensor, it is

$$Q_{ij} = Q_0\left(\chi_{ij} - \frac{\delta_{ij}}{3}\sum_k \chi_{kk}\right) \tag{70}$$

where Q_0 is a normalizing constant. The susceptibility χ is determined

from the correlation between the magnetization M and the magnetic field h:

$$M_i = \chi_{ij} h_j \tag{71}$$

In the isotropic liquid $\chi_{ij} = \chi\delta_{ij}$ and all the components Q_{ij} vanish. In the uniaxial nematic, choosing the axes in such a way that the matrix Q_{ij} becomes diagonal, we have

$$Q_{ij} = Q_0 \begin{bmatrix} \frac{1}{3}(\chi_\perp - \chi_\parallel) & 0 & 0 \\ 0 & \frac{1}{3}(\chi_\perp - \chi_\parallel) & 0 \\ 0 & 0 & \frac{2}{3}(\chi_\parallel - \chi_\perp) \end{bmatrix} \tag{72}$$

In the model of rigid rods[42] there is a simple connection between the macroscopic anisotropy and the scalar order parameter Q which is determined by Eq. (1):

$$\chi_\parallel - \chi_\perp = \frac{N}{V}(\alpha_\parallel - \alpha_\perp)Q \tag{73}$$

where $\alpha_\parallel - \alpha_\perp$ is the macroscopic anisotropy of the response of a molecule to the magnetic field, N is a number of molecules. Anisotropy of the dielectric susceptibility or refractive index could just as well be chosen. Optical measurements are very precise. However the difficulties arising at the attempt to correlate the macroscopic anisotropy with the microscopic characteristics, appear to be more essential in this case: electric molecular interactions can not consider to be weak unlike the magnetic ones. Essential assumptions should be made while extracting the parameter Q from the NMR spectrum.[43] Therefore one should interpret the temperature dependence of the measured order parameter with a definite cautiousness: it is not a best test for the validity of any theory.

The usual values of Q at the NI transition temperature lie between 0.3 and 0.5.[44,45] The uncertainty of Q_{NI} is usually large, due to the difficulty to extrapolate the data to the transition temperature and to the dependence of the result upon the technique used (Figure 7). Noticeably, the value of Q_{NI} deduced from the birefringence of the

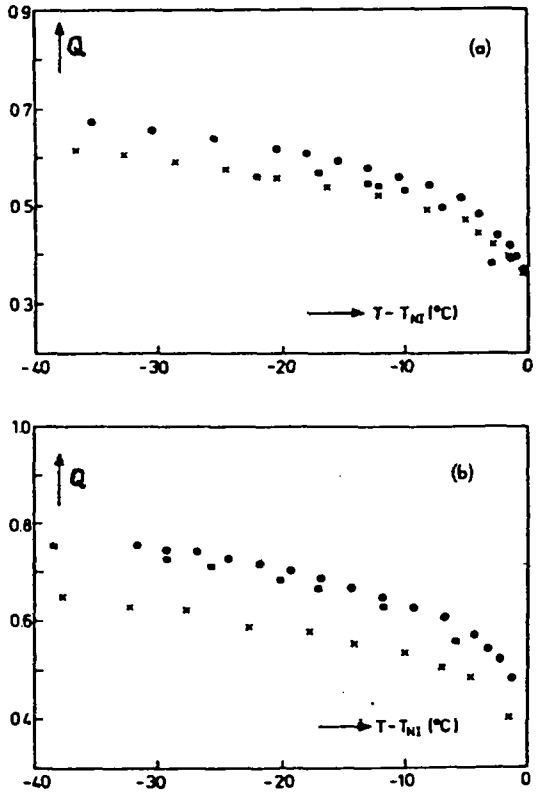

FIGURE 7 Nematic order parameter in PAA (a) and PAP (b)[44] determined by different methods: squares are proton–proton splitting, circles are para-carbon-13 chemical shift, crosses are magnetic susceptibility.

sample can vary by up to a factor of 2 according to the chosen model for the local electric field.[44] Anyway the large gap Q at the transition means (see Eq. 9) that the coefficients B and C are of the same order of magnitude, in other words, that both B and C are small.

Fitting formula (14) to the experimental temperature dependences of Q is made difficult by the fact that Q varies only weakly (~50%) within the nematic phase, a restriction which is the direct consequence of the large value of Q_{NI}. The more general form

$$Q = Q^{**} + k(T^{**} - T)^{\beta} \tag{74}$$

(with Q^{**}, T^{**}, k and β as adjustable parameters) can be successfully

fitted to the experimental data.[44–49] Unfortunately there is a large variety in the values of the effective exponent β though the most data are closer to the tricritical value β = 1/4 then to the ordinary mean-field value β = 1/2 (see Ref. 49).

A more stringent test of the Landau-de Gennes model is to compare the values of Q at T_{NI} and that at T^*. In any case the difference Q^*-Q_{NI} is found of the order of a few percent instead of 50% as predicted by Eqs. (9) and (10). This fact as well as the tricritical values of the effective exponent β in (74), obtained in many cases, can be easily explained by the smallness of the coefficient C (C ~ B << 1). If C is small the fifth and sixth-order terms in the expansion (5) must be taken into account. Thus the observable behaviour of $Q(T)$ is somewhat similar to the tricritical one.

Susceptibility

Measurements of the susceptibility χ are usually performed in the isotropic phase, where the Curie-Weiss law behaviour (18) is expected from the Landau-de Gennes theory. As pointed out by Lin Lei[50] the behaviour in the nematic phase is definitely less simple (no power law) due to the temperature dependence of the order parameter.

χ is the response of the medium to an external constraint which can be a magnetic field (Cotton-Mouton effect), an electrical field (Kerr effect) or an electrical field gradient (flexoelectrical coupling). As a consequence of the fluctuation-dissipation theorem,[2] χ can be obtained equivalently from the fluctuations of the anisotropy of the system.

Light scattering connected with the fluctuations of molecular orientation (fluctuations of anisotropy) appeared to be the most natural and reliable way for studying the susceptibility of the isotropic phase.[30,51–55] Light scattering intensity in the isotropic phase of nematics increases very much while approaching the NI transition point, resembling the critical opalescence in fluids. When approaching the NI transition temperature, the correlation length ξ increases as near critical points of fluids, though it scarcely reaches 100-120Å at $T = T_{NI}$ because of the first-order of the transition (Figure 8). Therefore the measurements of ξ in MBBA[52,53] using the "paltry" asymmetry of scattering diagram were a great experimental achievement. The temperature dependence of the measured correlation length agrees with mean-field dependence

$$\xi = \xi_0\left(\frac{T - T^*}{T^*}\right)^{-1/2}$$

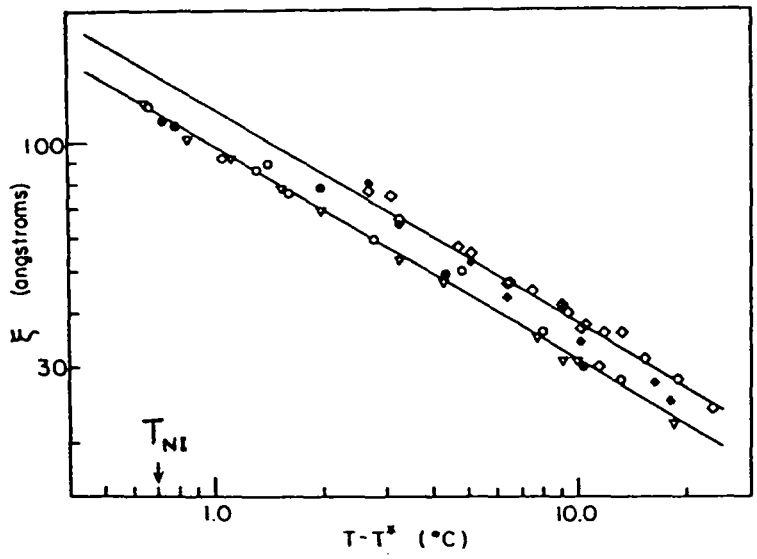

FIGURE 8 Temperature dependence of the correlation length in the isotropic phase of MBBA.[53] Upper curve represents data of Ref. 52 with the straight line denoting $\xi = (6.8 \pm 1.0)t^{-0.5}$Å. Lower curve is Ref. 53's data with $\xi = (5.5 \pm 0.2)t^{-0.5}$Å. Points of different forms correspond to different polarizations of the scattered light.

with $\xi_0 = 6 \pm 1$Å. However the temperature dependence of ξ in Ref. 52 and 53 might be determined in the narrow an interval of $(T - T^*)$ and the value of the extrapolation parameter T^* differs from that obtained from the temperature dependence of the scattering intensity.

Detailed analysis of the most accurate susceptibility measurements,[30,51-58] performed by various methods shows in all cases that in the vicinity of T_{NI} the Curie-Weiss law is violated (Figures 9 and 10). The observable effects exceed any possible systematic errors, e.g. multiple scattering. Extrapolation value of a temperature divergence of the susceptibility (T^*) strongly depends on the temperature interval and, therefore, it changes depending on the view-point of the interpretor. Thus for 8CB many different values of $T_{NI} - T^*$ were obtained: from 9.6 K[57] to 1.9 K[58]. Curvature of the temperature dependence of the inverse susceptibility may be described by Formulas (52) and (54). One can see that the main fluctuation correction, connected with the cubic term in the free energy expansion (4), is always negative.

The additional circumstances complicating interpretation of deviations from the Curie-Weiss law is the dependence of the value and

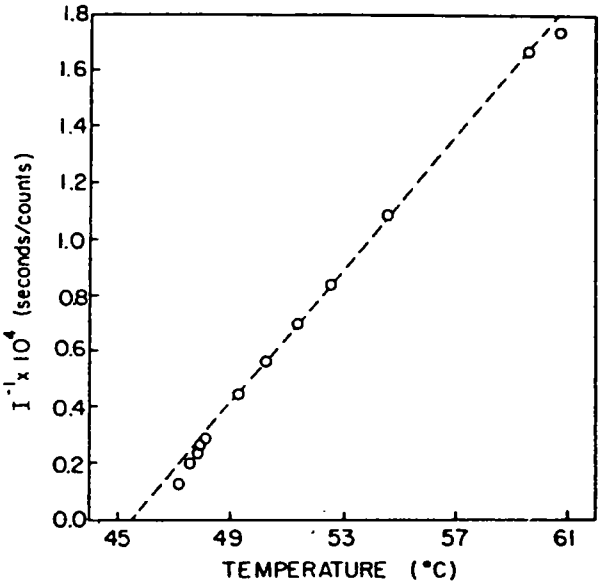

FIGURE 9 Temperature dependence of the inverse light-scattering intensity in the isotropic phase of MBBA (the angle of scattering is 21.4°).[53]

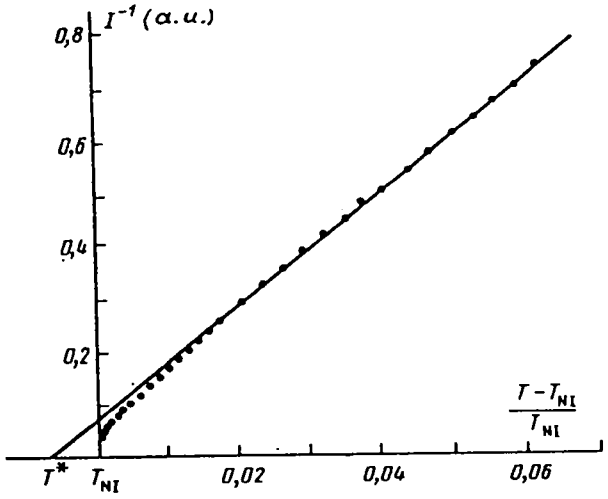

FIGURE 10 Temperature dependence of the inverse light-scattering intensity in the isotropic phase of BMOAB (the angle of scattering is 90°).[73]

the character of these deviations on the width of the nematic range (Figure 11). This effect can be connected with the coupling between orientational and translational ordering and will be discussed in Section 5.

Specific heat anomaly

The results of the early investigation[59–62] of the heat capacity anomaly near the NI transition were so contradictory that sometimes they did not allow even a qualitative interpretation. It is well known now that the widely used technique of differential scanning calorimetry (DSC), being nonequilibrium, fails to separate correctly pretransitional effects in the anomaly of the heat capacity from a diffuse δ-function which is related to the latent heat.

During recent years more accurate (and much closer to equilibrium) adiabatic calorimetry experiments in the vicinity of the NI transition were carried out[63–65] and the situation has become clearer. The results of the specific heat measurements of MBBA, BMOAB and MBBA + 3 molar % *n*-decane are shown in Figure 12. On Figure 13 the

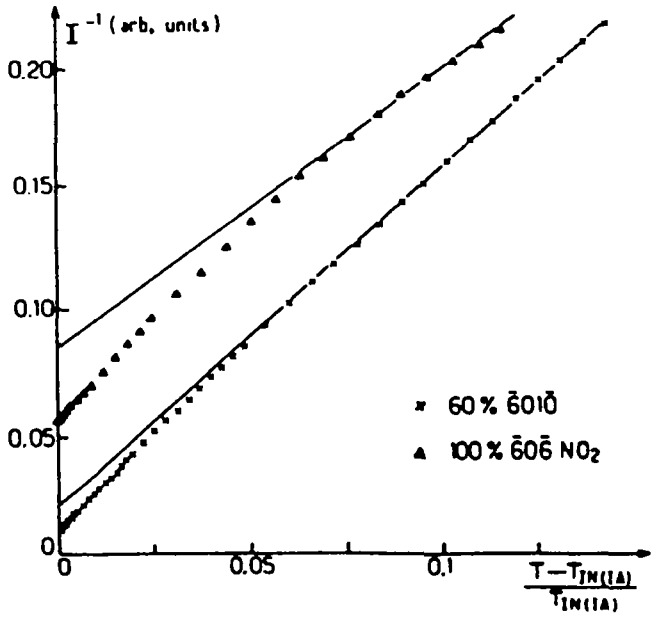

FIGURE 11 Temperature dependence of the inverse light-scattering intensity in the isotropic phase of 60% $\bar{6}01\bar{0}/\bar{6}0\bar{6}NO_2$ mixture near the NAI triple point, and that in the pure $\bar{6}0\bar{6}NO_2$ which has only AI transition.[70]

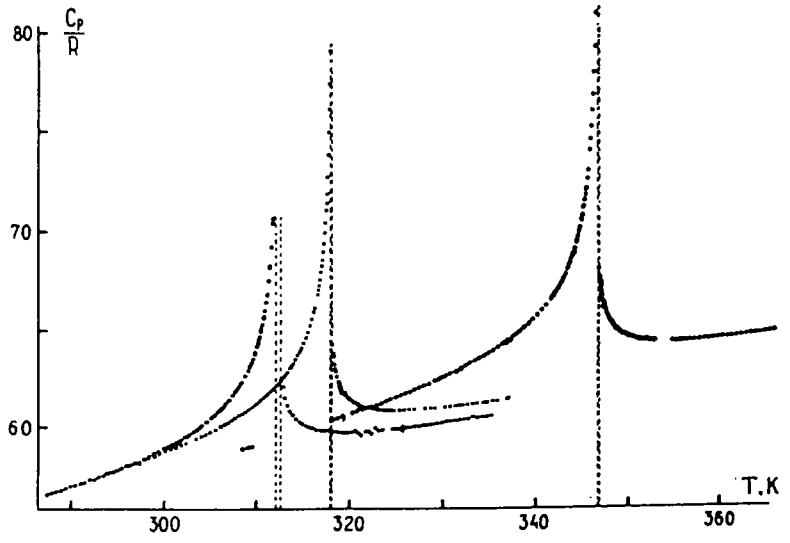

FIGURE 12 Specific heat in the vicinity of the NI transition:[63] BMOAB (filled diamonds), MBBA (crosses) and MBBA + 3% n-decane (dots).

same results in the immediate vicinity of the transition point are represented.

These results can be understood taking into account the presence of not more than 1% impurities in the pure specimen. The character of the specific heat anomaly distortion in the impure specimen depends substantially on whether the impurities are in thermodynamical equilibrium or not. In absolutely pure and uniform specimens, a δ-function in the specific heat corresponds to a first order transition point. The presence of a small amount of impurities in equilibrium converts the δ-function into a narrow trapezoid, its width depending on the concentration of impurities. The area of this trapezoid defines the latent heat of transition, which was calculated to be $\Delta H/RT_{NI} = 0.102 \pm 0.001$ for MBBA and 0.110 ± 0.001 for BMOAB. Non-uniformly distributed out of equilibrium impurities distort the δ-function in another way. Each small section of the speciment has its own beginning and end of the transition depending on impurity concentration: the δ-function is smeared out. The results may be reproducible if the relaxation time of the inhomogeneity is much larger than the duration of a measurement. For instance the value of the NI latent heat obtained by the DSC method[59] was twice the correct one.

The results of the measurements outside of the coexistence region

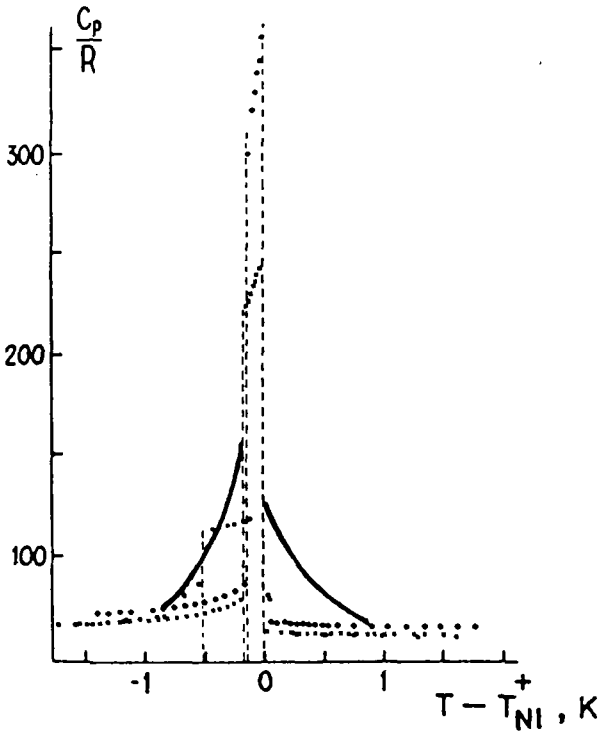

FIGURE 13 Specific heat in the immediate vicinity of the NI transition. Notations are the same as in Figure 12. Solid curve represents smearing of delta-function of C_p which was virtually observed in Ref. 60.

were fitted with the form

$$C_p/R = A_0(T/T^*)|t|^{-\alpha_{eff}} + A_1 + A_2 t + A_3 t^2 \qquad (75)$$

and by the crossover formula:

$$C_p/R = (T/T^*)(B_1|t|^{1/2} + B_2|t|^{\alpha})^{-1} + B_3 + B_4 t + B_5 t^2 \qquad (76)$$

Both yield adequate fitting. The effective exponent α_{eff} strongly depends on the range of fitting and has the value 0.3–04 for both substances in the nematic phase. Fixing α_{eff} to the mean-field value 0.5 leads to an inadequate fitting.

In the isotropic phase because of the smallness of the anomaly the result of fitting strongly depends on whether the A_3t^2 term is included or not. When it is included one may obtain the adequacy at least for BMOAB, while fixing $\alpha_{eff} = 0.5$ but the value $T - T^*$ appears to

be only 0.13°C. The crossover Formula (76) also gives good fitting of the heat capacity in the nematic as well as in the isotropic phase if α is fixed, for example, to the value of 0.1. But the term $B_1 t^{0.5}$ plays a dominant role. As in the previous case the adjusted value of $T - T^*$ is too small and in contradiction with the susceptibility measurements. One can see that the heat capacity behaviour is not simple and the obtained values of the critical exponents must probably are effective. Nevertheless if one tries to describe the nematic pretransitional behaviour using expansion (5) one could come to the value of the parameters similar for MBBA as well as for BMOAB presented in Table I.

In addition to the anomalously small value of $T - T^*$ obtained from the heat capacity measurements there is an even more important difference between the experiment and the calculations. There is no jump in the background part of the heat capacity while the theory [in the framework of expansion (5)] predicts a jump $(a^2/2C) \simeq 10R$. The real absolute jump in the heat capacity $C_p^- - C_p^+ \approx 20R$ arises from the anomalous part of the heat capacity but according to the Formulas (15) and (16) it should be twice more. The agreement between the calculations and experiment can be improved taking into account the fifth- and sixth-order terms in the Landau-de Gennes expansion:

$$F - F_0 = \frac{1}{2} a t Q^2 - \frac{1}{3} BQ^3 + \frac{1}{4} CQ^4 - \frac{1}{5} DQ^5 + \frac{1}{6} EQ^6 + \frac{1}{2} L(\nabla Q)^2 \quad (77)$$

This is understandable because the fourth-order coefficient C appears to be almost as small as the third-order coefficient B (see Table I).

TABLE I

The NI parameters of the Landau-de Gennes theory for MBBA

	Q_{NI}	$\Delta H/RT_{NI}$	$T_{NI} - T^*$ (K)	$T^{**} - T_{NI}$ (K)	A_0 ($\alpha_{eff} = 0.5$)	a	B	C
Experiment	0.4	0.1	1–2 (susceptibility) 0.13 (heat capacity)	0.24	0.68			
Calculations			1.9	0.24	0.8	1.4	0.06	0.1

Using the Formulas (8,9,12,15,16,17)

Using the values of the constants a, B, and C given in Table I and taking into account the sixth-order term in the expansion (77) one can sufficiently improve the description of the heat capacity in the nematic phase and eliminate the jump ~ 10R in the background. To determine the sixth-order coefficent E the amplitude of the anomalous part of C_p was used as an additional initial parameter. The best value of E appears to be 0.33.†

If (for the pretransitional part of the heat capacity in the isotropic phase) the exponent α_{eff} is fixed at the mean-field value of $\alpha = 0.5$, one can calculate the bare coherence length ξ_0 [see Formula (48)]. It appears to be 5.6 A which is in good agreement with the results of the light scattering measurements ($\xi_0 = 6 \pm 1$ Å if one chooses $\nu = 0.5$ and $\alpha = 0.5$). As a matter of fact one can determine the mean-field value $\nu = 0.5$ and $\alpha = 0.5$ with the same accuracy as for the Curie-Weiss law of susceptibility. Both of them are not punctual and the scaling relation $2 - \alpha = 3\nu$ is not satisfied. At the same time the fundamental relation between the susceptibility and the heat capacity (see Ref. 85 and Eq. 61) appears to be justified (Figure 14):

$$\delta C_p = (nRT^2 v_0 a^{-3/2}/16\pi\ \xi_0^3)\ (\partial\chi^{-1}/\partial T)^2\ \chi^{1/2} \qquad (78)$$

where n is a number of fluctuating modes, $n = 5$ in the isotropic phase. When $\chi^{-1} = at$ Eq. (78) transforms to Eqs. (48).

The smallness of the coefficient C explains so-called "tricritical hypothesis."[49,63-66] Indeed, the NI transition behavior looks like that near tricritical points where $C = 0$. Closeness of the effective exponent β in Formula (74) to the tricritical value 0.25, obtained in many cases, also reflects the essential role of the sixth-order term in describing the temperature dependence of the order parameter. Therefore the "tricritical behavior" of the heat capacity only indicates the necessity of taking into account the sixth-order term in the free energy expansion.

In Ref. 30 the approximation of the susceptibility as well as the heat capacity in the isotropic phase of BMOAB by Eqs. (54) and (55) was carried out using a unified set of the constant. Peculiarity of their adjustment was the negative (and small) value of the coefficient C. The temperature dependence of the order parameter was approximated well with the same constants. However the description

†The fifth-order coefficient D was assumed to be equal to zero.

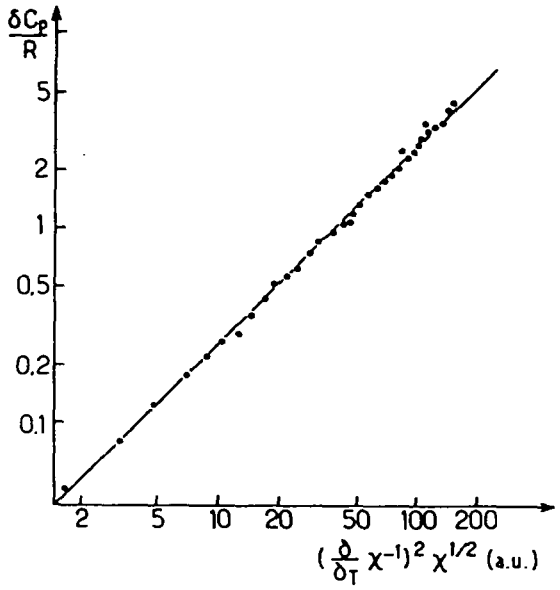

FIGURE 14 *Test of the relation (78) between excessive specific heat and susceptibility in the isotropic phase of BMOAB.*[77]

of the heat capacity in the nematic phase required another set of constants. One should note that in the vicinity of the NI transition $CQ^4 \sim EQ^6$, i.e. the experiment is carried out in the range of crossover from the tricritical-like behaviour to the critical or to the usual mean-field one. Probably in this range all the terms of the expansion (77) beginning with CQ^4 have the same order of magnitude. Therefore coordination of all the physical properties could require more and more expansion terms, and the description would become especially empirical.

Influence of non-mesogenic impurities to NI transitions

Additions of impurities to the initial pure nematic leads to broadening of the NI transition and appearance of a two-phase region. This effect is important from an experimental viewpoint since all real nematics contain impurities. The impurities which do not form a mesophase usually decrease the NI transition temperature. For small concentration of impurities a phase diagram has the form presented in Figure 15. Depression of the NI transition temperature is connected with

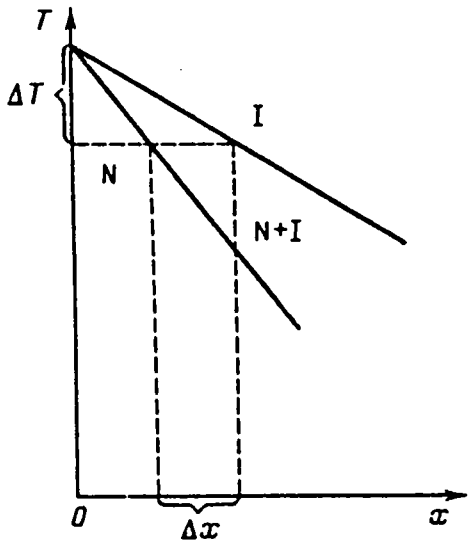

FIGURE 15 Phase diagram of a dilute solution of a nonmesogenic substance in a nematic liquid crystal.

the width of the two-phase region and the latent heat of the transition:[2,67]

$$T^0_{NI} - T_{NI} \approx \Delta x (RT^0_{NI}) \Delta H^{-1}_{NI} \tag{79}$$

where T^0_{NI} is the temperature of the NI transition in a pure specimen.

The NI transition latent heat in BMOAB was calculated in Ref. 64 using the parameters of the BMOAB-*n*-heptane phase diagram. The calculated value $\Delta H_{NI}/RT_{NI} = 0.12 \pm 0.02$ agrees with the result of the calorimetric measurements $\Delta H_{NI}/RT_{NI} = 0.110 \pm 0.001$.

Phase diagrams at large impurity concentrations (Figure 16) substantially differ from that presented in Figure 15. Their form is determined by two factors: 1) anomalously small values of the coefficients B and C in expansion (77), 2) nonideality of the mixture. The smallness of B means that the transition is close to a second order. In the case of $B = 0$ nonideality of the solution may lead to the appearance of a tricritical point due to the coupling between the order parameter and concentration.[10] Below the tricritical point the stratification of the mixture occurs. If the transition in a mesogenic solvent is very near to tricritical point ($C << 1$), the phase diagram for a dilute solution has the form presented in Figure 17. In the case of

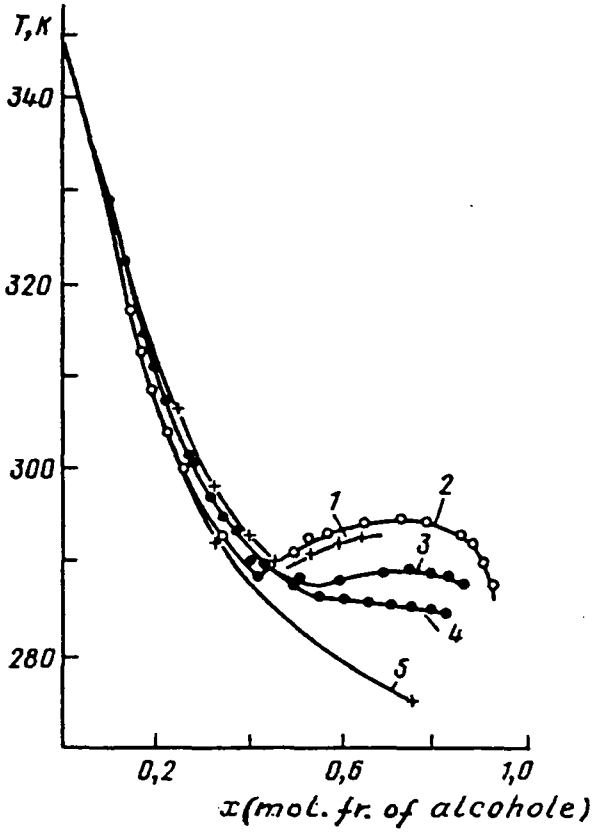

FIGURE 16 Clearing temperatures for BMOAB-alcohol mixtures:[67] propylalcohol (1), isopentylalcohol (2), butylalcohol (3), pentylalcohol (4), dethylalcohol (5).

C = 0 the width of a two-phase region[67]

$$\Delta x \sim x^2,$$

otherwise in the ordinary case

$$\Delta x \sim x.$$

Estimates[67] show that at C ~ 0.1, the contribution of x^2—term to the phase diagram is the same as the linear one when $x \sim 0.1$. For understanding the character of the phase diagram of nematic-non-mesogenic mixtures one should take into account the nonideality of

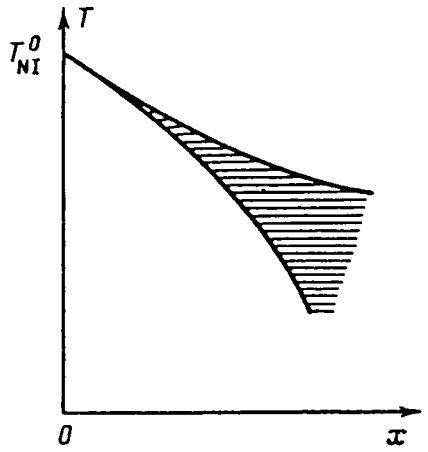

FIGURE 17 Phase diagram of a dilute solution in the case of tricritical behavior for the pure solvent.

the mixture, which may lead sometimes to the phase separation in the isotropic phase (Figure 18). It is interesting to note that the critical behaviour near the liquid–liquid equilibrium critical point in the such mixture ($\alpha = 0.11$[65,67]) is equivalent to that in simple fluids.

5. INFLUENCE OF SMECTIC FLUCTUATIONS TO THE PRETRANSITIONAL BEHAVIOUR IN THE ISOTROPIC PHASE

The neighbourhood of a smectic phase has a noticeable influence on the pretransitional phenomena in the isotropic phase. This influence is manifested in the following effects:

1) the "background" part of the heat capacity increases when the width of the nematic range decreases,

2) the narrower the width of the nematic range the larger the deviations from the Curie-Weiss law for the susceptibility,

3) the latent heat of the NI transition increases on approaching the NAI triple point, though the jump of the nematic order parameter does not change essentially.

These effects are closely connected with the infinite number of possible characteristic wavevectors for the smectic density wave in the isotropic phase (Brazovskii[40]). Therefore the divergent contribution to the entropy and, hence, to the heat capacity appears (see Formula 63). The temperature of the divergency T_{AI}^{*} lies much lower

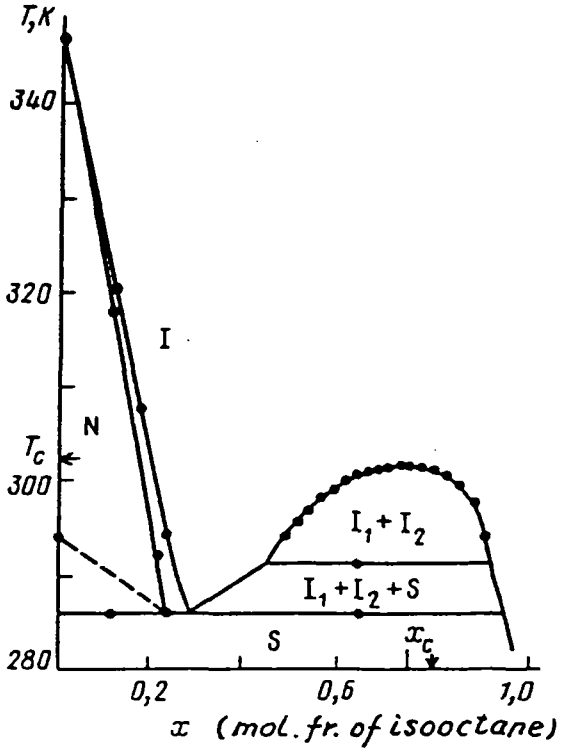

FIGURE 18 Phase diagram of BMOAB-isooctane mixture.[67] T_c and x_c correspond to the isotropic liquid–liquid critical point.

than the NI transition temperature. So the anomaly (63) can be considered as an addition to the background of C_p in the isotropic phase. Experiment[68] shows that such an addition really exists.

Furthermore, the smectic fluctuations in the isotropic phase result in the renormalization of the character of the smectic fluctuations and change the temperature dependence of the susceptibility[36,38] (see Section 3).

The expression (59) for the renormalized susceptibility and the expression (61) for the heat capacity qualitatively agree with the experiment. What is more, the results of the experiment and calculation can be coordinated for each individual case.[36] However such an agreement should not be overstated. The constants included in Formulas (59–61) are adjustable when fitting the experiment. One cannot be sure that the influence of the smectic fluctuations is the only effect that leads to the departures from the Curie-Weiss law for the susceptibility and from the root divergence for the heat capacity.

Results of the theoretical investigation of the influence of the nematic fluctuations on the susceptibility and the heat capacity in the isotropic phase[30] show that the corresponding deviations have the same character and the same order of magnitude. Therefore accurate division of the effects properly related to the NI transition and the effects dependent on the existence of the smectic phase should precede the quantitative analysis. Thus for example, Zink and de Jeu[69] stated their opinion on the basis of the interpretation of the light-scattering study in the homologous nCB series that there was no noticeable correlation between the departures from the Curie-Weiss law and the nearness of the smectic phase.

In view of this result it was interesting to carry out an experiment in a mixture of two liquid crystals. One component should have the AI transition. Thus the possible even-odd effects would be eliminated. In Refs. 70–73 the results of the accurate light scattering study of $\bar{6}O\bar{6}NO_2$-$\bar{6}O1\bar{0}$, $\bar{6}O\bar{8}$-$\bar{6}O1\bar{0}$, $\bar{6}O1\bar{0}$-$\bar{6}O1\bar{2}$ mixtures as well as of pure BMOAB, 8CB and 9CB are presented (See Figures 19 and 20). Noticeable deviations from the Curie-Weiss law were observed everywhere (Figure 21). One could merely compare the amplitudes of these deviations at the same distances from the transition temperature for the different samples.[69] But this way is not quite correct. The first order character of the NI and, especially, AI transitions depends on

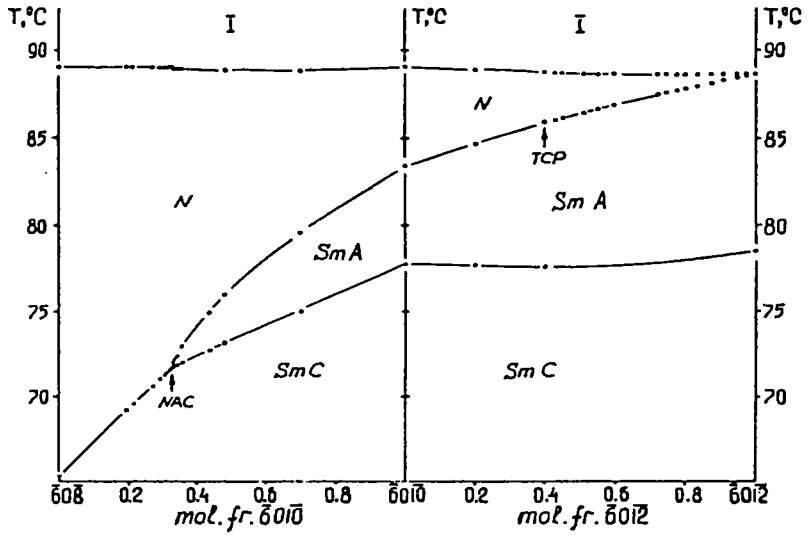

FIGURE 19 Phase diagram of $\bar{6}O\bar{8}$–$\bar{6}O1\bar{0}$–$\bar{6}O1\bar{2}$ mixtures.

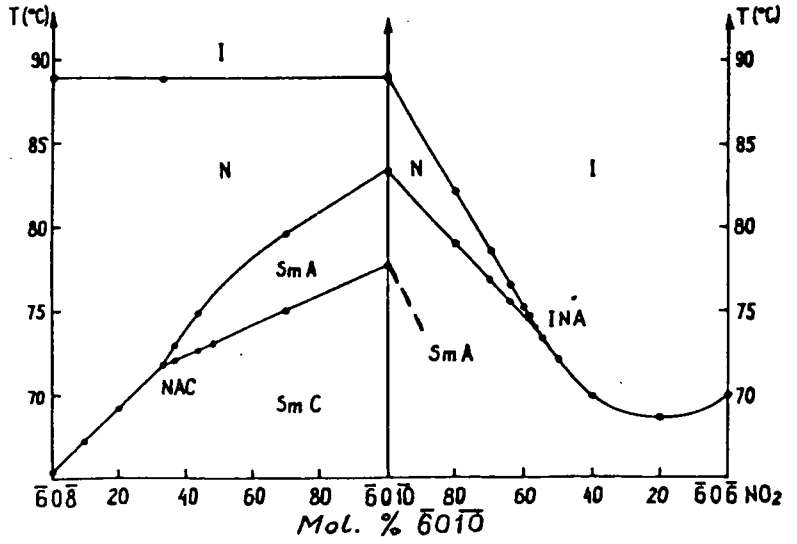

FIGURE 20 Phase diagram of $\bar{6}O\bar{8}$–$\bar{6}O\bar{10}$–$\bar{6}O\bar{6}$ NO_2 mixtures.

the mixture concentration and, e.g., that is much stronger for $\bar{6}O\bar{6}NO_2$ than for $\bar{6}O1\bar{0}$. Therefore the different samples in the phase transition point are at different distances from the absolute stability limit of the isotropic phase. So the effective departures from the Curie-Weiss law increase when one moves from $\bar{6}O1\bar{1}$ to $\bar{6}O\bar{6}$ NO_2 (Figure 22). Moreover fitting the temperature dependence of the susceptibility by the empirical formula

$$\chi^{-1} \sim \frac{T}{I} = A\, t^{\gamma} \tag{80}$$

where γ is an effective exponent which characterizes the curvature of the inverse light scattering intensity I, showed that γ decreased while approaching the transition point. Indeed, there is a suspicion that the temperature of the intensity curves over the entire experimental range of temperature. The data were fitted by Eq. (80) in two temperature ranges:

a) "wide range" was from $t = 0.01$ up to $t = 0.1$
b) "asymptotic range" was $t \leq 0.01$.

The effective exponent behaviour is shown in Figure 23. The value of γ in the "wide range" for the liquid crystals with various nematic

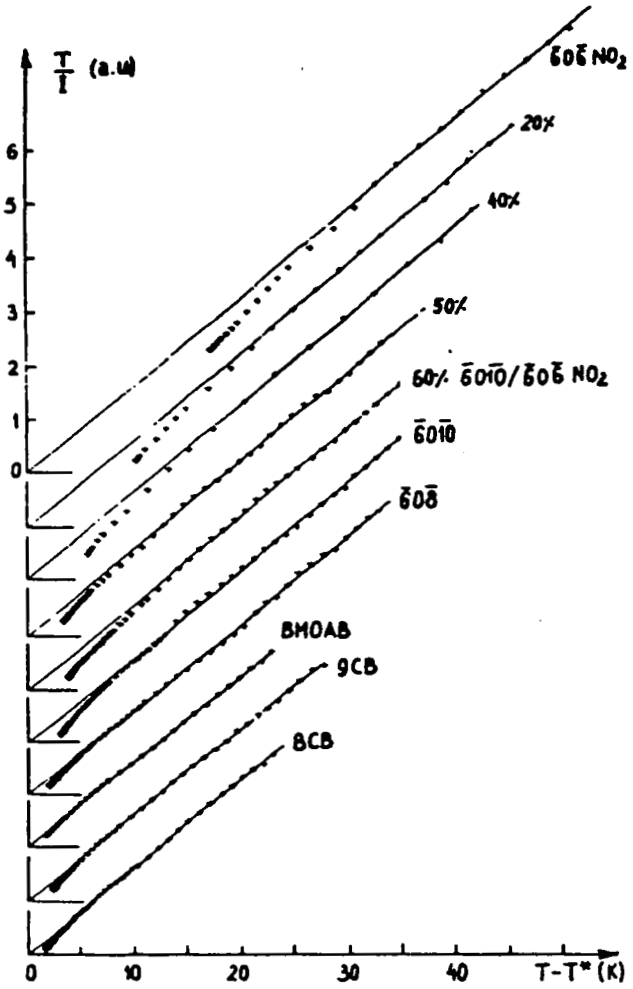

FIGURE 21 Inverse light-scattering intensity for the set of liquid crystals and liquid crystalline mixtures.[71]

ranges changes slightly and it is about 0.9. But the result of data fitting in the "asymptotic range" exhibits the influence of the smectic phase. The effective exponent γ has a sharp minimum close to the NAI point for the mixture $\bar{6}O\bar{6}NO_2/\bar{6}O\bar{1}\bar{0}$. The effective exponents of 8CB and 9CB are close to those of the mixture $\bar{6}O\bar{6}NO_2/\bar{6}O\bar{1}\bar{0}$ at the same nematic ranges. The value of the scattering intensity at the transition points, normalized to the amplitude A is also shown in Figure 23.

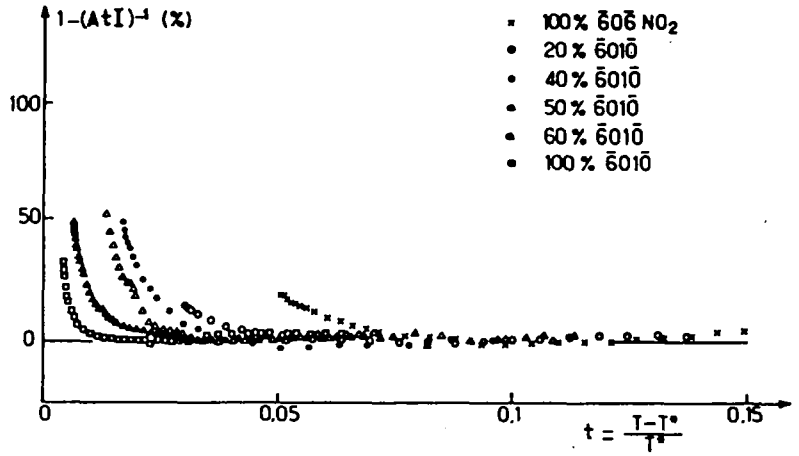

FIGURE 22 Relative deviations of the inverse light-scattering intensity from the linear law.[70,71]

It characterizes the first-order "power" of the transition. We can see from the figure that this value (B) increases rapidly for the AI transition upon moving away from the INA point. The experimental data for the crystals with narrow nematic range are quantitatively

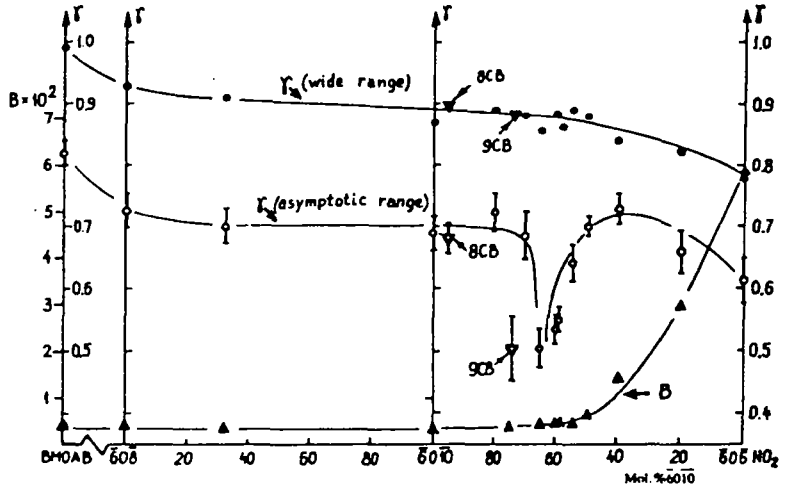

FIGURE 23 Effective curvature (circles) of the temperature dependence of the inverse light-scattering intensity and the first-order power (triangles) for the NI and AI phase transitions.[71] Inversed triangles are related to values of γ for 8CB and 9CB at the same nematic ranges.

described in the framework of the theory of a coupling between the nematic and smectic fluctuations.[36,38] In Refs. 71–73 the light scattering data were fitted by the simplified equation (59) taking into account the main correction term

$$\frac{T}{aI} = \frac{T - T^*_{NI}}{T^*_{NI}} - \frac{B^2_{Q\psi}\, T^{*3/2}_{NI}}{(T - T^*_{NI} + \Delta)^{3/2}} \tag{81}$$

where $\Delta = T^*_{NI} - T^*_{AI}$

This physically justified equation satisfies the experimental data in all temperature ranges. It has an obvious advantage as compared to the empirical formula (80) in which the effective exponent γ is really dependent upon temperature. In Eq. (81) $B_{Q\psi}$ determines the magnitude of the deviations from the linear law while $T - T^*_{NI} + \Delta$ characterizes the increase of the curvature upon approaching the transition point. The smaller Δ, the larger the curvature. The evolution of the parameter Δ for the $\bar{6}O\bar{6}NO_2/\bar{6}O\bar{1}0$ and $\bar{6}O\bar{8}-\bar{6}O1\bar{0}-\bar{6}O\bar{1}2$ mixtures is shown in Figure 24. One can note that the region of the small values of Δ corresponds to the small values of γ (see Figure 23). It is remarkable that negative values of Δ were obtained for the AI transition, which means that the bare absolute stability limit of the isotropic phase for AI transition is higher than that for the NI one. Increase of the NI transition latent heat near the triple NAI point can also be explained by a change of the character of the smectic fluctuations in the isotropic phase as compared to the nematic one.[74] The entropy of the N-phase is lower than the entropy of the I-phase:

$$S_I - S_N = \int_{T_{NI}}^{T_0} \delta C_p dT + (\Delta S_{NI})_0 \tag{82}$$

In Eq. (82) C_p is the anomalous (fluctuational) part of the heat capacity in the N-phase near the NA transition:

$$C_p \sim |T - T_{NA}|^{-\alpha} \tag{83}$$

$(\Delta S_{NI})_0$ is a bare entropy jump. The anomaly is absent when $T > T_{NI}$. Quantitative estimates are difficult here since one should set the definite form of the temperature dependence of the heat capacity related to the smectic fluctuations in the nematic phase and choose correctly the upper integration limit T_0 in Eq. (82). This is the temperature at which the smectic fluctuation contribution should be used up even in lack of the NI transition. The other reason of changing the entropy of the isotropic phase due to the Brazovskii

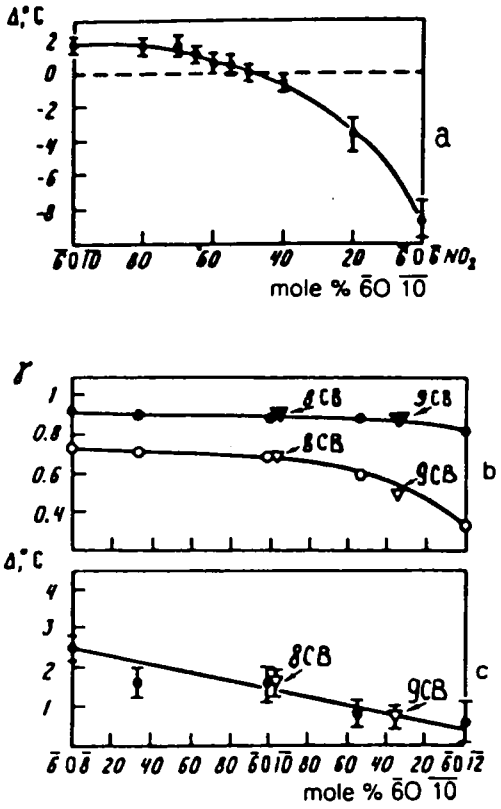

FIGURE 24 (a) The evolution of the bare nematic–smectic gap in the $\bar{6}O\bar{1}\bar{0}$–$\bar{6}O\bar{6}NO_2$ mixture.[71]
(b) Effective curvature for the $\bar{6}O\bar{8}$-$\bar{6}O1\bar{0}$–$\bar{6}O1\bar{2}$ mixture.[72]
(c) The evolution of the bare nematic–smectic gap in the $\bar{6}O\bar{8}$–$\bar{6}O1\bar{0}$–$\bar{6}O1\bar{2}$ mixture. Notations see at Figure 23.

effect is apparently less essential since the temperature of divergence of the smectic fluctuations in the isotropic phase T^*_{AI} is much lower than T_{NA}. Qualitative (order of magnitude) estimates performed for a number of substances[74] agree with the experiment.

6. UNIVERSALITY OF CRITICAL DYNAMICS IN THE VICINITY OF THE NI PHASE TRANSITION

Sound absorption and dispersion are homogeneous functions

The Ni phase transition belongs to a dynamic universality class different from that relevant to critical points in fluids. The nematic order

parameter is not conserved. The characteristic relaxation time depends on the susceptibility χ and effective "viscosity" η:

$$\tau = \chi\eta \tag{82}$$

while in fluids the critical relaxation time depends on the space scale:

$$\tau_q^{-1} = 2Dq^2 \tag{83}$$

(q is a wave vector; at $q << \xi^{-1}$, $D = \dfrac{kT}{6\pi\eta\xi}$).[84]

Recently the nature of the critical dynamics near the NI transition was cleared up in details with the help of acoustic relaxation investigations[75,76] (see also Ref. 77). A quantitative agreement between dynamics and statics was shown to hold. It is important that no assumptions connected with the nature of pretransitional behaviour of the equilibrium properties were used. In particular the temperature of the susceptibility singularity T^* was never used as an adjustable parameter. The following questions were posed:

1) Are there homogeneous functions of variables ω (frequency) and τ (relaxation time) which describe the acoustic relaxation in the isotropic as well as in the nematic phase?

2) Have these functions (if they exist!) a universal form?

3) What restrictions to the transitional behaviour of the statics are imposed with the universality of the dynamics?

Two substances were investigated, MBBA and BMOAB, because accurate heat capacity measurements were performed for them previously. Experimental data for sound absorption and velocity are presented in Figures 25, 26 and 27. Both the excess sound absorption and sound velocity dispersion were found to be homogeneous functions of ω and τ in the iosotropic as well as in the nematic phase (Figures 28 and 29):

$$1 - (u/u_\infty)^2 = A(\tau)\phi_1(\omega\tau) \tag{84}$$

$$\alpha_s\lambda = \pi A(\tau)\phi_2(\omega\tau) \tag{85}$$

where u_∞ is the velocity of sound extrapolated to $\omega \to \infty$, it is a regular function, λ is the sound wave length. The dispersion of sound velocity and the absorption are determined by the real and imaginary parts

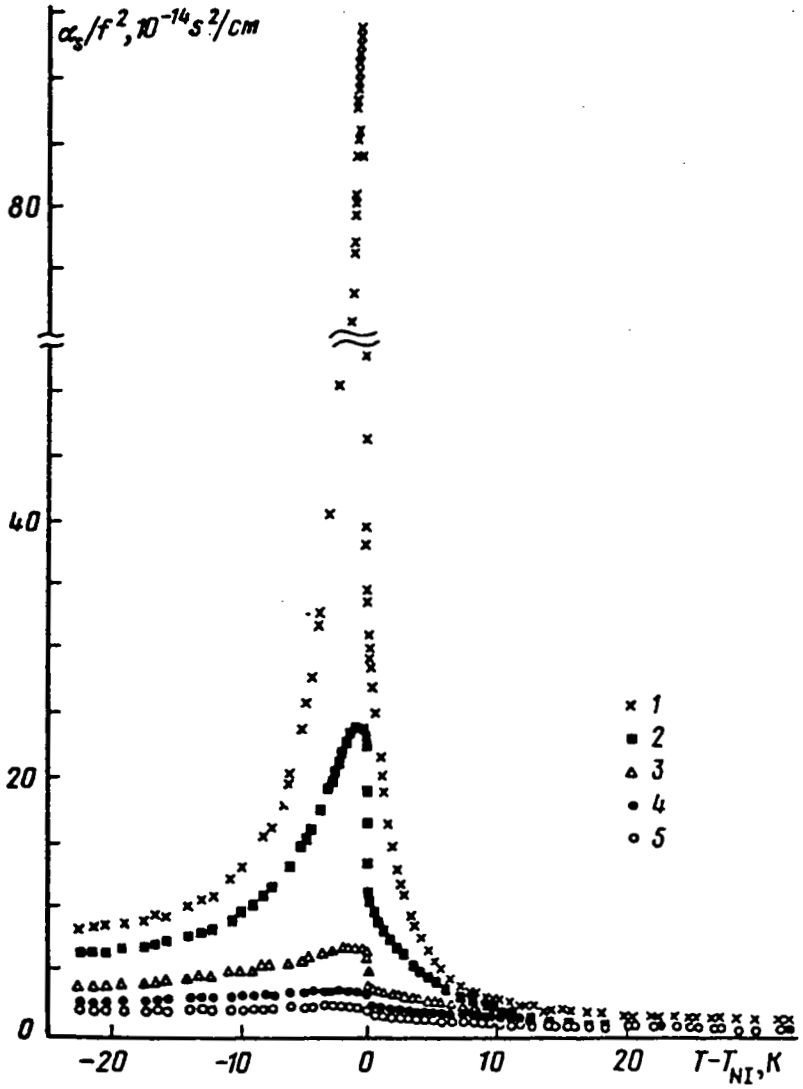

FIGURE 25 Sound absorption in MBBA near its NI transition:[76] $f = \omega/2\pi$ (1–5 notations correspond to f = 1.5, 3.8, 9.4, 15.1, and 20.9 MHz)

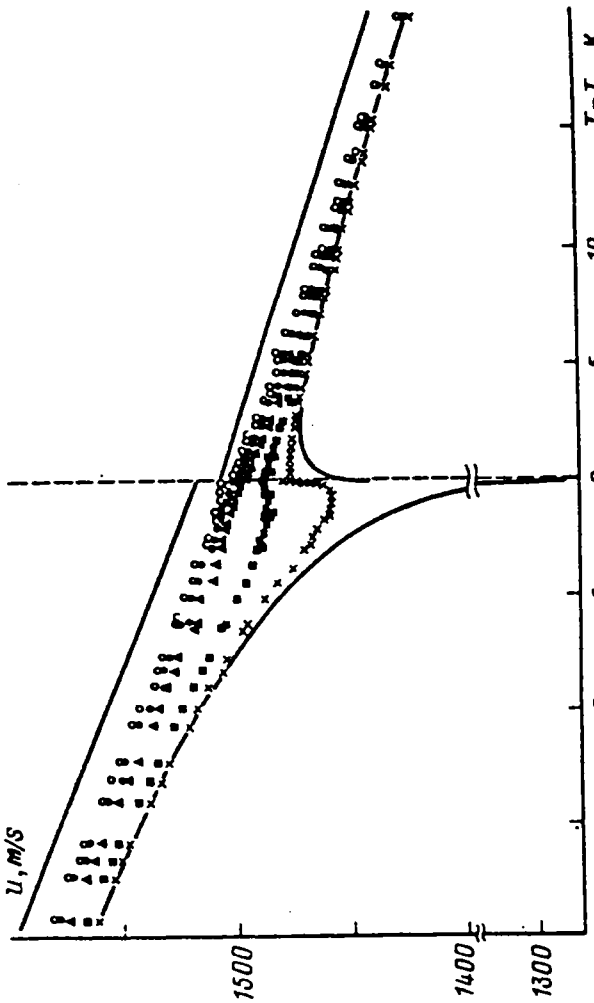

FIGURE 26 Sound velocity in MBBA near its NI transition.[76] Lower and upper solid lines correspond to the thermodynamical ($\omega = 0$) and extrapolated to $\omega = \infty$ sound velocity. Notations are the same as in Figure 25.

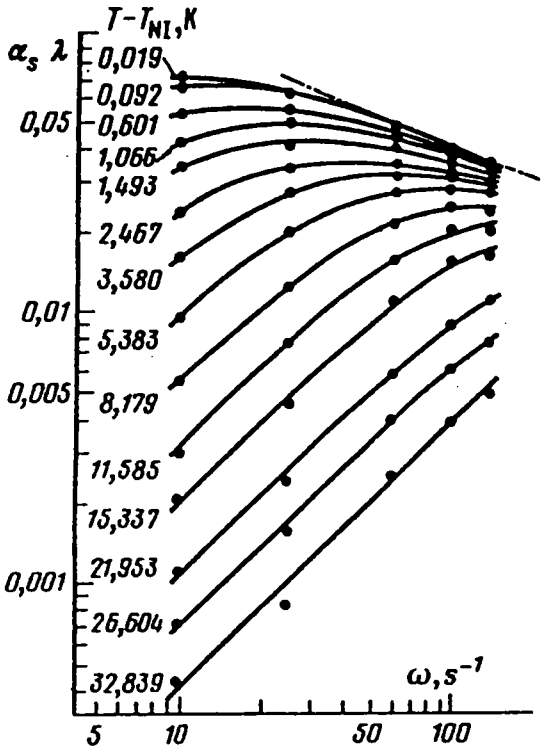

FIGURE 27 Excess sound absorption in the isotropic phase of MBBA. Slope of the dashed line corresponds to the value of $y = 0.4$ which is nonasymptotic and probably should increase up to 0.5 in a high frequency limit.

of the complex adiabatic compressibility $\bar{\beta}_s$

$$\bar{u}^2 = u_\infty^2 - \Delta\bar{u}^2 \tag{86}$$

where

$$\bar{u}^2 = (\rho\bar{\beta}_S)^{-1}$$

$$\mathrm{Im}(\Delta\bar{u}^2/u_\infty^2) = \alpha_s\lambda/\pi \tag{87}$$

$$\mathrm{Re}(\Delta\bar{u}^2/u_\infty^2) = 1 - (u/u_\infty)^2 \tag{88}$$

In the nematic phase the pretransition absorption and dispersion are determined by at least two mechanisms: the relaxation of the

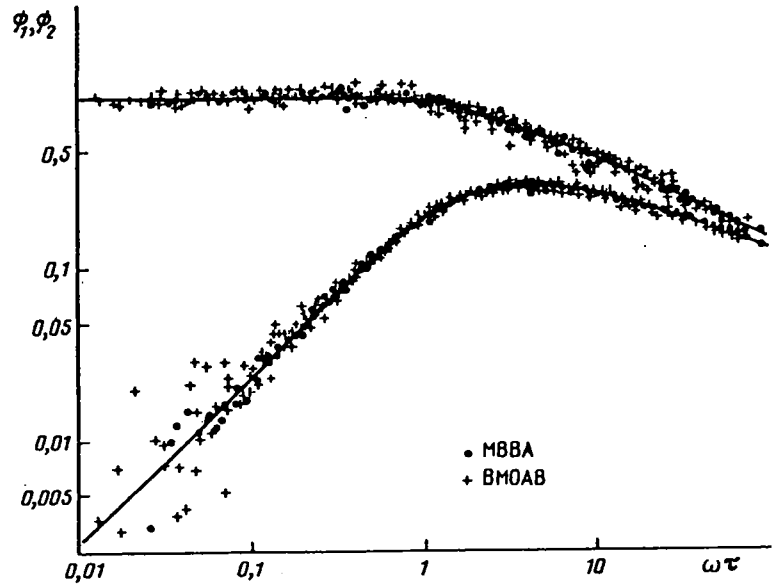

FIGURE 28 Universal scaling functions ϕ_1 and ϕ_2 for the isotropic phase of MBBA (circles) and BMOAB (crosses). The continuous curves represent the Imura-Okano functions given by Eqs. (107).

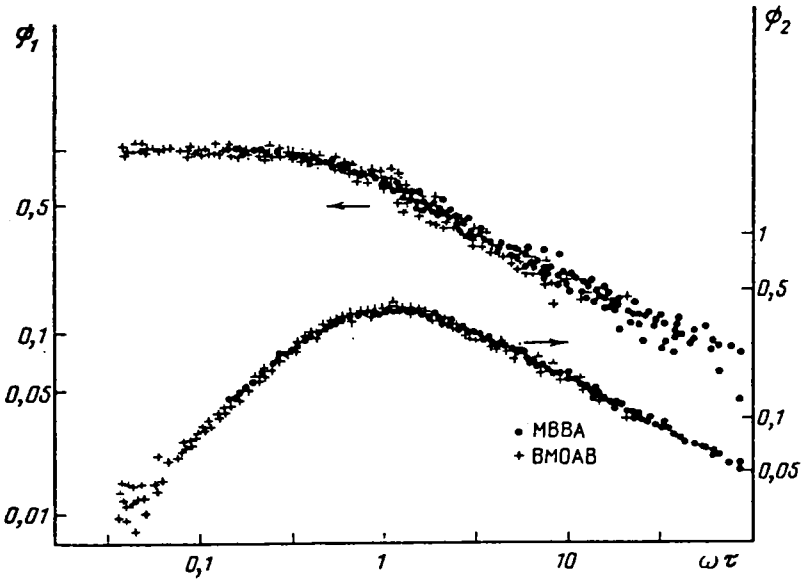

FIGURE 29 Universal functions ϕ_1 and ϕ_2 for the nematic phase of MBBA (circles) and BMOAB (crosses). The scales for ϕ_1 and ϕ_2 are shifted relative to one another to avoid crossing.

order parameter and the relaxation of the order parameter fluctuations. In the isotropic phase only the fluctuation mechanism exists.

Mean-field approximation

In the mean-field approximation[78]

$$\Delta\overline{u}^2(\omega\tau) = A_1(T)F_1(x) + A_2(T)F_2(x) \tag{89}$$

where $x = i\omega\tau$

$$F_1(x) = (1 + x)^{-1} \tag{90}$$

$$F_2(x) = (x/2)^{-1/2}[(2/x - 1)^{-1/2} - (2/x)^{1/2}] \tag{91}$$

$$A_1(T) = (\partial P/\partial Q)_S(\partial Q/\partial \rho)_S \tag{92}$$

$$A_2(T) = 1/32\pi(\partial^2 P/\partial Q^2)_S(\partial \chi^{-1}/\partial \rho)_S \nu_0 L^{-3/2} \tag{93}$$

The approximate expressions of $A_1(T)$ and $A_2(T)$, if calculated with the Landau-de Gennes expansion (77), have the form

$$A_1(T) = \frac{\partial Q}{\partial T}\frac{\partial}{\partial T}\left(\frac{\partial F}{\partial Q}\right) \tag{94}$$

$$A_2(T) = g\left[\frac{\partial}{\partial T}(\chi^{-1})\right]^2 RT(\chi^{-1}a^{3/2})^{-1/2}\frac{\nu_0}{32\xi_0^3} \tag{95}$$

where g is a constant.

The first term in the expression (89) is connected with the relaxation of the order parameter,[78,79] the second is connected with the relaxation of the correlation function and is proportional to the fluctuation part of the heat capacity.[80] The conditions of the homogeneity are satisfied only if the temperature dependence of the functions $A_1(T)$ and $A_2(T)$ is identical. It is easy to see that the forms of the functions $A_1(T)$ and $A_2(T)$ are determined by the fine interplay of the coefficients of the expansion (77). The identical temperature dependence of $A_1(T)$ and $A_2(T)$ exists only with a special choice of the values of the coefficients (e.g. $B = C = D = 0$). An attempt was made in Ref. 76 to bring the acoustic and calorimetric data to coincidence in the nematic phase of MBBA using just the same (as in Section 4) set of the coefficients of the expansion (77) with account of the sixth-order term: $a = 1.4$, $B = 0.06$, $C = 0.1$, $D = 0$, $E = 0.33$, $\xi_0^2 =$

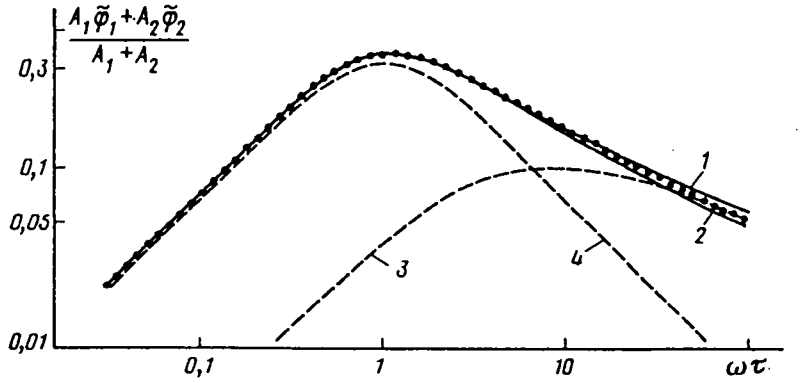

FIGURE 30 Results of calculation of the sound absorption functions for the nematic phase of MBBA in the mean-field approximation while using Eqs. (89–91, 94 and 95). Here $\tilde{\phi}_1 = \mathrm{Im}F_1$ and $\tilde{\phi}_2 = \mathrm{Im}F_2$: (1) $T_{NI} - T = 0.1K$, (2) $T_{NI} - T = 1.0K$, (3) $A_2\mathrm{Im}F_2$ for $T_{NI} - T = 0.1K$, (4)$A_1\mathrm{Im}F_1$ for $T_{NI} - T = 0.1K$. The points represent the experimental behaviour.

36 Å.[2] One can see on Figure 30 that the violation of the homogeneity is small and in general is of the same order of magnitude as the error of the description of the equilibrium properties. Perhaps taking into account the next terms of the perturbation theory and varying the new adjustable parameters one can succeed to bring into agreement quantitatively all the experimental data including the temperature dependence of the order parameter. But this way seems to be rather artificial and at least impractical.

It is not likely that the homogeneity found experimentally for the two substances, which is indeed a universal property of the NI transition, is the result of a random (and fairly fine) interplay of constants. Moreover, it is worth noting the large value of the fluctuation contribution to the properties of the nematic phase: A_2/A_1 varies from 0.2 for $T_{NI} - T = 15K$ to 0.33 for $T_{NI} - T = 0.1K$. At high frequencies the fluctuation mechanism is practically the only one, because $\lim_{x\to\infty} F_1(x) \sim x^{-1}$ and $\lim_{x\to\infty} F_2(x) \sim x^{-1/2}$. Estimates of Ginzburg criterion, made in Section 3, show that in the vicinity of the NI transition one could expect the crossover from mean-field behavior to critical.

Dynamic scaling

Therefore a more natural representation of the experimental results can be obtained in the scaling form[81]:

$$\Delta\bar{u}^2/u_\infty^2 = \tau^\nu\psi(x) \tag{96}$$

where

$$y = \alpha/z$$

α and z are the critical exponents of the heat capacity and relaxation time correspondingly.

In the hydrodynamic regime ($x << 1$)

$$\psi(x) = \psi(0) + \psi'(0)x + \frac{1}{2}\psi''(0)x^2 + \ldots. \tag{97}$$

$$(u_\infty^2 - u^2)/u_\infty^2 = \mathrm{Re}(\Delta\bar{u}^2/u_\infty) = \tau^y\left[\psi(0) - \psi'(0)\frac{\omega\tau}{2}\right] \tag{98}$$

$$\frac{1}{\pi}\alpha_s\lambda = \mathrm{Im}(\Delta\bar{u}/u_\infty) \approx \tau^y\psi(0)\omega\tau \tag{99}$$

In the critical regime ($x >> 1$)

$$\psi(x) = A_\infty x^{-y} \tag{100}$$

$$(u_\infty^2 - u^2)/u_\infty^2 = A_\infty\omega^{-y}\cos(\pi y/2) \tag{101}$$

$$\alpha_s\lambda/\pi = A_\infty\,\omega^{-y}\sin(\pi y/2) \tag{102}$$

One can see that according to dynamic scaling the asymptotic behaviour of the absorption and dispersion in the hydrodynamic as well as in the critical regime is determined by the same critical exponent y and in the limit $x \to \infty$ the relation of the dispersion to the absorption tends toward constant value:

$$\begin{aligned}(u_\infty^2 - u^2)/u_\infty^2\alpha\lambda &= \mathrm{Re}\,\psi(x)/\mathrm{Im}\psi(x)^{y^-} \\ &= \phi_1(\omega\tau)/\phi_2(\omega\tau) = ctg(\pi/2)y\end{aligned} \tag{103}$$

One can see in Figures 28 and 29 as well as in Figures 27 and 31 that both predictions of the scaling theory are justified. The value of the critical exponent y is near the mean-field result $y = 0.5$ (Table II). The value of the ratio is $\phi_1/\phi_2 = 1 \pm 0.2$ for both substances in both phases. It is remarkable that the experimental value $y \approx 0.5$ is near the mean-field prediction while the pretransition behaviours of both the heat capacity and the susceptibility do not have the pure mean-field exponents (the effective critical exponents $\gamma < 1$ and $\alpha < 0.5$, see Section 4).

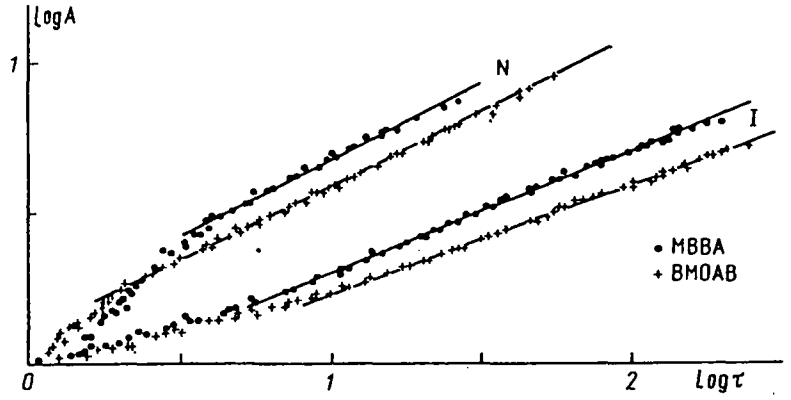

FIGURE 31 Asymptotic behaviour of the critical aplitude of the sound absorption in both phases of MBBA and BMOAB in the hydrodynamic regime. Comparing Eqs. (85) and (99) one can see that $A(T) = \psi(0)\tau^{y}$.

The values of the critical exponents demand the adjustable parameter T^* for the extrapolation and can be considered to be effective but not true. Only the choice of the relaxation time as a scale instead of the temperature leads to the discovery of the true exponent behaviour.

The scaling description seems to be attractive in that at least it allows one to avoid the large number of adjustable parameters of the expansion (77). It is worth noting only that the critical exponent y is close to the mean-field (more strictly to Gaussian) value 0.5.

Explicit form of functions describing acoustic relaxation (relaxation time, critical amplitudes, universal functions)

If one supposes that the effective "viscosity" in Eq. (82) has the same temperature dependence as the shear viscosity:

$$\eta = \eta_0 \exp(\theta/T) \tag{104}$$

where $\theta = 4200K$, then the relaxation time calculated from the For-

TABLE II

Experimental values of critical exponent y ((*) nonasymptotic values)

	Isotropic phase		Nematic phase	
	MBBA	BMOAB	MBBA	BMOAB
$\omega\tau << 1$ (absorption)	0.36 ± 0.05*	0.40 ± 0.05*	0.50 ± 0.05	0.50 ± 0.05
$\omega\tau >> 1$ (dispersion)	0.45 ± 0.10	0.48 ± 0.10	0.43 ± 0.05	0.50 ± 0.05
$\omega\tau >> 1$ (absorption)	≈0.4*	≈0.4*	0.50 ± 0.05	0.50 ± 0.05

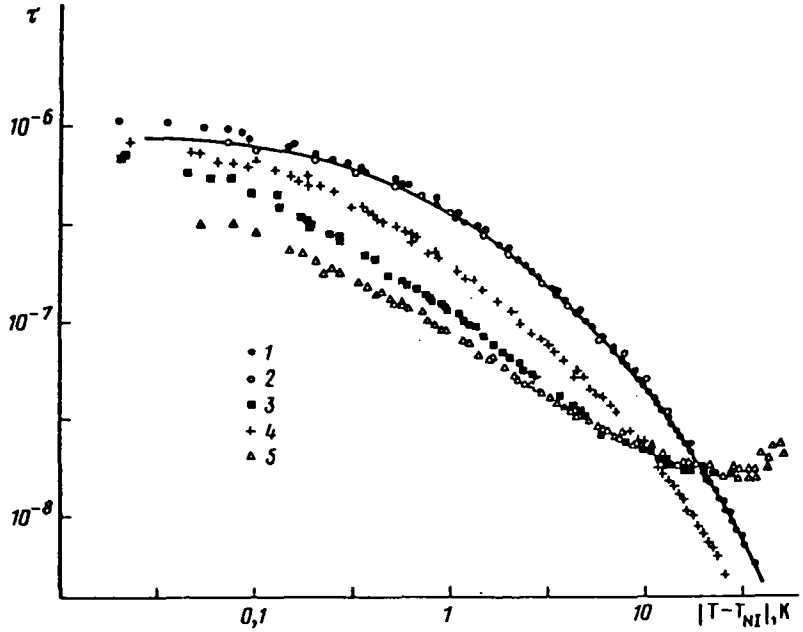

FIGURE 32 Relaxation times of MBBA and BMOAB near the NI transition. MBBA: isotropic phase (Ref. 82's data (1) and Ref. 76's data (2)), nematic phase (3), the continuous line is a result of calculation[76] with the help of the susceptibility data. BMOAB: isotropic phase (4), nematic phase (5).

mula (82), using light-scattering data for χ is in good agreement with independent experiments in MBBA (Figure 32).[82] The difference between the values of the relaxation times of MBBA and BMOAB (approximately a factor of 2) was clearly due to the corresponding difference in the shear viscosity.

The pretransitional amplitudes of the absorption and dispersion appeared to be proportional to the pretransitional amplitude of the heat capacity (Figure 33). Moreover the coefficient of proportionality is close to one. The value of the ratio

$$g = A(T)\,(C_p)_0/\delta C_p \tag{105}$$

[$(C_p)_0$ is a regular part (background) of the heat capacity] was calculated by Imura and Okanao[80] who followed Fixman[83] proposed the identical anomalous parts in the heat capacities at constant pressure C_p and constant volume C_v. It corresponds to the neglect of the dependence of the transition temperature on pressure.[84] Taking into account in first approximation the pressure dependence of T_{NI} gives

$$g = (\gamma_0 - 1) + 2\gamma_0(\partial P/\partial T)_v(dT_{NI}/dP) \tag{106}$$

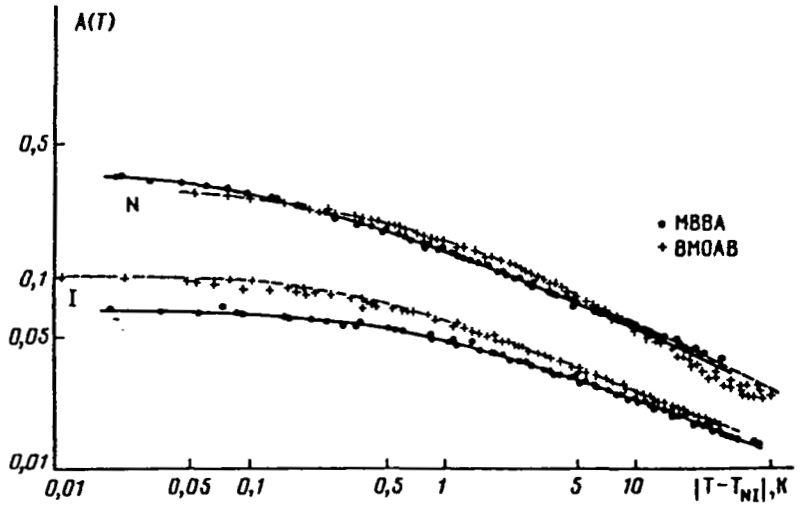

FIGURE 33 Relation between the critical amplitude of the sound absorption and the specific heat anomaly. The continuous lines are the temperature dependences of the excess specific heats for MBBA and BMOAB.

Using the experimental values of the parameters of Eq. (106) $[(\partial P/\partial T)_v \approx 1$ MPa/K, $\gamma_0 = (C_p)_0/(C_v)_0 \approx 1.2$, $(dT_{NI}/dP) = 0.35$K/MPa] one can obtain the estimate (with accuracy 10–20%)$g \approx 1$ in an agreement with the experiment.

In the isotropic phase the universal functions $\phi_1(\omega\tau)$ and $\phi_2(\omega\tau)$ follow the prediction of Imura-Okano theory based on the Ornstein-Zenike (Gaussian) approximation:

$$\phi_1(\omega\tau) = \mathrm{Re}F_2(x) = \left(\frac{4}{\omega\tau}\right)^{1/2}\left[\frac{2}{\omega\tau} + \left(1 + \frac{4}{\omega^2\tau^2}\right)\right]^{-1/2} \tag{107}$$

$$\phi_2(\omega\tau) = \mathrm{Im}F_2(x) = \left(\frac{4}{\omega\tau}\right)^{1/2}\left\{\left[\frac{2}{\omega\tau} + \left(1 + \frac{4}{\omega^2\tau^2}\right)^{1/2}\right]^{1/2} - \left(\frac{4}{\omega\tau}\right)^{1/2}\right\}$$

In the nematic phase the universal functions $\phi_1(\omega\tau)$ and $\phi_2(\omega\tau)$ can be presented by the following linear combinations of F_1 and F_2:

$$\begin{aligned}\phi_1(\omega\tau) &= m\,\mathrm{Re}F_1(x) + (1-m)\,\mathrm{Re}F_2(x)\\ \phi_2(\omega\tau) &= m\,\mathrm{Im}F_1(x) + (1-m)\,\mathrm{Im}F_2(x)\end{aligned} \tag{108}$$

where $m = 0.75$. The value of m is close to the results of the cal-

culations in the mean-field approximation but does not depend on the proximity of the transition point. It means the identical temperature dependence of the amplitudes A_2 and A_2 in the Formula (89) and this is an additional argument for using of the scaling approach. This scaling approach is compatible with the mean-field (better to say Gaussian) dynamic exponent $y = 0.5$.

One can remark that the asymptotics of the dynamic scaling functions allow to make a conclusion about the nature of the order parameter dynamic universality class. For conserved order parameter of critical fluids (density or concentration) $y = \alpha/(2 - \alpha)$. Indeed for investigated critical fluids[84] $\alpha \approx 0.11$ and $y \approx 0.06$ while in Gaussian approximation $\alpha = 0.5$ and $y = 1/3$. Nematic order parameter is not conserved, so $y = \alpha/z$. In Gaussian approximation $\alpha = 0.5$ $z = 1$ and $y = 0.5$.

7. NATURE OF THE NI CRITICAL PHENOMENA

Universality of the critical dynamics in nematic liquid crystals as well as the character of the asymptotic universal functions allows one to state some new opinions on the NI transition. The tensor character of the order parameter and, hence, the first-order nature of the NI transition is the main reason for the absence of simple power laws either mean-field or scaling. Approximation to the divergence temperature of the susceptibility is limited by the range of temperatures

$$t = \frac{T - T^*}{T^*} \geq \frac{T_{NI} - T^*}{T^*} \sim 10^{-2} - 10^{-3}.$$

Experimentalists have only one order of magnitude of temperature change for determination of the power laws. Moreover one can not be sure that they are the simple power laws connected with each other by universal correlations as near a second order phase transition. One can give an example of the following analogy with critical fluids. If the density of a fluid differs from the critical one, the transition is a first order. Temperature dependences of the physical values do not follow simple power laws in this case (critical exponents cannot be found directly). Nevertheless it is possible to preserve a universal description, if one uses the susceptibility or the heat capacity instead of temperature as a scale.[84] Existence of the cubic invariant in liquid crystals wrecks the universal correlation between temperature dependences of the physical values. Using the relaxation time as a scale,

we restore the universality and reveal the true critical behaviour. Universality would be also restored if one chose the susceptibility or the heat capacity as a scale instead of $T - T^*$. Such a choice of the scale was natural for the description of equilibrium properties. In Section 4 Figure 14 demonstrated the connection between the heat capacity anomalous part and the susceptibility, given by Formula (78).

One should note that this correlation is correct in scaling theory if the small difference of the correlation function from the Ornstein-Zernike approximation is neglected (see Refs. 84 and 85). So the correlation (78) can be considered as an "equation of state" of liquid crystals in the isotropic phase near the NI transition. This equation of state is apparently universal and does not depend on the microscopic nature of the departures of the susceptibility from the Curie-Weiss law and that of the heat capacity from the root divergence. One can expect that there also exists a universal connection between the heat capacity and the susceptibility in the nematic phase. This assertion requires experimental testing. Though the restored universal picture is apparently characterized by the critical exponents, which describe the Gaussian fluctuation behaviour, the used approach has the scaling form.

Specificially, in this case there is no need to distinguish the fluctuation contribution to the anomalies of the physical properties in the nematic phase from that connected with the temperature dependence of the order parameter. It means that account of fluctuations may not reduce to small corrections.

One can also state additional considerations concerning the smallness of the Ginzburg criterion for the NI transition and thus the existence of the Gaussian fluctuation behaviour. It was shown in Section 2 that there are a number of reasons which lead to the weakness of the first-order nature of the NI transition (smallness of the coefficient B). In the mean-field approximation such a reason may be biaxiality of mesogenic molecules. On the other hand, the coupling of orientational ordering with conformation of the flexible fragments of molecules (Formula 23) is the simplest reason for the smallness of the coefficient C for the fourth power of the order parameter. The real smallness of the coefficient $C \approx 0.1$ means the corresponding decrease of the Ginzburg number in 100 times. In addition, note that the value of the bare correlation length near the NI transition $\xi_0 \approx$ 6Å is larger (approximately by a factor of 3) than that for the critical points of fluids, whereas the average distance between the molecules in nematics is only 20–30% larger than such a value in fluids. In the mixture BMOAB-isoctane near its critical point $\xi_0 \approx 3$Å[67] and the average volume per molecule does not differ very much from this

value in pure BMOAB. In the Ginzburg criterion the ratio $v_0^{1/3}/\xi_0$ is included in the sixth power. It leads to the appearance of the additional smallness in it as compared to the usual liquids. Physically it means the existence of the definite long-range interaction when the orientational order is formed. If the value ξ_0 in simple liquids, which are mainly composed of spherical molecules, is approximately equal to the radius of a molecule, ξ_0 in the nematics is apparently determined by averaging of the longitudinal and transverse sizes of the anisotropic molecules.

8. EXPERIMENTAL STUDY OF NA TRANSITION

The character of critical phenomena near NA transition points is not yet understood completely. Nevertheless one can note several important questions which were reliably examined in past years.

Specific heat anomaly and the order of NA transition

Even the more or less simple question about the order of the NA transition was a subject of the discussion during many years. Numerous experiments on various liquid crystals with the help of DSC and NMR techniques, investigations of the specific volume as well as anisotropy of the refractive index and magnetic susceptibility indicated that entropy, nematic order parameter, and density had a discontinuity at the NA transitions.[86,87] These discontinuities seemed to decrease with an increase in the width of the nematic range, disappearing at

$$\Delta = 1 - \frac{T_{NA}}{T_{NI}} \approx 0.10 - 0.15.$$

The value of $\Delta = 0.1 - 0.15$ is close to the position of the tricritical point on the NA transition line predicted by the MacMillan's mean-field model.[13] In that model $\Delta_{tcp} = 0.13$. It is well known, however, that the DSC method is essentially nonequilibrium and does not allow a correct separation of pretransitional (fluctuation) effects from a smeared δ-function, which is related to the latent heat of the transition (see Section 4). Recently performed high-resolution calorimetric experiments[88–94] show that the latent heat is virtually absent in the same liquid crystals as well as in others up to values of $\Delta \leqslant 0.01$ (see Figures 19 and 34–36). One should note that the effective critical exponent α varies from $\alpha \approx 0.5$ near the NA tricritical points to $\alpha \approx 0$ at $\Delta \approx 0.06$. This fact probably manifests the crossover from

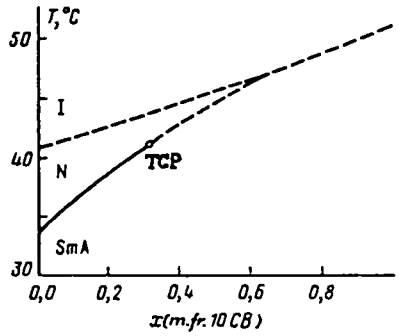

FIGURE 34 Phase diagram of 8CB–10CB mixture.[95] Dashed lines are first-order transitions.

the tricritical behaviour to the "helium-like" one (see Table III). Simultaneously, the heat capacity critical amplitude drastically decreases, so that the anomaly virtually disappears at $\Delta \approx 0.1$ (Figure 37). Hence, one can conclude that the disappearance of the NA peaks on DSC thermograms indicated vanishing of the fluctuation part of the heat capacity, but not the latent heat.

One can see that the disappearance of the nematic order parameter and density "jumps," quoted above, on the second-order side of the NA transition line is related to vanishing of the heat capacity critical anomaly.[74]

The singular part of the free energy according to fluctuation theory is

$$\delta F \sim A_0|t|^{2-\alpha} \tag{109}$$

where A_0 is the critical amplitude of the heat capacity ($\delta C_p \approx A_0|t|^{-\alpha}$). Since T_{NA} is a smooth function of pressure, chemical potential and other fields, including the field h conjugated to the nematic order parameter, the fluctuation parts of entropy, specific volume and concentration (in a mixture) have the form:

$$\begin{aligned} \delta S &\sim A_0|t|^{1-\alpha} \\ \delta Q &\sim A_0(dT_{NA}/dh)|t|^{1-\alpha} \\ \delta V &\sim A_0(dT_{NA}/dP)|t|^{1-\alpha} \\ \delta x &\sim A_0(dT_{NA}/d\mu)|t|^{1-\alpha} \end{aligned} \tag{110}$$

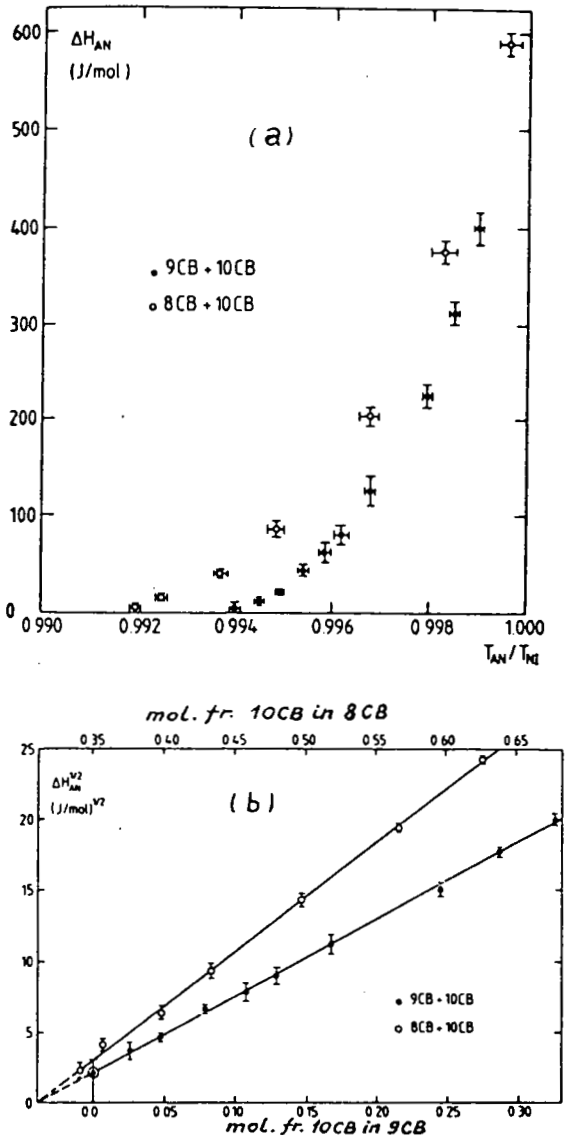

FIGURE 35 Vanishing of the latent heat on the first-order side of the NA transition line in 9CB–10CB and 8CB–10CB mixtures.[95]

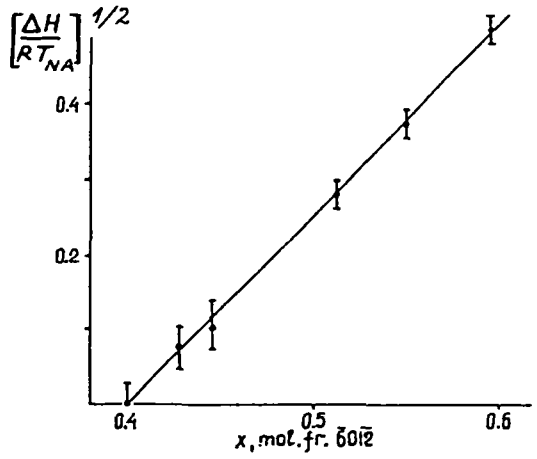

FIGURE 36 Vanishing of the NA latent heat in $\bar{6}O1\bar{0}$–$\bar{6}O1\bar{0}$ mixture.[93]

TABLE III

Results of experimental study of NA transition (Refs. 88–91, 102–111, 124).

	T_{NA}/T_{NI}	$\alpha^{\pm}$	γ^{+}	$\nu_{\perp}^{+}$	$\nu_{\parallel}^{+}$	$\alpha+2\nu_{\perp}+\nu_{\parallel}$
6OCB–8OCB	0.895		1.75	0.73	0.95	
6OCB–8OCB	0.898		1.77	0.70	0.93	
7S5–8S5	0.904		0.31	0.70	0.72	
7S5–8S5	0.908		1.21	0.67	0.64	
7S5–8S5	0.911		1.52	0.68	0.82	
8OCB–7S5	0.911	−0.55(0.35)	1.58(1.03)	0.78(0.505)	0.90(0.58)	1.92
6OCB–8OCB	0.920		1.61	0.61	0.81	
7S5–8S5	0.924		1.45	0.68	0.81	
4O7	0.926	−0.03	1.46	0.65	0.78	2.05
8S5	0.936	0	1.53	0.68	0.83	2.19
CBOOA	0.940	0.15	1.30	0.62	0.70	2.09
4O8	0.958	0.15	1.31	0.57	0.70	1.99
$\bar{6}O1\bar{0}$ + $\bar{6}O\bar{8}$	0.960	0				
8OCB	0.963	0.2	1.32	0.58	0.71	2.09
9S5	0.967	0.22	1.31	0.57	0.71	2.07
8CB	0.977	0.31	1.26	0.51	0.67	2.00
$\bar{6}O1\bar{0}$	0.980	0.24				
10S5	0.984	0.45	1.1	0.51	0.61	2.08
9CB	0.994	0.53	1.1	0.37	0.57	1.84
Helium analogy		−0.02	1.32	0.67	0.67	2.0
Tricritical behaviour		0.5	1.0	0.5	0.5	2.0

Symbols ($\pm$) correspond $T > T_{NA}(+)$ and $T < T_{NA}(-)$. Values of critical exponents for 8OCB–7S5 mixture (in brackets) are calculated dividing experimental (renormalized) values by $1 - \alpha$.[95b]

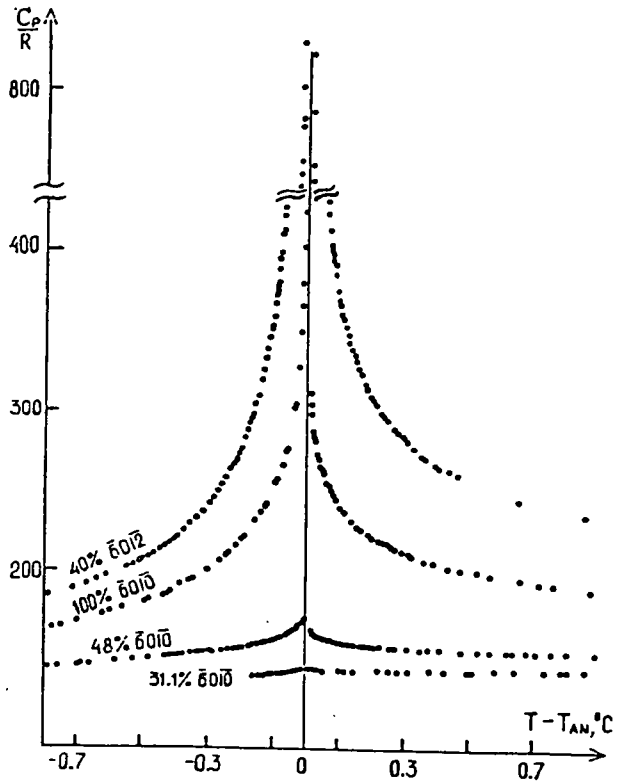

FIGURE 37 Depressing of the NA specific heat anomaly in $\bar{6}O\bar{8}$–$\bar{6}O\bar{1}\bar{0}$–$\bar{6}O\bar{1}\bar{2}$ mixtures while passing from the tricritical point to the NAC multicritical point.

Therefore the fluctuation parts of all these values, regarded as the "smeared jumps," should vanish simultaneously.

The reason of the small tricritical value of Δ is obviously the small value of the nematic–smectic coupling constant λ in expansion (27), since, according to Eq. (29), at $C = 0$

$$\Delta_{tcp} = \frac{A_N}{a_N} = \frac{2\lambda^2}{a_N C_0} \tag{111}$$

The value of the coupling constant λ is determined by the dependence of the NA transition on the smectic order parameter:

$$\lambda = -\frac{1}{2}\frac{a_0}{T_{NA}}\frac{dT_{NA}}{dQ} \tag{112}$$

In mixtures

$$\lambda = \frac{a_0}{T_{NA}} \frac{dT_{NA}}{dx} \left(\frac{dx}{dQ}\right)_{NA} \tag{113}$$

Assuming $a_N \approx 1$, $C_0 \approx 1$, $\frac{dx}{dQ} \approx 1$ and taking into account the value of $(dT_{NA}/dx) \approx 0.07$ in 8CB–10CB mixture, one can obtain

$$\lambda \approx 0.07 \qquad \text{and} \qquad \Delta_{tcp} \approx 5.10^{-3}$$

in a qualitative agreement with experiment.[95]

The only exception, manifected the large value $\Delta_{tcp} \approx 0.06$ for $\bar{7}$S5 – 8OCB mixture,[96b] supports the proposed explanation of the small Δ_{tcp} in the other systems. Indeed, the value of dT_{NA}/dx in $\bar{7}$S5–8OCB is unusually large (289K), and the coupling constant λ should be much larger as well.

Sometimes high-resolution calorimetry shows a small latent heat for the NA transition (and small two-phase region) in liquid crystals for which the second order is firmly established (e.g. in 8OCB[19,97]). The most probable explanation of the effect is the influence of impurities.[74] Impurity leads to the renormalization of the coefficient C in front of the fourth power ψ term in the smectic free energy expansion[10,84]:

$$C^* \approx C - 2T_{NA}^{-2} (dT_{NA}/dx)x \tag{114}$$

where x is a concentration of the impurity. If the constant C is already small due to the coupling between nematic and smectic ordering, even a small amount of impurity can change the transition to the first order one.

Though the situation around the calorimetric investigations of the NA transition seems to be more or less clear, there are some facts requiring a more detailed explanation. First of all the nature of the zero-like value of the critical exponent α remains discussionable. The crossover from tricritical behavior ($\alpha = 0.5$) to helium-like ($\alpha = -0.02$) seems to be observable (see Tables III and IV). However one should not forget that the values of α close to zero were sometimes obtained near the re-entrant point or near the multicritical NAC point. In both these cases the NA heat capacity anomaly vanishes. How to distinguish the crossover effect of changing α from the depression of C_p anomaly? The situation becomes even more complicated

TABLE IV

Fit by formula $C_p/R = A^{\pm}(t^{-\alpha\pm} - 1) + C^{\pm}$ of the heat capacity near the NA transitions in the $\bar{6}O\bar{8}$–$\bar{6}O\bar{1}\bar{0}$ and $\bar{6}O\bar{1}\bar{0}$–$\bar{6}O\bar{1}2$ mixtures $\bar{A}^-$, $\bar{C}^-$ and $\bar{A}^+$,$\bar{C}^+$ correspond to fit with $\alpha^- = \alpha^+$)[93]

	α^- ($\delta\alpha^-$)	α^+ ($\delta\alpha^+$)	A^- (δA^-)	A^+ (δA^+)	C^- (δC^-)	C^+ (δC^+)	$\alpha^- = \alpha^+$	$\bar{A}^-$ ($\delta\bar{A}^-$)	$\bar{A}^+$ ($\delta\bar{A}^+$)	$\bar{C}^-$	$\bar{C}^+$	$\frac{T_{AN}}{T_{NI}}$
0.400 mol.fr.	0.576	0.476	2.18	4.20	111.9	163.5	0.518	3.79	2.75	94.0	177.5	0.9923
$\bar{6}O\bar{1}2$ in $\bar{6}O\bar{1}0$	(0.012)	(0.015)	(0.1)	(0.7)	(1.7)	(5.2)		(0.02)	(0.01)			
$\bar{6}O\bar{1}0$	0.246	0.255	28.2	14.9	69.8	136.1	0.25	26.0	16.5	76.7	1.35	0.9843
	(0.02)	(0.03)	(6.8)	(7.7)	(10.7)	(10)		(1.2)	(1.1)			
0.481 mol.fr.	−0.065	−0.039	−177.8	−107.8	85.3	127.2	−0.05	−204.2	−95.7	90	124.3	0.9644
$\bar{6}O\bar{1}0$ in $\bar{6}O\bar{8}$	(0.033)	(0.04)	(42)	(76)	(5.5)	(1.0)		(3.2)	3.7			

in mixtures where there may be effects of renormalization of the critical exponents if measurements are carried out at constant concentration. The heat capacity C_p at constant concentration does not diverge at the NA transition point in a mixture, and its critical exponent is renormalized from α to $\alpha_R = -\alpha/1 - \alpha)$ for $\alpha > 0$.[98,99] The range of the temperature where α has already been renormalized ($t << t_0$) can be estimated by following formula[84,99]:

$$t_R \sim \left[A_0 x(1 - x)\left(\frac{1}{T_{NA}} \frac{dT_{NA}}{dx}\right)^2\right]^{1/\alpha} \tag{115}$$

where A_0 is a critical amplitude of the non-renormalized heat capacity (in units of R). Far from re-entrant and NAC points the value of (dT_{NA}/dx) is small in a majority of cases, and the renormalization is not accessible. In the vicinity of re-entrant and NAC points the slope of the NA line becomes large and the renormalization must be taken into account. The remarkable exception among other systems is $\bar{7}$S5–8OCB mixture, investigated in Ref. 96b, where because of the unusual value of dT_{NA}/dx the renormalization $\alpha \rightarrow \alpha_R$ was observed. The

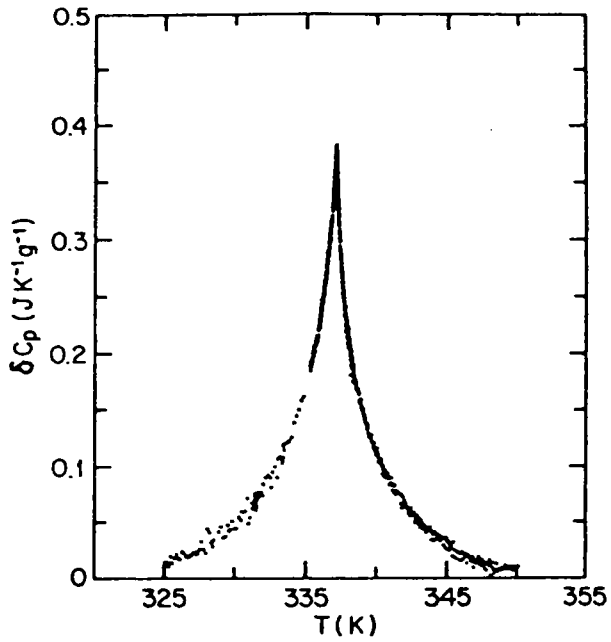

FIGURE 38 Finite cusp of the renormalized excess specific heat in the nearly tricritical $\bar{7}$S5–8OCB mixture.[96b]

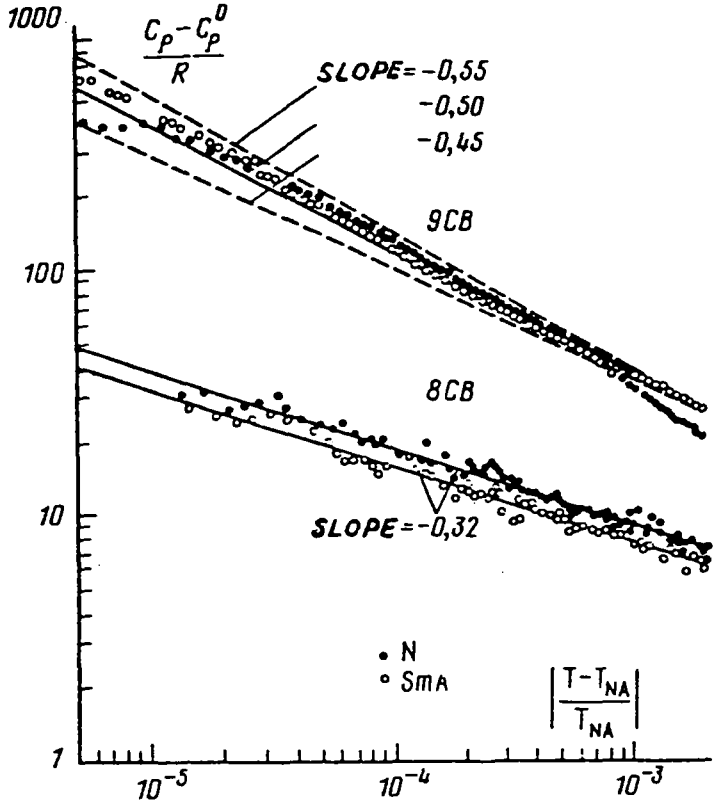

FIGURE 39 Character of the NA specific heat singularities in 9CB and 8CB.[90]

finite cusp in C_p near the tricritical point (see Figure 38) yields $\alpha_R = -0.93 \pm 0.17$. Since $\alpha_R = -\alpha/(1-\alpha)$, this corresponds to $\alpha = 0.48 \pm 0.05$. The other discussionable question of the NA critical phenomena is the character of the NA tricritical behaviour. The NA tricritical point does not look like usual tricritical points. Tricriticial points are characterized by a sharp asymetry in the C_p anomaly above and below tricritical temperature (see, e.g. Ref. 100). Renormalization group theory predicts the tricritical amplitude ratio $A_0/A_0^+ = 5\sqrt{5}/\pi$ (see Ref. 10) which obviously contradicts to the NA tricritical behaviour. Experiment (see Refs. 90, 93, Table IV, Figures 37 and 39) shows that A_0^+ does not differ from A^- so much, i.e. there is the unusual large fluctuation part of C_p above T_{tcp} (in the nematic phase). What is the reason of the such large fluctuation anomaly in the vicinity of the Gaussian point? The question still remains open.

EVIDENCE OF THE HALPERIN-LUBENSKY-MA EFFECT FOR THE NA TRANSITION

There is another important difference betweeen theoretical predictions and NA tricritical behaviour. Landau-de Gennes theory predicts that the latent heat along the first order side of the transition line should be linear function of the distance to the tricritical point, i.e. in a mixture

$$\Delta H_{NA} \sim x - x_{tcp} \tag{116}$$

Results, presented in Figures 35 and 36, show that this prediction is not proved in the case of the NA transition. In Ref. 94 there was shown that the natural reason of the observed nonlinear behaviour of the NA latent heat was Halperin-Lubensky-Ma (HLM) effect.[34] As it was mentioned in Section 3, according to HLM, transverse fluctuations of a nematic director should result in a cubic invariant in the smectic A free energy expansion and, hence, make the NA transition to be a first order. The free energy near the NA transition can be written in the following form:

$$F - F_0 = \frac{1}{2} at|\psi|^2 - \frac{1}{3}B|\psi|^3 + \frac{1}{4}C|\psi|^4 + \frac{1}{6}E|\psi|^6 \tag{117}$$

where

$$B \approx \left(\frac{ak_0^2\xi_{0\perp}^2 v_0^{2/3}}{K}\right)^{3/2} \tag{118}$$

a and C are effective constant, renormalized by the coupling between smectic and nematic ordering, $k_0 = 2\pi/l$ (l is a distance between smectic layers), K is the Frank constant. Existence of three different Frank constants in a real situation is not very important for a qualitative description of the HLM effect.[101] Eqs. (117) and (118) are written with neglect of ψ-fluctuations. Nevertheless such an approximation might be appropriate in the vicinity of the Gaussian tricritical point.

Taking $v_0 K^{-3/2} \approx 1$, $a \approx 1$ and $k_0\xi_{0\perp} \approx \xi_\perp/\xi_{||} \approx 1/5$ we get $B \approx 10^{-2}$ in the usual situation. One should note that the smallness of B is a result of relatively weak coupling of the director fluctuations with the smectic lattice. The combination $ak_0^2\xi_{0\perp}^2$ plays the role of the amplitude of such coupling. One can estimate the NA latent heat

with the help of the following formula which is equivalent to Eq. (17):

$$\frac{\Delta H_{NA}}{RT_{NA}} = \frac{2aB^2}{9C^2} \tag{119}$$

In the usual situation when $C \approx 1$, $\Delta H_{NA}/RT_{NA} \leqslant 10^{-5}$. One can see that the NA latent heat, generated by the HLM effect, is inaccessible even to the highest-resolution adiabatic calorimetry, since its sensitivity is not better than 10^{-3} RT.[91,93,102] However, while passing along the NA line to the NAI triple point, the values of the effective constants a and C change: a increases and C decreases (see Eqs. 28 and 29). When $C = 0$ (in the mean-field tricritical point, predicted by McMillan[13] and de Gennes)[1] the estimate of the NA latent heat gives

$$\left(\frac{\Delta H_{NA}}{RT_{NA}}\right)_{C=0} \approx \frac{1}{2}a\left(\frac{B}{2E}\right)^{2/3} \tag{120}$$

Taking $a \approx 1$, $E \approx 1$ and $B \approx 10^{-2}$, one can obtain

$$\left(\frac{\Delta H_{NA}}{RT_{NA}}\right)_{C=0} \approx 0.02$$

i.e., the value which is quite accessible to observation.

Putting into expansion (117) the mean-field dependence of C on the mixture concentration along the NA transition line,

$$C = C_0(x - x^*) \tag{121}$$

(x^* is a concentration of the McMillan-de Gennes tricritical point, $C_0 < 0$) one can obtain the analytic expression for $\Delta H_{NA}(x)$. One should note that if

$$-C_0(x - x^*) >> B^{2/3}E^{1/3} \tag{122}$$

ΔH_{NA} along the first-order side of the NA line is a linear function of the concentration:

$$\frac{\Delta H_{NA}}{RT_{NA}} = \alpha(x - x^*) \tag{123}$$

where

$$\alpha = -3aC_0/8E$$

The inequality (122) means neglecting of the HLM effect, so the position of the McMillan-de Gennes point and the value of α can be found by the linear extrapolation of $\Delta H_{NA}(x)$. One should stress that the point $x = x^*$ would be tricritical only in the absence of the HLM effect.

If inequality (122) is not valid, the nonlinear universal dependence of $\Delta H_{NA}(x)$ follows from the HLM theory:

$$\frac{\Delta H_{NA}}{\Delta H^*_{NA}} - \left[\frac{\Delta H_{NA}}{\Delta H^*_{NA}}\right]^{-1/2} = y - y^* \qquad (124)$$

where $\Delta H^*_{NA} = (\Delta H_{NA})_{C=0}$ given by Eq. (120), the dimensionless variable $y = \alpha R T^*_{NA}/\Delta H^*_{NA} x$, $T^*_{NA}$and y^* are the values of T and y at the McMillan-de Gennes point.

In Ref. 93 and 94 the experimental results of the study of the NA transition latent heat in the mixture $\bar{6}O1\bar{0}$–$\bar{6}O1\bar{2}$ were presented (see the phase diagram in Figure 19). Measurements were performed by slow scanning adiabatic calorimetry (see Refs. 91, 93, 102). The rate of scanning was 10^{-5} K/s. The nonlinear (close to quadratic) dependence of $\Delta H_{NA}(x)$ was found as well as in Ref. 95 for 9CB–10CB and 8CB–10CB mixtures (Figures 35 and 36). In Ref. 94 the NA latent heats, obtained for $\bar{6}O1\bar{0}$–$\bar{6}O1\bar{2}$[93] as well as for 9CB–10CB and 8CB–10CB mixtures,[95] were fitted by the universal function (124) (see Figure 40).

The values of the adjustable parameters are:

	α	x^*	ΔH^*_{NA}
$\bar{6}O1\bar{0}$–$\bar{6}O1\bar{2}$	1.95	0.482	0.040
8CB–10CB	0.99	0.423	0.026
9CB–10CB	0.54	0.098	0.019

It is interesting to note that the linear part of $\Delta H_{NA}(x)$ is absent for 8CB–10CB and 9CB–10CB mixtures since in that case the McMillan-de Gennes point ($x = x^*$) is located too close to the NAI triple point.

Thus the NA transition with a narrow nematic range is a first order one. The order of the NA transition is determined by two reasons: the classical McMillan-de Gennes mechanism of a coupling between

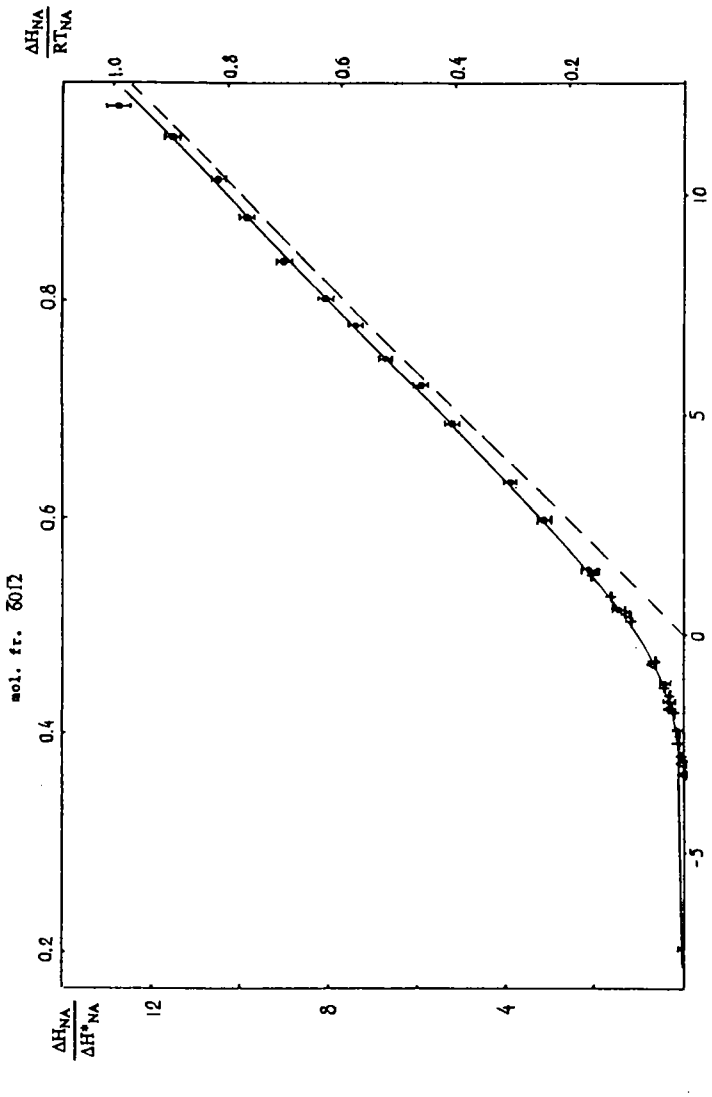

FIGURE 40 Evolution of the relative NA transition latent heat in the vicinity of the McMillan-deGennes tricritical point. Continuous line is the universal function (124) following from the HLM theory.[94] Circles are $\bar{6}O\bar{1}\bar{0}$–$\bar{6}O\bar{1}\bar{2}$ mixtures,[93] triangles are 8CB–10CB mixture, and crosses are 9CB–10CB mixture.[95] The $\Delta S_{NA} - x$ plane is related only to the mixture $\bar{6}O\bar{1}\bar{0}$–$\bar{6}O\bar{1}\bar{2}$.

smectic and nematic ordering and the fluctuation Halperin-Lubensky-Ma effect. The first order character of the NA transition for $x < x^*$, which is continuous in the mean-field approximation is, due to the HLM effect. As the nematic range increases the latent heat of the NA transition decreases and tends to the small but nonzero limit. Finally it becomes less than the experimental error. Then apparent quadratic dependence $\Delta H_{NA}(x)$, presented in Figures 35 and 36, reveals this tendency, i.e. $x = x_{tcp}$ is not the real tricritical point there. At large widths of the nematic range fluctuations of the smectic order parameter are essential, and the approach used above may appear to be incorrect.

Correlation properties near NA transitions

The correlation properties near NA transition points (form of the correlation function, longitudinal and transverse correlation lengths) were investigated in many works by high-resolution X-ray scattering[103–106] and indirectly by light scattering (measurements of elastic constants).[107,108] It was mentioned in Section 3 that in smectics, according to the Landau-Peierls theorem,[2] true long-range order is impossible because the fluctuations in layer position diverge logarithmically with the sample size. For the heat capacity anomaly this slow logarithmic divergence probably is not very important. However, as for the correlation function, which should vanish algebraically as

$$G(r) \sim r_{||}^{-\eta} \tag{125}$$

where η is a small number of order 0.1, it increases slowly while passing to the NA transition point. When $G(r)$ decays algebraically, the Bragg peaks of the X-ray scattering are replaced by power-law singularities of the form

$$I \sim (k_{||} - k_0)^{-2+\eta} \tag{126}$$

where $k_0 = 2\pi/l$ is a smectic density wave number, $k_{||}$ is a wave number of the X-ray scattering along the smectic wave. Experimentally it is difficult to distinguish between the δ-function of Bragg scattering and the power-law singularity (126), and the very high angular resolution is necessary. Such an experiment was performed by Als-Nielsen and his coworkers.[103–106] As a result the prediction of the Landau-Peierls theory was brilliantly approved (Figure 41). In

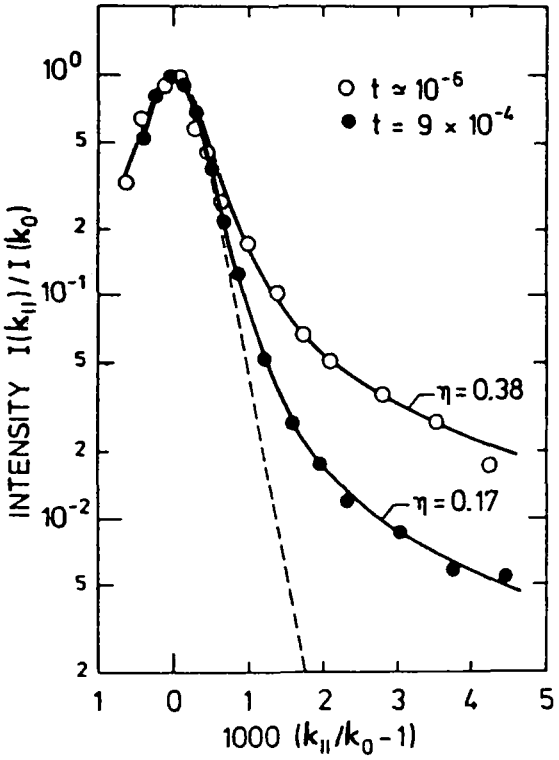

FIGURE 41 Intensity profile for X-ray scattering from the smectic A density waves in 8OCB.[104] The dashed line is the spectrometer resolution function. The solid curves are a convolution of the resolution function from algebraic decay of the correlation function.

this connection Litster and his coworkers[109] suggested the following classification of phase transitions based on existence of two marginal dimensionalities of space: the upper marginal dimensionality d^* and the lower marginal dimensionality d_0. At $d \geq d^*$ fluctuations are small and mean-field approximation is correct. At $d \leq d_0$ fluctuations are so large that the long-range order is impossible. The interval $d_0 < d < d^*$ corresponds to the critical regime, at least in the asymptotic vicinity of a transition point. For usual crystallization $d_0 = 2$, but for the one-dimension crystallization in three-dimension smectics $d_0 = 3$. For fluids and mixtures near their critical points $d^* = 4$ and $d_0 = 1$, therefore at $d = 2$ and $d = 3$ the appearance of long-range ordering is accompanied by critical fluctuations. It is important that $d^* = 3$

at tricritical points, i.e. a tricritical point is Gaussian in usual three-dimensional systems. Incidentally $d^* = 6$ for the first-order NI transition due to existence of the cubic invariant in the effective Hamiltonian. (The value $d^* = 6$ is too far from $d = 3$, therefore it is impossible to apply $\epsilon = (d^* - d)$-expansion method for description of the NI transition).

Let us return to the NA transition. In all investigated systems the correlation length $\xi_{\|}$ and $\xi_{\perp}$ increase while approaching the NA transition point (Figure 42), but $\xi_{\perp} < \xi_{\|}$. If one fits the correlation lengths by the simple power laws,

$$\begin{aligned} \xi_{\|} &= \xi_{0\|}|t|^{-\nu_{\|}} \\ \xi_{\perp} &= \xi_{0\perp}|t|^{-\nu_{\perp}} \end{aligned} \tag{129}$$

the value of $\nu_{\|}$ appears to be often close to "helium" value 2/3, meanwhile the value of $\nu_{\perp}$ is always less (see Table IV). One can not say that the situation here is quite clear. One should note that there

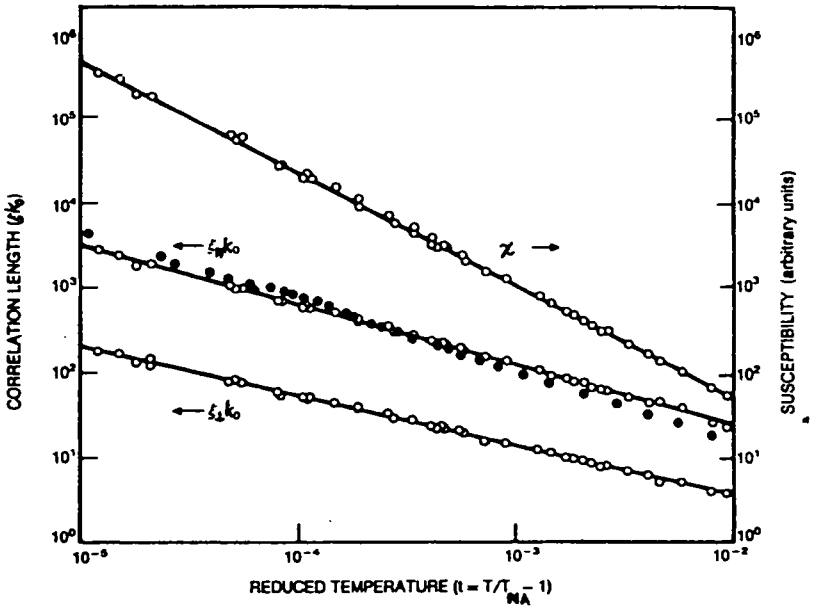

FIGURE 42 Susceptibility (χ) and the correlation lengths of smectic A fluctuations in the nematic phase of 408.[12] Unfilled circles are X-ray scattering data ($k_0 = 0.222\text{Å}^{-1}$). Filled circles are the values of $\xi_{\|}$ deduced from light-scattering measurements of the divergence of the nematic bend elastic constant. The solid lines are power-law fits with the exponent $\nu_{\|} = 0.70$ and $\nu_{\perp} = 0.58$.

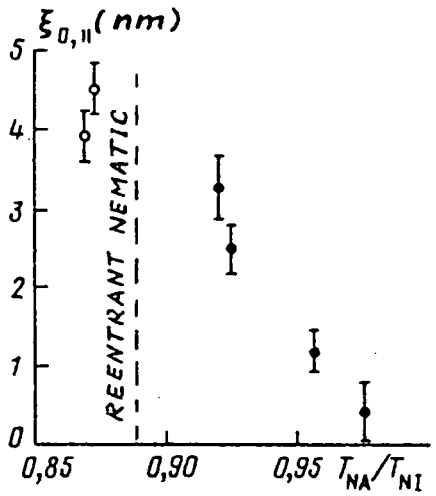

FIGURE 43 Effective bare correlation length in 6OCB–8OCB mixture.[18]

are such rough effects as an increase in $\xi_{0\parallel}$, $\nu_{\parallel}$ and γ with an increase in the nematic range in 6OCB–8OCB mixture[18,106] (Figure 43 and Table IV). This can be explained by the proximity of the re-entrant point which occurs at $T_{NA}/T_{NI} \approx 0.88$ in this mixture. At the re-entrant point the critical exponent should be doubled, meanwhile in its proximity all the values are effective due to crossover phenomena (see Section 3). Near the NAC multicritical point there are another effect: reducing $\xi_{0\perp}$. Both these effects may interfere, confusing the picture. Without taking such effects into account, there is no sense to discuss more delicate theoretical questions such as distinctions between "helium analogy" and anisotropic fixed point. It is remarkable, however, that the anisotropic scaling relation between the effective critical exponents,

$$\nu_{\parallel} + 2\nu_{\perp} = 2 - \alpha \tag{130}$$

is valid (see Table IV). Moreover, there is a constant product $A_0\xi_{0\parallel}\xi_{0\perp}^2$ for the effective heat capacity critical amplitude A_0 and the bare correlation lengths (two-scale-factor universality).

At large nematic ranges it is noticeable a tendency towards the violation of Eq. (130). In the re-entrant region the critical exponent are doubled and this relation should be modified:

$$\nu_{\parallel} + 2\nu_{\perp} = 4 - \alpha \tag{131}$$

where all the critical exponents are effective. Virtually, there is crossover from the behaviour (130) to the behaviour (131).

9. EXPERIMENTAL STUDY OF AC TRANSITION

In all the studied systems the AC transition appeared to be a second order. In the most of the latest works it is confirmed that experimental results are well described by the mean-field theory. Thus in Ref. 110 the mean-field value of the critical exponent β, which characterizes the temperature dependence of the tilt angle in a C-phase, was clearly demonstrated (Figure 44). The best value of β was 0.47 ± 0.04. Light scattering study[111] of the same liquid crystal ($\bar{8}S5$) has led to the following results: $\gamma = 1.10 \pm 0.12$, $\xi_{0\parallel} = 13.5 \pm 2$Å and $\xi_{0\perp} = 21 \pm 9$Å. Large values of the bare correlation lengths result in the validity of the mean-field approximation (Ginzburg number is about $10^{-5} - 10^{-6}$).

Specific heat experiments are also in agreement with the mean-field theory, however the sixth-order term in the free energy expansion should be taken into account (see Refs. 112–114 and Figure 45). Physically it may signify the proximity to the tricritical point. Besides the fluctuation addition to the mean-field jump of the AC specific heat was reported in Refs. 91–93 (see below).

It is quite easy to understand the microscopic nature of the validity of the mean-field approach in the vicinity of the AC transition. Tilt

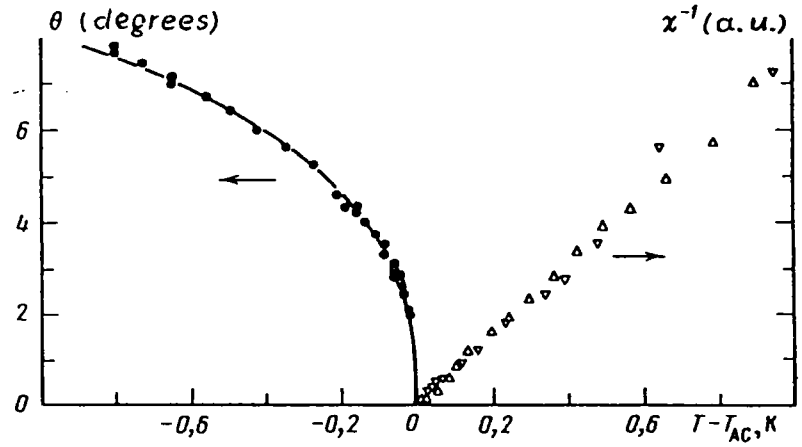

FIGURE 44 Temperature dependence of the mean molecular tilt and susceptibility of 4O7 near the AC transition.[109]

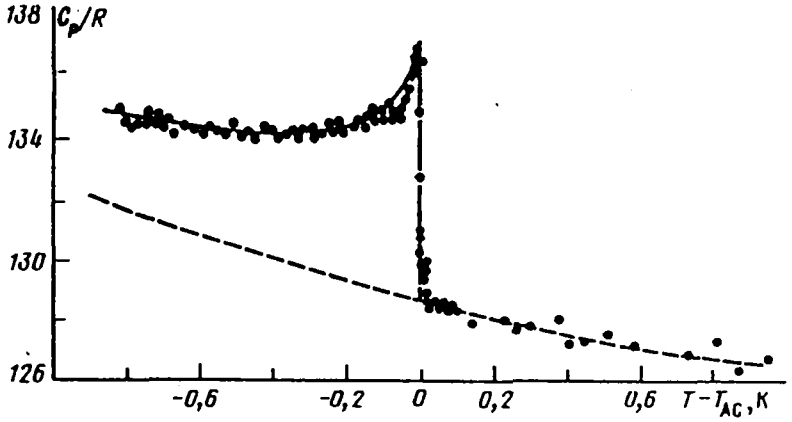

FIGURE 45 Specific heat near AC transition in 4O7.[109,114] Continuous line corresponds to the mean-field approximation.

of molecule in a smectic layer is carried out on the whole molecular length and with many other molecules simultaneously. It corresponds to the large values of the bare correlation length $\xi_{0\parallel}$ and $\xi_{0\perp}$.

10. NATURE OF A NAC MULTICRITICAL POINT

Since a NAC (nematic–smectic A–smectic C) multicritical point was discovered experimentally[115,116] significant efforts both of the theorists[20,37,117,118] and experimentalists[91,92,112,119–124] were made for understanding the nature of this phenomena. The description of the NAC point as a Lifshitz point[20] implies the first order character of the NC transition as result of the tilt fluctuations in the nematic phase (see Section 3), furthermore the NC latent heat has to disappear at the NAC point.[41] This prediction has been supported by experiment.[91,119,120] However, there were important disagreements between the observed experimentally phase diagram topologies. In the mean-field models with the director tilt depending on the existence of the smectic ordering,[16,20] the NA and NC lines are continuous at the NAC point while the AC line is coming in obliquely. The previously observed phase diagrams[119,120] seemed to have an opposite behaviour: the AC and NC lines were continuous, while the NA line approached the NAC point obliquely. Furthermore accurate study of several systems[122–124] have shown that there is the universal NAC topology which is in evident contradiction with any mean-field theory (Figure

46). All the lines, converging in the NAC point, have nonanalytic character. It can mean the fluctuation nature of the NAC point.

A comprehensive study of the phase diagram and the phase transitions in the vicinity of the NAC multicritical point in the $\overline{7}$S5–8OCB mixture has been recently performed by Martinez-Miranda, Kortan and Birgeneau[124] with the help of the high-resolution X-ray scattering. They found that the smectic fluctuations near the NAC point were well described by the Lifshitz-point model. The universality of the NAC topology was also confirmed. One can conclude that the NAC phase diagram is described by the following equations:

$$T_{NA} - T_{NAC} = A_{NA}(x - x_{NAC})^{\phi} + B(x - x_{NAC}) \quad (132)$$

$$T_{NC} - T_{NAC} = A_{NC}(x - x_{NAC})^{\phi} + B(x - x_{NAC}) \quad (133)$$

$$T_{AC} - T_{NAC} = A_{AC}(x - x_{NAC})^{\phi_{AC}} + B(x - x_{NAC}) \quad (134)$$

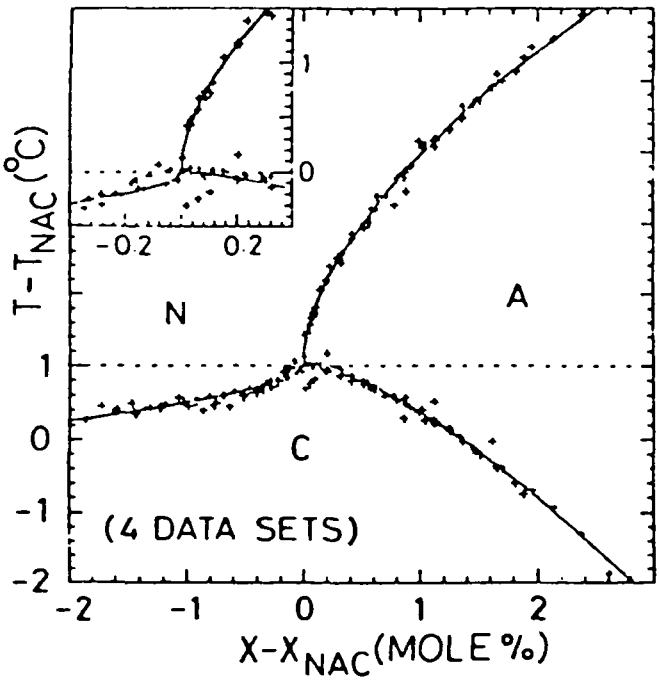

FIGURE 46 Universal topology of a NAC multicritical point.[123] Data[122] for the phase diagrams of four binary systems are shown together after suitable normalization.

where $\phi \simeq 0.5 - 0.6$, $\phi_{AC} \simeq 1.5 - 1.6$.[122-124] A_{NA}, A_{NC} and A_{AC} are not universal. There is no theory of such universality until now.

In this connection it is important to consider the result calorimetric study of the NAC point and to compare it with the results obtained by different techniques and in different systems. In Refs. 91–93 the results of the first high-resolution adiabatic calorimetry study of the NAC point was reported. The $\bar{6}O\bar{8}$–$\bar{6}O1\bar{0}$ mixture was investigated. One can note on the phase diagram of this mixture (Figures 1 and 47) the peculiarity on the NI transition line at the concentration corresponding to the NAC point.

Let us consider separately the phase transition lines converging in the NAC point.

NC transition line

NC transitions are first order ones (compare Figures 48a and 48b). The NC transition heat decreases while approaching the NAC point. Whereas the NC latent heat in the pure $\bar{6}O\bar{8}$ is about 0.1 RT_{NC}, in the mixture containing 0.325 mol. fr. $\bar{6}O1\bar{0}$ it is only 4.10^{-4} RT_{NC}! Such a "paltry" latent heat becomes noticeable only when the slowest scanning rate is used (Figure 49a). Otherwise the transition looks as a second order one (Figure 49b). The change of the concentration only in 0.1% leads to the second order transition within the limits of

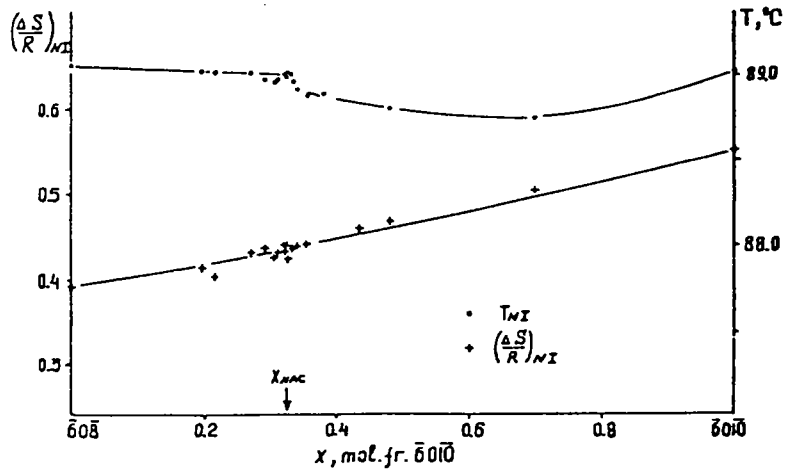

FIGURE 47 NI transition line and the NI transition entropy of $\bar{6}O\bar{8}$–$\bar{6}O1\bar{0}$ mixture.

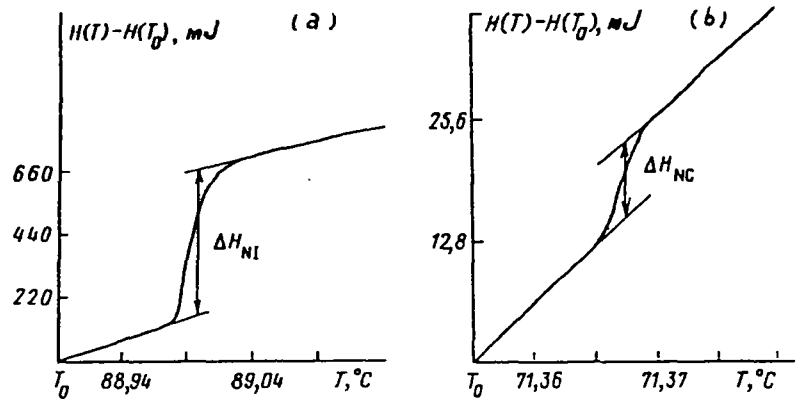

FIGURE 48 NI(a) and NC(b) enthalpy in 0.306 mol.fr. $\bar{6}O1\bar{0}/\bar{6}O\bar{8}$ mixture. The rate of scanning is $5.3 \cdot 10^{-5}$ K/s.

the experimental accuracy (Figure 50). The concentration dependence of the NC latent heat can be fitted by a power-law formula:

$$\Delta H_{NC} \sim (x_{NAC} - x)^{\psi} \tag{135}$$

with $\psi = 0.84 \pm 0.02$ (Figure 51). The extrapolation of the NC latent heat to zero value gives the NAC point position between 0.325 and 0.326 mol. fr. $\bar{6}O1\bar{0}$. Of course, the nonobvious assumption that the point of the NC latent heat disappearance and the NAC point are identical has to be made (see also Figure 51).

The results of the heat capacity measurements near the NC transitions for two samples (pure $\bar{6}O\bar{8}$ and the closest to the NAC point) are shown in Figure 52. The heat capacity anomaly can be qualitatively explained within the framework of the Landau-de Gennes theory with a negative coefficient at the fourth-order term in the free energy expansion (see Section 2). Fit by the formula

$$\frac{C_p}{R} = A_0[|(t| + t_0)^{-\alpha} - 1] + A_1 + A_2 t + A_3 t^2 \tag{136}$$

was good for the pure $\bar{6}O\bar{8}$, when the value of $\alpha = 0.5$ was fixed and t_0 was taken as adjustable parameter, which appeared to be about 10^{-3}. One can see, however, from Figure 52 that fluctuation correction to C_p in the nematic phase of the pure $\bar{6}O\bar{8}$ is noticeable. Therefore a more attentive analysis is probably necessary (see also Ref. 96a).

Close to the NAC point the NC latent heat becomes extremely small. In 0.324 mol. fr. $\bar{6}O1\bar{0}$ mixture it is about 10^{-3} RT_{NC}. According

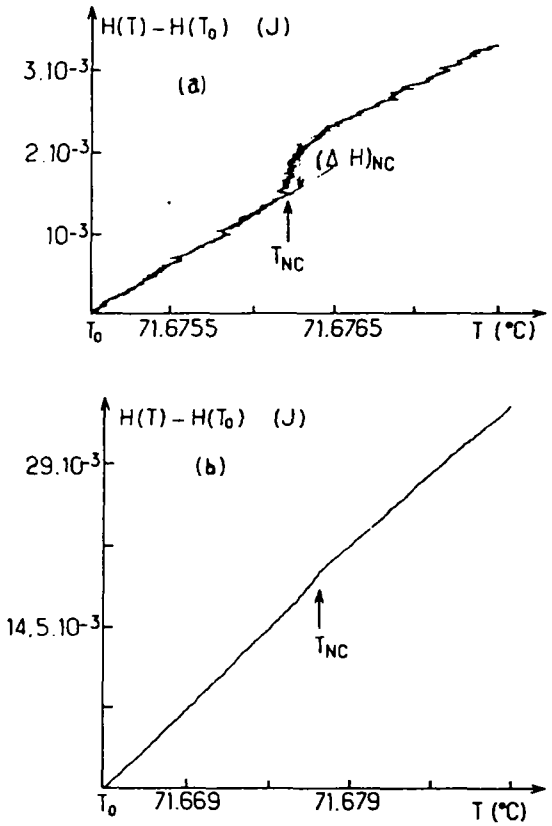

FIGURE 49 NC enthalpy in the immediate vicinity of the NAC point of $\bar{6}O\bar{8}$–$\bar{6}O1\bar{0}$ mixture (0.325 mol.fr. $\bar{6}O1\bar{0}$): a) the rate of scanning is $2.2 \cdot 10^{-6}$K/s, b) it is $1.4 \cdot 10^{-5}$ K/s.

to formulae (38) and (40) it means that $C = -2.10^{-3}$ and $t_0 \simeq 4.10^{-7}$ at $a \approx E \approx 1$. So one would think that the heat capacity should manifest a tricritical behaviour. On the contrary, the fit with fixed $\alpha = 0.5$ was not good anywhere in the vicinity of the NAC point. The better fit was obtained by the crossover formula

$$\frac{C_p}{R} = A_0[(|t| + t_0)^{-0.5} - 1] + A_0^*(|t|^{-\alpha} - 1) + A_1 + A_2 t + A_3 t^2 \quad (137)$$

The value of t_0 appeared to be of several orders more than the previous one and $\alpha = 0.4$–0.5. This fact as well the nonlinear $\Delta H_{NC}(x)$ dependence may correspond to the nonlinear shape of the NC line

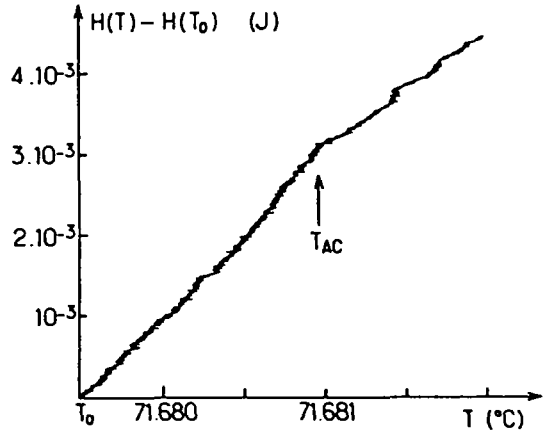

FIGURE 50 NA enthalpy in the immediate vicinity of the NAC point (0.326 mol.fr. $\bar{6}O1\bar{0}$). The rate of scanning is $1.4 \cdot 10^{-6}$K/s.

in the immediate vicinity of the NAC point (see Figure 53). In the nematic phase of the $\bar{7}S5$–8OCB mixture above the NC boundary, there found the Lifshitz line along which the fluctuation change from being SmA-like to SmC-like and $L_\perp = 0$[124] (see Sections 2 and 3). The Lifshitz line appeared to be a natural prolongation of the AC transition line (Figure 54). Near this line the unusual behaviour of the correlation lengths occurred. Hardly noticeable on Figure 52 smeared maximum C_p in the nematic phase close to the NAC point might correspond to these effects.

AC transition line

The results of the heat capacity measurements near the AC transition[91–93] are shown in Figure 55. Data of only two samples of the $\bar{6}O\bar{8}$–$\bar{6}O1\bar{0}$ mixture are represented as examples. Like in the case of the NC transition the fit by formula (136) with $\alpha = 0.5$ was not good in the vicinity of the NAC point. The best value of α is about zero at $t_0 = 0$. Using the crossover formula (137) one can obtain a good fit with $\alpha \simeq 0.2$–0.4 and $t_0 \approx 10^{-3}$. Thus the C_p behaviour appears to be more complicated than the mean-field prediction. It seems strange, incidentally, that the tilt behaviour is in a good agreement with the mean-field theory ($\beta \simeq 0.5$) for $\bar{7}S\bar{5}$–8OCBN mixture even in the immediate vicinity of the NAC point!).[124] The reason of such discord is not yet clear.

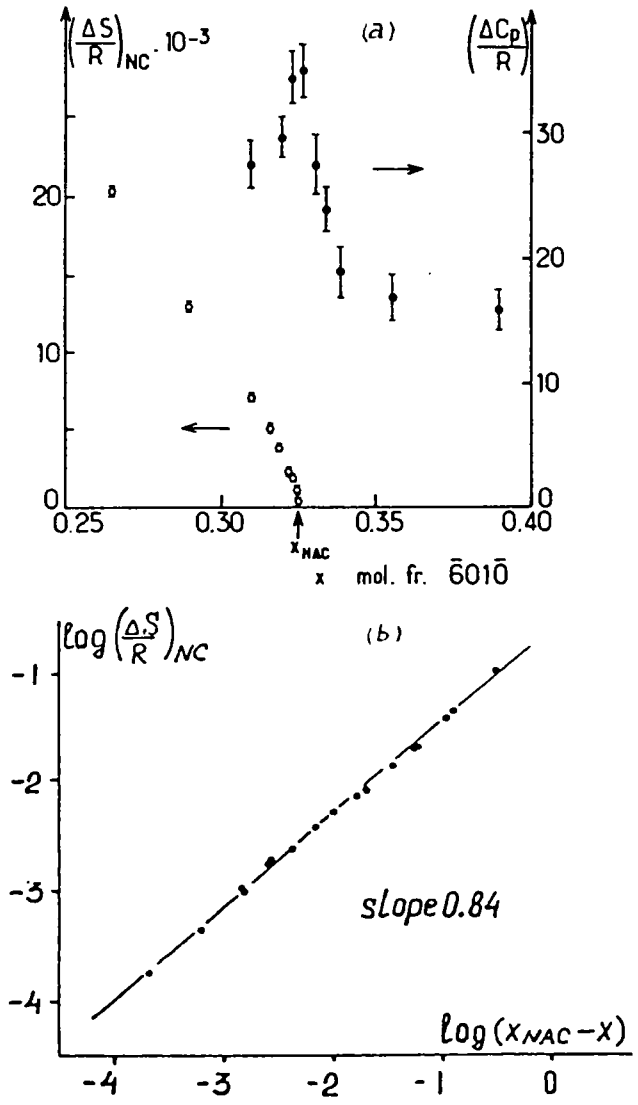

FIGURE 51 a) NC transition entropy and heat capacity jumps near the NAC point. b) Fit of the NC transition entropy by the power law (135).

NA transition line

Near the NAC multicritical point the NA transitions are second order. Furthermore there is a drastic decrease of the heat capacity anomaly upon approaching the NAC point (see Figure 37). Therefore it is

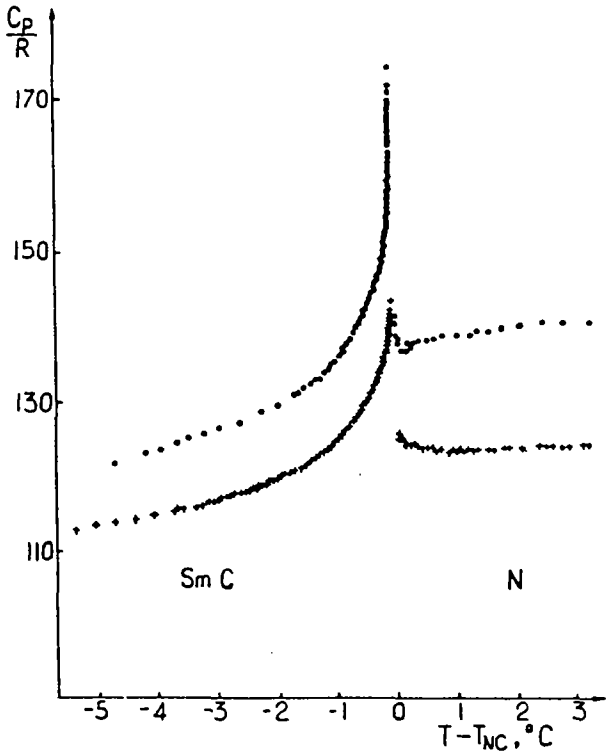

FIGURE 52 Heat capacity near the NC transition in the pure $\bar{6}O\bar{8}$ (crosses and 0.325 $\bar{6}O\bar{1}0/\bar{6}O\bar{8}$ mixture (dots).

difficult to know the exact shape of the NA line in the immediate vicinity NAC point using the calorimetric technique. The other measurements[122–124] show that there is a vertical slope of the NA line there like in a re-entrant point. Some questions arise with this issue: how to distinguish the effects of doubling critical exponents, their "Fisher renormalization" and the probable crossover from Gaussian behaviour to critical? What values of critical exponents are true? Even the best critical exponent data, recently reported in Ref. 124, do not give the answer.

Alternative universality of a NAC point topology

Voronov[125] recently suggested the alternative variant of a NAC point universal topology. He assumed that there should be equal critical

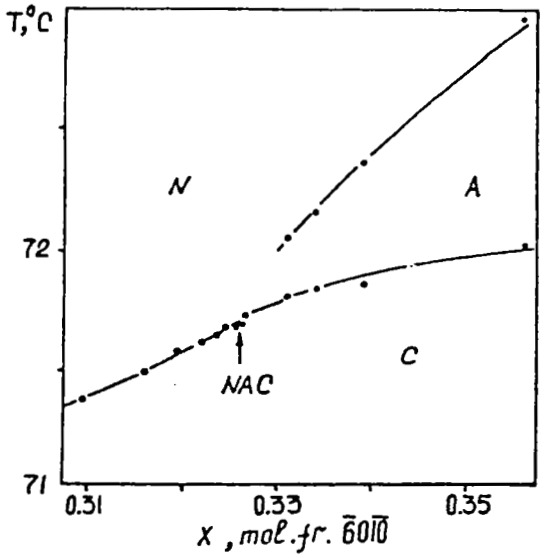

FIGURE 53 Phase diagram of $\bar{6}O\bar{8}$–$\bar{6}O1\bar{0}$ mixture in the vicinity of the NAC point.

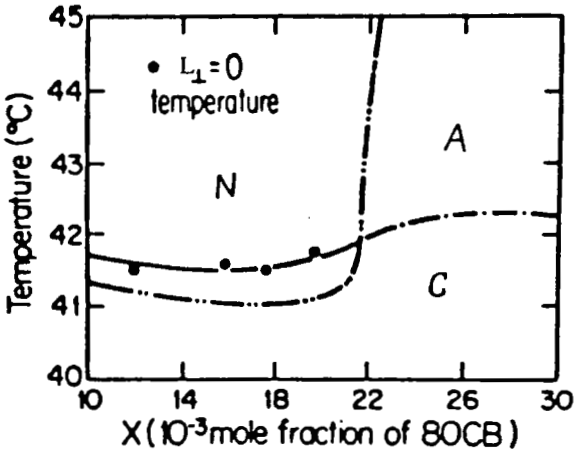

FIGURE 54 Lifshitz line ($L_\perp = 0$) in the immediate vicinity of the NAC point of $\bar{7}S\bar{5}$–8OCB mixture.[124]

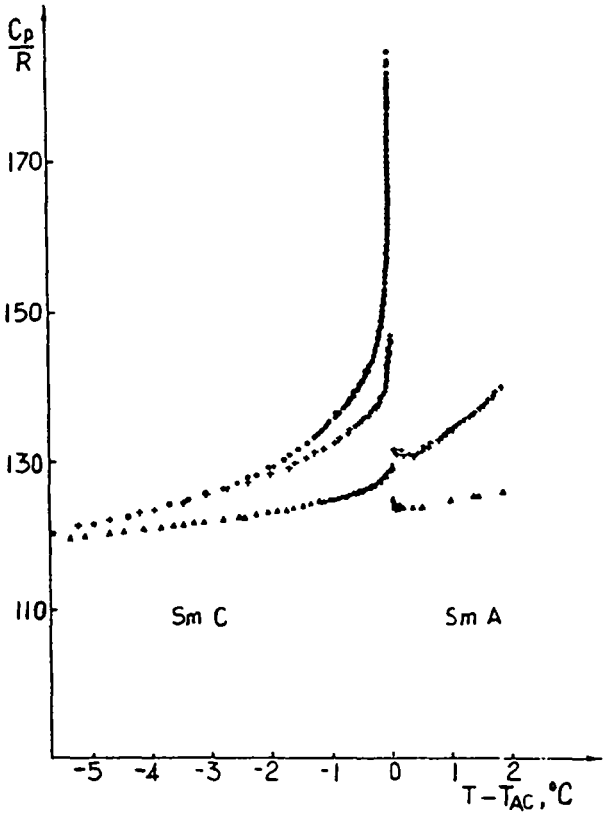

FIGURE 55 Heat capacity near the AC transition in 0.326 mol.fr. $\bar{6}O1\bar{0}/\bar{6}O\bar{8}$ (dots) 0.48 mol.fr. $\bar{6}O1\bar{0}/\bar{6}O\bar{8}$ mixture (crosses), and in the pure $\bar{6}O1\bar{2}$ (triangles).[93]

exponents of NA and AC lines, i.e.:

$$T_{NA} - T_{NAC} = A_{NA}(x - x_{NAC})^{\phi} + B(x - x_{NAC}) \quad (138)$$

$$T_{AC} - T_{NAC} = A_{AC}(x - x_{NAC})^{\phi} + B(x - x_{NAC}) \quad (139)$$

$$T_{NC} - T_{NAC} = A_{NC}(x - x_{NAC})^{\phi_{NC}} + B(x - x_{NAC}) \quad (140)$$

The NC line exponent ϕ_{NC} should be independent. The result of fitting $T_{NA} - T_{AC}$ for different systems is shown in Figure 56. The nonuniversality of amplitudes A was eliminated by appropriate normalization procedure. The slope corresponds to the universal exponent $\phi = 0.67 \pm 0.03$. The obtained value of ϕ allows to deduce the

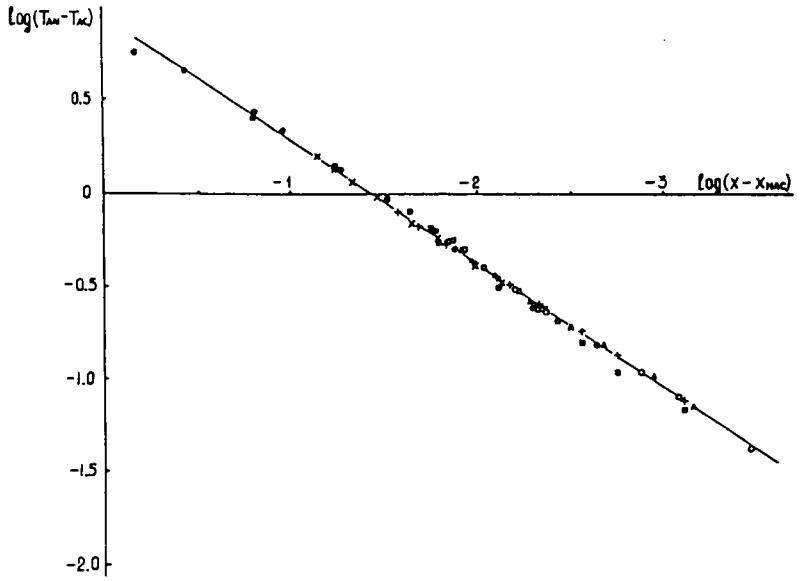

FIGURE 56 Fit of $T_{NA} - T_{AC}$ for seven liquid crystalline systems by Eqs. (138) and (139): $\bar{6}O\bar{8}$–$\bar{6}O\bar{10}$ (dots), $\bar{6}O\bar{10}$-HOPBPOCPC (filled squares)[125] $\bar{7}S5$–$9S5$ (pluses), $\bar{8}O8$–XC (triangles), $\bar{7}S5$-XC (circles), 7 one–8OCB (unfilled squares)[122] 7APCBB (crosses).[123]

"base-line" $B(x - x_{NAC})$ and obtained the value of ϕ_{NC}. The fit of NC lines by the formula

$$\Delta = \frac{1}{A_{NC}}[(T_{NC} - T_{NAC}) - B(x - x_{NAC})] = (x - x_{NAC})^{\phi_{NAC}} \quad (141)$$

is represented in Figure 57. One can see that the exponent ϕ_{NC} is also universal. The proposed universality allows to avoid some contradictions mentioned above:

1) In the new NAC point topology all transition lines are "continuous" since $\phi < 1$ and $\phi_{NC} < 1$. AC line is a prolongation of NC line in accordance of the heat capacity behaviour.

2) The value of the universal exponent $\phi_{NC} = 0.87 \pm 0.04$ coincides within the limits of experimental error with exponent of the NC latent heat dependence ($\psi = 0.84 \pm 0.02$). The universal phase diagram for various systems is shown in Figure 58. The axis $\Delta = 0$ is the base-line of the proposed in Ref. 125 universality while the base-line of the universal topology, suggested in Ref. 122, is the dashed lne. Both of the proposed universal topologies are in agree-

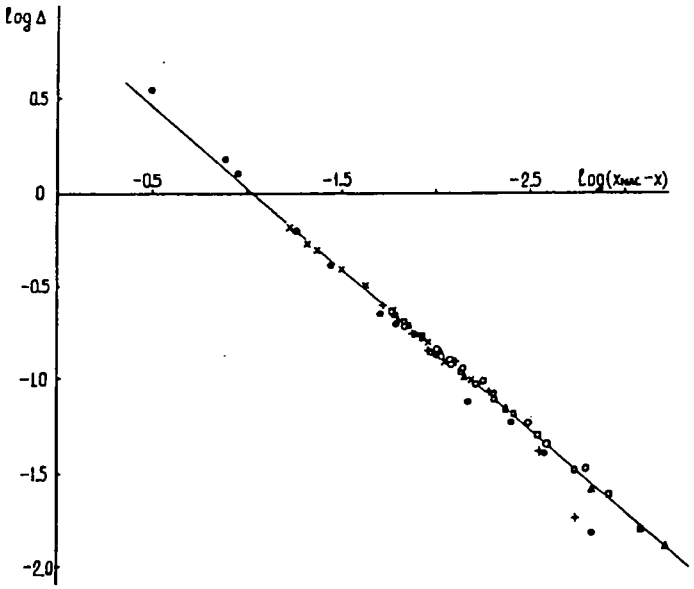

FIGURE 57 Fit of NC lines for the seven systems by Eq. (141). Notations see at Figure 56 caption.

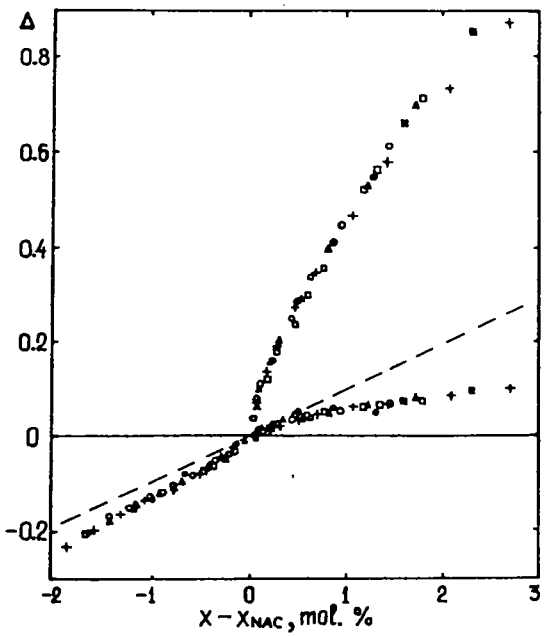

FIGURE 58 Universal NAC phase diagram.[125] Notations see at Figure 56 caption.

ment with experiment. Indeed, one may agree with the authors of Ref. 124, saying about the NAC problem: "The principal issues appear to be on the theoretical front."

11. CONCLUSION

All the main types of critical phenomena are also inherent to liquid crystals: mean-field behaviour near AC transition, large fluctuations frustrating long-range order in smectics, fluctuations driving NC and NA second-order transitions to first order, crossover from tricritical behaviour to critical on NA transition line, etc.

Though many questions still remain unanswered (the nature of the NA transition being the most important among them), it is undoubtedly clear that liquid crystals may be successfully included in the universal picture of the physics of critical phenomena.

References

1. P. G. de Gennes, *The Physics of Liquid Crystals*, Oxford U. P., London (1974).
2. L. D. Landau and E. E. Lifshitz, *Statistical Physics*, 3rd ed. Pergamon, New York (1980).
3. E. F. Gramsbergen, L. Longa and W. H. de Jeu, *Physics Reports*, **135**, 195, No. 4 (1986).
4. V. L. Pokrovskii and E. I. Kats, *Sov. Phys. JETP*, **46**, 405 (1977).
5. P. B. Vigman, A. I. Larkin and V. M. Filev, *Sov. Phys. JETP*, **68**, 944 (1975).
6. L. J. Yu and A. Saupe, *Phys. Rev. Lett.*, **45**, 1000 (1980).
7. V. N. Kachinskii, V. A. Ivanov, S. M. Stishov, *Sov. Phys. JETP*, **48**, 273 (1978).
8. Z. Y. Chen and J. M. Deutch, *J. Chem. Phys.*, **80**, 2151 (1984).
9. M. A. Anisimov, J. Prost and B. Poulingly, Bordeaux (1985) (unpublished).
10. M. A. Anisimov, E. E. Gorodetskii and V. M. Zaprudsii, *Sov. Phys. USPEKHI*, **24**, 57 (1981).
11. E. M. Averianov, *Sov. Phys. Solid State*, **24**, 149 (1982); **24**, 1609 (1982).
12. J. D. Litster and R. J. Bergeneau, *Physics Today*, May 26 (1982).
13. W. L. McMillan, *Phys. Rev.*, **A4**, 1238 (1971).
14. K. C. Chu and W. L. McMillan, *Phys. Rev.*, **A15**, 1181 (1977).
15. S. A. Pikin and V. L. Idenbom, *Sov. Phys. USPEKHI*, **21**, 487 (1978).
16. E. E. Gorodetskii and V. E. Podnek, *Sov. Phys. Crystallography*, **29**, 618 (1984).
17. D. Guillon, P. E. Cladis and J. Stamatoff, *Phys. Rev. Lett.*, **41**, 1598 (1978).
18. J. D. Litster, G. W. Garland, K. T. Lushington and R. Schaetzing, *Mol. Cryst. Liq. Cryst.*, **63**, 145 (1981).
19. G. B. Kasting, K. T. Lushington and C. W. Garland, *Phys. Rev.*, **B22**, 321 (1980).
20. J. H. Chen and T. C. Lubensky, *Phys. Rev.*, **A14**, 1202 (1976).
21. R. M. Hornreich, M. Luban and S. Shtrikman, *Phys. Rev. Lett.*, **35**, 1678 (1975).
22. D. R. Nelson and R. A. Pelcovits, *Phys. Rev.*, **B16**, 9191 (1977).
23. E. I. Kats, *Sov. Phys. USPEKHI*, **27**, 42 (1984).
24. Sh.K. Ma, *Modern Theory of Critical Phenomena*, W. A. Benjamin, Reading, Mass. (1976).

25. K. G. Wilson and J. Kogut, *Phys. Reports*, **12C**, 75 (1974).
26. E. E. Gorodetskii and V. M. Zaprudskii, *Sov. Phys. JETP*, **41**, 103 (1978).
27. A. L. Korzhenevskii and V. N. Shalaev, *Sov. Phys. JETP*, **49**, 1094 (1979).
28. C. P. Fan and M. J. Stephen, *Phys. Rev. Lett.*, **25**, 500 (1970).
29. R. G. Priest, In: *Liquid Crystals*, Proc. Int. Conf. in Bangalore, Heyden (1980), p. 361.
30. L. V. Adzhemyan, L. T. Adzhemyan, A. Y. Valkov, L. A. Zubkov, I. V. Melnik and V. P. Romanov, *Sov. Phys. JETP*, **60**, 712 (1984).
31. S. G. Dunn and T. C. Lubensky, *J. de Physique*, **42**, 1201 (1981).
32. D. R. Nelson and J. Toner, *Phys. Rev.*, **B24**, 361 (1981).
33. T. C. Lubensky and A. J. McKane, *J. de Physique*, **43**, L217 (1982).
34. B. I. Halperin, T. C. Lubensky and Sh.K. Ma, *Phys. Rev. Lett.*, **32**, 292 (1974).
35. T. C. Lubensky (private communication).
36. M. A. Anisimov, E. E. Gorodetskii and V. E. Podnek, *JETP Lett.*, **37**, 414 (1983).
37. E. E. Gorodetskii and V. E. Podnek, *JETP Lett.*, **39**, 624 (1984).
38. A. Gohin, C. Destrade, H. Gasparoux and J. Prost, *J. de Physique*, **44**, 427 (1983).
39. V. P. Podnek (private communication).
40. S. A. Brazovskii, *Sov. Phys. JETP*, **41**, 85 (1975).
41. J. Swift, *Phys. Rev.*, **A14**, 2274 (1976).
42. W. Maier and A. Sauper, *Z. Naturforsch*, **16A**, 816 (1961). J. Nehring and A. Saupe, *Mol. Cryst. Liq. Cryst.*, **8**, 403 (1969).
43. W. H. de Jeu, Physical Properties of Liquid Crystalline Materials, Gordon and Breach, New York (1980).
44. W. H. de Jeu and P. Bordevijk, *J. Chem. Phys.*, **68**, 109, 116 (1978). W. H. de Jeu and W.A.P. Claassen, *J. Chem. Phys.*, **68**, 102 (1978).
45. I. H. Ibrahim and W. Haase, *Z. Naturforsch*, **31A**, 1644 (1976).
46. J. Haller, H. A. Huggins, H. R. Lilienthal and T. R. McCuire, *J. Chem. Phys.*, **77**, 950 (1973).
47. E. G. Hanson and Y. R. Shen, *Mol. Cryst. Liq. Cryst.*, **36**, 193 (1976).
48. P. I. Collins and J. R. McColl, *Sol. St. Comm.*, **28**, 997 (1978).
49. P. H. Keyes, *Phys. Lett.*, **A67**, 132 (1978).
50. Lin Lei, In: *Liquid Crystals*, Proc. Int. Conf. in Bangalore, Heyden (1980), p. 355.
51. T. W. Stinson and J. D. Litster, *Phys. Rev. Lett.*, **25**, 503 (1970).
52. T. W. Stinson and J. D. Litster, *Phys. Rev. Lett.*, **30**, 688 (1973).
53. E. Gulary and B. Chiu, *J. Chem. Phys.*, **62**, 798 (1975).
54. T. W. Stinson, J. D. Litster and N. A. Clark, *J. de Physique*, **33**, 69 (1972).
55. A. Gohin, Thesis, Bordeaux (1979) (unpublished).
56. B. Malraison, Y. Poggi and C. Filippini, *Sol. St. Comm.*, **31**, 843 (1979).
57. K. Muta, H. Takezoe, A. Fukuda and E. Kuze, *Jap. J. Appl. Phys.*, **18**, 2073 (1979).
58. B. Poulingny, J. P. Marcerou, J. R. Lalane and E. Coles, *Mol. Phys.*, **49**, 583 (1983).
59. K. Hirakawa and Sh. Kai, *J. Phys. So. Jap.*, **37**, 1472 (1974).
60. B. I. Ostrovskii, S. A. Taraskin, B. A. Strukov and A. S. Sonin, *Sov. Phys. JETP*, **44**, 363 (1976).
61. J. Mayer, T. Waluge and J. A. Janik, *Phys. Lett.*, **A41**, 102 (1972).
62. M. Sorai, T. Nakamura and S. Seki, *Bull. Chem. Soc. Jap.*, **47**, 2192 (1974).
63. M. A. Anisimov, V. M. Mamnitsky and E. L. Sorkin, In: *Liquid Crystals*, Proc. Int. Conf. in Bangalore, Heyden (1980), p. 347.
64. M. A. Anisimov, S. R. Garber, V. S. Esipov, V. M. Mamnitskii, G. I. Ovodov, L. A. Smolenko and E. L. Sorkin, *Sov. Phys. JETP*, **45**, 1042 (1977).
65. M. A. Anisimov, E. L. Sorkin and V. M. Mamnitskii, *Sov. J. Eng. Phys.*, **39**, 1385 (1981).

66. M. A. Anisimov, V. M. Zaprudkii, V. M. Mamnitskii and E. L. Sorkin, *JETP Lett.*, **30**, 491 (1979).
67. E. L. Sorkin, Thesis, Moscow (unpublished) (1980).
68. V. P. Voronov (private communication).
69. H. Zink and W. H. de Jeu, *Mol. Cryst. Liq. Cryst.*, **124**, 287 (1985).
70. M. A. Anisimov, V. I. Labko, G. L. Nikolaenko and I. K. Yudin, *Mol. Cryst. Liq. Cryst. Lett.*, **2**, 77 (1985).
71. M. A. Anisimov, S. A. Konev, V. I. Labko, G. L. Nikolaenko, G. I. Olefirenko and I. K. Yudin, *Mol. Cryst. Liq. Cryst.*, **146**, 421 (1987).
72. M. A. Anisimov, V. I. Labko, G. L. Nikolaenko and I. K. Yudin, *JETP Lett.*, **45**, 111 (1987).
73. G. L. Nikolaenko, Thesis, Moscow (1987) (unpublished).
74. M. A. Anisimov, *JETP Lett.*, **37**, 11 (1983).
75. M. A. Anisimov, V. P. Voronov, Yu.F. Kiyachenko and V. M. Merkulov, *Mol. Cryst. Liq. Cryst.*, **104**, 273 (1984).
76. M. A. Anisimov, V. P. Voronov, A. S. Goldenstein, E. E. Gorodetskii and V. M. Merkulov, *Sov. Phys. JETP*, **60**, 1134 (1984).
77. M. A. Anisimov, *Mol. Cryst. Liq. Cryst.*, **146**, 435 (1987).
78. L. D. Landau and E. M. Lifshitz, *Fluid Mechanics*, 3rd ed., Pergamon, Oxford (1966).
79. L. D. Landau and I. M. Khalatnikov, In: the *Collected Papers of L. D. Landau*, Pergamon, Oxford (1965).
80. H. Imura and K. Okano, *Chem. Phys. Lett.*, **19**, 387 (1973).
81. R. A. Ferrell and J. K. Battacharjee, *Phys. Rev.*, **B23**, 2434 (1981).
82. G. K. Wong and Y. R. Chen, *Phys. Rev.*, **A10**, 1277 (1974).
83. M. Fixman, *J. Chem. Phys.*, **36**, 1961 (1962).
84. M. A. Anisimov, *Critical Phenomena in Liquids and Liquid Crystals* (in Russian), Nauka, Moscow (1987).
85. L. Mistura, *J. Chem. Phys.*, **57**, 2311 (1972).
86. F. Hardouin, G. Sigaud, M. F. Achard and H. Gasparoux, *Ann. de Physique*, **34**, 381 (1978).
87. T. McKee and J. McCall, *Phys. Rev. Lett.*, **34**, 1076 (1975).
88. D. Brisbin, R. De Hoff, T. E. Lockhart and D. L. Johnson, *Phys. Rev. Lett.*, **43**, 1171 (1979).
89. C. W. Garland, G. B. Kasting and K. J. Lushington, *Phys. Rev. Lett.*, **43**, 1420 (1979). G. B. Kasting, C. W. Garland and K. J. Lushington, *J. de Physique*, **41**, 879 (1980).
90. H. Marynissen, J. Thoen and W. Van Dael, *Mol. Cryst. Liq. Cryst.*, **97**, 149 (1983). J. Thoen, H. Marynissen and W. Van Dael, *Phys. Rev. Lett.*, **52**, 204 (1984).
91. M. A. Anisimov, V. P. Voronov, A. O. Kulkov and F. Kholmurodov, *J. de Physique*, **46**, 2137 (1985).
92. M. A. Anisimov, V. P. Voronov, A. O. Kulkov and F. Kholmurodov, *JETP Lett.*, **41**, 302 (1985).
93. M. A. Anisimov, V. P. Voronov, A. O. Kulkov, V. N. Petukhov and F. Kholmurodov, *Mol. Cryst. Liq. Cryst.*, **150** b, 399 (1987).
94. M. A. Anisimov, V. P. Voronov, E. E. Gorodetskii, V. E. Podnek and F. Kholmurodov, *JETP Lett.*, **45**, 425 (1987).
95. H. Marynissen, J. Thoen and W. Van Dael, *Mol. Cryst. Liq. Cryst.*, **124**, 195 (1985).
96. a) C. W. Garland and M. E. Huster, *Phys. Rev.*, **A35**, 2365 (1987). b) M. E. Huster, K. J. Stine and C. W. Garland, Phys. Rev., **A36**, 2364 (1987). C. W. Garland (private communication).
97. D. L. Johnson, C. F. Hayes, R. J. De Hoff and C. A. Schantz, *Phys. Rev.*, **B18**, 4902 (1978).
98. M. E. Fisher, *Phys. Rev.*, **176**, 257 (1968).

99. M. A. Anisimov, A. V. Voronel and E. E. Gorodetskii, *Sov. Phys. JETP*, **33**, 605 (1971).
100. M. A. Anisimov, V. M. Zaprudskii, T. A. Milner and E. I. Ponomarenko, *Sov. Phys. JETP*, **53**, 397 (1981).
101. V. E. Podnek (private communication).
102. J. Thoen, H. Marynissen and W. Van Dael, *Phys. Rev.*, **A26**, 2886 (1982).
103. J. Als-Nielsen, R. J. Birgeneau, M. Kaplan, J. D. Litster and C. R. Safinya, *Phys. Rev. Lett.*, **39**, 352 (1977).
104. J. Als-Nielsen, J. D. Litster, R. J. Birgeneau, M. Kaplan, C. R. Safinya, A. Lindegaard-Andersen and S. Mathiesen, *Phys. Rev.*, **B22**, 312 (1980).
105. J. D. Litster, R. J. Birgeneau, M. Kaplan, C. R. Safinya and J. Als-Nielsen, In: *Ordering in Strongly Fluctuating Condensed Matter Systems*, ed. T. Riste, Plenum Press, New York (1980), p. 357.
106. B. M. Ocko, R. J. Birgeneau, J. D. Litster and M. E. Neubert, *Phys. Rev. Lett.*, **52**, 208 (1984).
107. J. D. Litster, J. Als-Nielsen, R. J. Birgeneau, S. S. Dana, R. Davidov, F. Garcia-Golding, M. Kaplan, S. R. Safinia and R. Schaetzing, *J. de Physique*, **40**, C3-339 (1979).
108. D. Davidov, S. R. Safinia, M. Kaplan, S. S. Dana, R. Schaetzing, R. J. Birgeneau and J. D. Litster, *Phys. Rev.*, **B19**, 1657 (1979).
109. R. J. Birgeneau, C. W. Garland, A. R. Kortan, J. D. Litster, M. Meichle, B. M. Ocko, C. Rosenblatt, L. J. Yu and J. Goodby, *Phys. Rev.*, **A27**, 1251 (1983).
110. C. R. Safinya, M. Kaplan, J. Als-Nielsen, R. J. Birgeneau, D. Davidov, J. D. Litster, D. L. Johnson and M. E. Neubert, *Phys. Rev.*, **B21**, 4149 (1980).
111. R. Schaetzing, Ph.D. Thesis, M.I.T. (1980).
112. C. C. Huang, J. M. Viner, *Phys. Rev.*, **A25**, 3385 (1982).
113. J. Thoen and G. Seynhaeve, *Mol. Cryst. Liq. Cryst.*, **127**, 229 (1985).
114. M. Meichle and C. W. Garland, *Phys. Rev.*, **A27**, 2624 (1983).
115. D. Johnson, D. Alender and R. De Hoff, C. Maze, E. Oppenheim and R. Reynolds, *Phys. Rev.*, **B16**, 470 (1977).
116. G. Sigaud, H. Hardouin and M. F. Achard, *Sol. St. Comm.*, **23**, 35 (1977).
117. G. Grinstein and J. Toner, *Phys. Rev. Lett.*, **51**, 2386 (1983).
118. L. Benguigui, *J. de Physique*, **40**, 419 (1979).
119. R. De Hoff, R. Biggers, D. Brisbin and D. L. Johnson, *Phys. Rev.*, **A25**, 472 (1982).
120. C. C. Huang and S. C. Lien, *Phys. Rev. Lett.*, **47**, 1917 (1981).
121. L. Solomon and D. L. Litster, *Phys. Rev. Lett.*, **56**, 2268 (1986).
122. D. Brisbin, D. L. Johnson, H. Fellner and M. E. Meubert, *Phys. Rev. Lett.*, **53**, 2141 (1984).
123. R. Shashidhar, B. R. Ratna and S. Krishna Prasad, *Phys. Rev. Lett.*, **53**, 2141 (1984).
124. L. T. Martinez-Miranda, A. R. Kortan and R. G. Birgeneau, *Phys. Rev.*, **A36**, 2372 (1987).
125. V. P. Voronov (private communication). M. A. Anisimov and V. P. Voronov (to be published).